VISUAL FIELD RESPONSIVENESS IN GLAUCOMA

AN EYE TRACKING APPROACH

DEEPMALA MAZUMDAR

Visual Field Responsiveness in Glaucoma: An Eye Tracking Approach

Deepmala Mazumdar

The making of this research and the dissertation was made possible by financial support from

The execution and publication of this research work has been made possible by the logistical support from

Visual Field Responsiveness in Glaucoma: An eye tracking approach

Reactiviteit van het gezichtsveld bij Glaucoom: Een eye-tracking-benadering

Thesis

to obtain the degree of Doctor from the

Erasmus University Rotterdam

by command of the

rector magnificus

Prof.dr. A.L. Bredenoord

and in accordance with the decision of the Doctorate Board.

The public defence shall be held on

Tuesday 7 December 2021 at 10:30 hrs

by

Deepmala Mazumdar

born in the Seven Sister's land, Assam, India

Erasmus University Rotterdam

Promotion Commission:

Promotors:	Prof.dr. J. van der Steen
	Prof.dr. R. J. George
Other Members:	Prof.dr. J.R. Vingerling
	Prof.dr. H.S.Tan
	Prof.dr. R. Baraas
Copromotor:	Dr.ir. J.J.M. Pel

Table of Contents

Chapter 1	General Introduction	7-31
Chapter 2	Comparison of SRT between normal and glaucoma using an eye movement perimeter. *Adapted from Indian Journal of Ophthalmology, 2014, Jan;62(1):55-9*	33-46
Chapter 3	Effect of age, sex, stimulus intensity and eccentricity on SRT in Eye Movement Perimetry *Adapted from: Translational Vision Science & Technology. 2019 Jul 30;8(4):13*	47-71
Chapter 4	A preliminary study to construct a normative database for Eye Movement Perimetry: does ethnicity affects SRT values? *Manuscript in Preparation*	73-76
Chapter 5	Visual field plots: A comparison study between Standard Automated Perimetry and Eye Movement Perimetry *Adapted from: Journal of Glaucoma. 2020 May;29(5):351-361*	77-102
Chapter 6	SRT in mirror image sectors across horizontal meridian in Eye Movement Perimetry *Adapted from: Scientific Reports. 2021 Jan 29;11(1):26-30*	103-125
Chapter 7	Comparison between monocular and binocular visual field responsiveness in glaucomatous eyes using Eye Movement Perimetry: An exploratory study *Manuscript in Preparation*	127-130
Chapter 8	General Discussion	131-148
Appendices	General Summary	151-154
	Reference List	155-165
	Portfolio	167-174
	List of Publications & Awards	175-176
	Acknowledgement	177
	Curriculum Vitae	178

CHAPTER 1

GENERAL INTRODUCTION

Being able to “see” is one of the most essential senses for human development and survival. The sense of seeing is often referred to as ‘sight’ and ‘vision’ although these are different entities. Sight is being able to see the objects be it close or/and far away, whereas vision is something more complex. Vision is the dynamic and interactive process by which the brain perceives and processes the visual information. Even with completely normal eyesight, problems with vision can still exist, for example when there are issues in using both the eyes together and in understanding the processed visual information. Our vision impacts us more than we realize because it enables us to perform activities as routine as navigating our world, identifying a word, or finding something on the page of a book or even negotiating the traffic. The process of perceiving and processing visual information involves an elaborate network of neuronal tracts that connects the eyes with many of the brain areas (Daw, 2006).

This network of visual information processing has its roots in both our eyes simultaneously. The incoming light travels through different structures of the eye, such as the cornea, the lens, and the pupil in tandem to focus the light rays onto the retina (fig 1.1A).

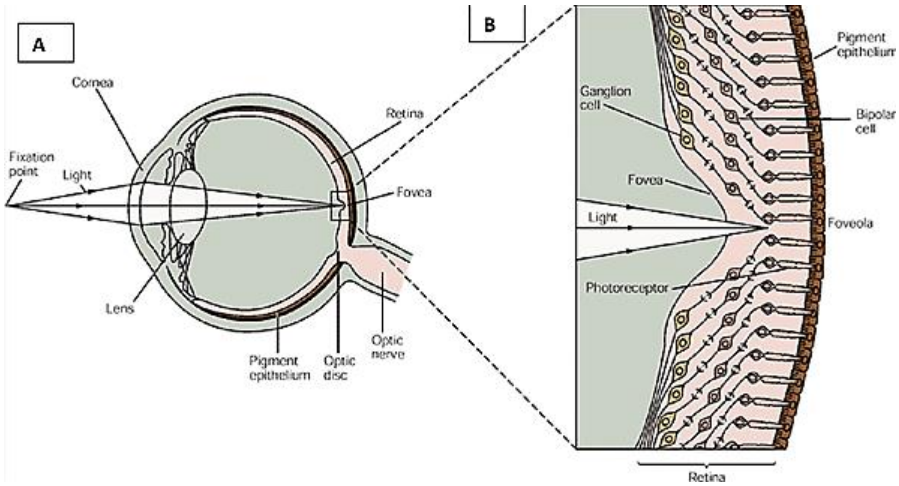

Figure 1.1: A, showing the primary structures within the eye through which the incoming light travels; **B**, showing the details of the neural retina, the light rays pass through the components of the neural retina including the photoreceptors and finally reaches the centre of the fovea, foveola. *(Reproduced from Kandel et al, 2000)*

Here, the light triggers different components of the neural retina, which consists of the photoreceptor cells; the retinal ganglion cells, the bipolar cells, the amacrine cells, the horizontal cells, the rods, and cones (fig1.1B). The neural layers overlying the photoreceptors absorb some of the passing light and thus reduce light scattering and image distortion which helps in translating visual information. The axons of the retinal ganglion cells transport the visual information from each eye through the optic nerve to the visual cortex, as shown in fig 1.2.

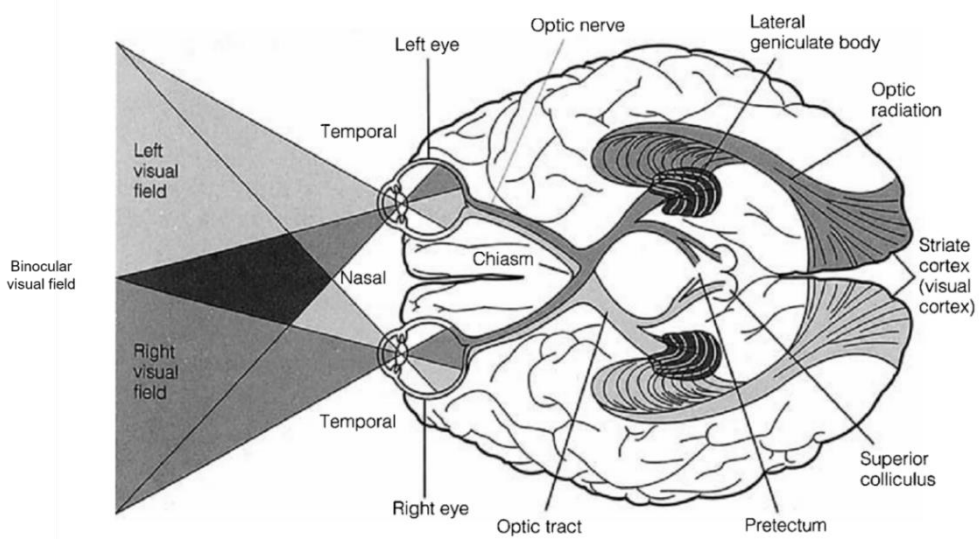

Figure 1.2: The visual pathway as visualised from below. The visual pathway with the course of visual information flows from the right and left hemi-fields of the two eyes' visual field. The visual information is transported by the axons of retinal ganglion cells from both the eyes through the optic nerve to the visual cortex. The axonal fibres from the nasal retina cross in the chiasm and the temporal retinal axons maintain their course without crossing. The right visual cortex perceives information from the left field of view and vice versa. (*Reproduced from Nigel W. Daw. Visual development. Vol. 9. New York: Springer, 2006*)

The visual cortex, otherwise known as the striate cortex, is divided into six critical areas: primary visual cortex (V1), extrastriate cortex (V2, V3, V4, and V5) and the inferotemporal cortex. Visual information first received at the primary visual cortex, V1, where information received

from the two eyes are converged and analysed. From V1 the visual information is transferred to the more specialised areas: the extrastriate cortex and the inferotemporal cortex. Each of these areas works in tandem to process specific visual information such as object recognition, motion, depth, colour (Daw, 2006). The result of this visual information being received and interpreted by different areas in the brain is called visual perception, which is a combination of vision and sight.

Any pathology in the visual information processing pathways (fig 1.2) results in loss of visual functions (Goetz, ed., 2007). Pathological changes in the form of a lesion or infarctions at any level in the visual pathway or level of the visual cortex can lead to specific loss of visual functions, visual neglect, motion processing deficit, loss of colour perception, visual field loss as well as complete loss of vision. At the level of the eye, any degenerative changes in the neural retina can manifest as impairment in visual acuity, loss of visual field or reduced contrast sensitivity. Thus, the process of visual perception requires a complete intact network from the eye up to the brain.

The presence of any form of visual function loss, in isolation or in combination can have a huge impact on a person's life. Some impairments that are related to structures of the eye are often temporary/stable and can be cured. For example, visual impairment due to cataract can be restored with intra-ocular lens implantation or refractive errors can be corrected using spectacles or contact lenses. Impairments that involve primary and higher-order visual pathways can result in irreversible loss of visual functions. One of the most prevalent ocular conditions is glaucoma, also known as "the silent thief of sight". The glaucomatous degenerative changes in the primary visual sensory pathway are manifested in the form of progressive permanent visual field loss which, if left untreated, can progress to complete blindness (Foster et al., 2002). The term "visual field" refers to the entire expanse of space one can see while fixating a central point. Any form of damage in the visual field impacts the quality of life (McKean-Cowdin R et al, 2008).

Glaucoma and its impact on the visual field:

Glaucomatous visual field loss occurs secondary to the loss of retinal nerve fibres because of the degenerative changes. Therefore, the visual field defects correspond to the anatomical disposition of the retinal nerve fibre layer (Garway-Heath et al., 2002). A typical glaucomatous visual field defect has traditionally been described as loss of vision at the outer edges i.e., 'peripheral vision'. Anecdotally, the subtle changes in the field of vision especially when it is at the periphery go unnoticed until it is progressed to advanced stages. However, any form of damage in the visual field has an impact on (outdoor)mobility, driving, reading, doing household chores and many day-to-day tasks which involve eye-hand coordination in turn challenging the state of mind (Popescu ML et al. 2012). The advanced stage of the irreversible visual field loss caused by glaucoma creates a 'tunnel vision' or as if "looking through a straw". Since visual field perception is a process which involves both the eyes, this perception of having 'tunnel vision' in real life under binocular condition is known to be a misnomer to both patients with visual field defect and clinicians. For patients with two functional eyes, if the visual field defect is present only in one eye or asymmetric, it is more likely to go unperceived at the early stages (Geroge, Ve, and Vijaya 2010). This can happen if the damage is restricted to only one of the overlapping regions of the visual field. Even if there are no overlapping regions this can be explained by the fact that either the brain is filling in 'missing parts' of the visual field or there is a combination of adaptation mechanism by the brain using head and eye movements (fig 1.3). The 'tipping point' of when the bilateral visual field damage becomes significant enough to cause disability is not well explored. The functional binocular visual field for a patient with glaucomatous visual field loss is still unexplored, especially in clinical practice. The current standard visual field test serves the purpose of monitoring and managing disease progression on a monocular basis yet, a more practical field test under binocular viewing

condition could address the questions about their visual status in terms of its impact on day-to-day life activities and quality of life.

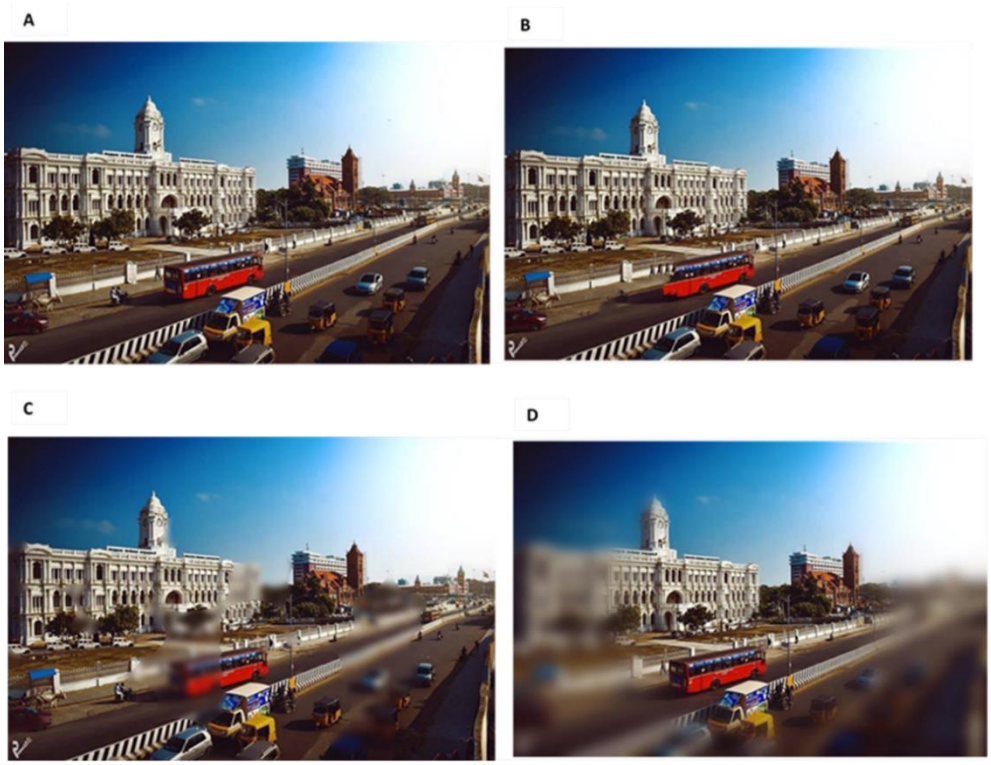

Figure 1.3: The image is from Chennai road scene, Panel A, is the scene perceived by an individual with normal vision. The image was then manipulated to create a speculated perception of patients with glaucomatous field defects. Panels B, C and D are based on the simulations of glaucomatous visual field defects at different stages of progression of the disease. The perception of visual field defects varies between patients.

New functional approaches to measure the extent and depth of the visual field

Over the past decades, efforts have been made to enhance glaucoma diagnostic techniques to improve early detection and to arrest the disease progression. Functional evaluation of the visual field has been the clinical standard for the detection and classification of glaucoma (Johnson, Wall, and Thompson 2011). In current ophthalmic practice, Standard Automated Perimetry (SAP) is the most widely used method

for testing the visual field and is regarded as the current clinical standard for assessing visual fields. The method, however, requires considerable patient co-operation in the form of maintaining steady fixation and suppressing reflex eye movements to perform the test reliably. Suppressing these reflexive eye movements causes discomfort and gives rise to complaints of fatigue from patients (Toepfer et al., 2008). The prolonged fixation requirement contradicts the natural urge of looking at newly appeared stimuli and thus often leads to unreliable test results. The complexity of performing an SAP test procedure raises interest in less demanding visual field tests addressing the drawbacks of the existing procedure.

In the 1980's the approach of testing visual field using reflex eye movements were reported by Jernigan ME (1980) and Trope (Trope, Eizenman, and Coyle 1989) where the key feature was to observe the participants eye movement while they were presented with peripheral targets during the visual field test. This procedure was named Eye Movement Perimetry (EMP). The advancements and availability of eye-tracking technology in the mid-1990s allowed the performance of visual field testing as well as quantification of eye movements objectively, first reported by Kim et al., (1995). This approach of testing the visual field allows the reflex eye movement as a test measure, thus making the task much easier and in turn also eliminates the false-positive calls. The EMP approach enables us to examine patient's interactions within the tested visual field under monocular as well as binocular viewing conditions.

In this thesis, I present an eye-tracking based approach that can assess 1) the extent of the visual field under monocular as well as under binocular viewing conditions and 2) the speed of the patient's response to the presented stimuli within the tested field of vision in terms of Saccadic Reaction Time (SRT). The measurements are primarily done in patients with glaucoma and healthy age-matched controls. The following chapter presents a brief overview of the pathophysiology and clinical manifestations of glaucoma. Next, the existing diagnostic methods for assessing visual field defects, their limitations, and the arguments for using an eye-tracking based

approach for assessing the visual field are explained. Finally, the aim of the thesis and the research questions are presented.

Pathophysiology of glaucoma and its impact on the visual field:

It was during the early 8th century BC when the use of the term '*glaukos'* was found in ancient Greek. It is thought that glaucoma is derived from the term *glaukos*, which described the colour of the pupil or clouded eye which might be a result of corneal oedema or mature cataract (Leffler et al., 2015; Stamper, Lieberman, & Drake., 2009). In the present era, the term 'glaucoma' refers to a panoply of diseases that share certain features including degeneration of the optic nerve head and corresponding functional loss especially in the form of visual field defects (Foster et al., 2002). Glaucoma is the leading cause of irreversible blindness worldwide affecting 64.3 million in 2013 and is predicted to increase to 111.8 million (~ 74%) in 2040 (Tham YC et al, 2014). Since the disease usually presents asymptomatically especially in the early stages, ~90% of those affected in the community remain unaware and undetected until the visual morbidity leads to disability (Weinreb RN et al., 2004; Foster PJ et al., 2002; George R et al., 2010). In terms of the global burden, the impact caused by Glaucoma is enormous. As the disease severity increases it affects health-related quality of life (HRQoL) and in many ways imposes a socioeconomic burden on the patient and on society (Tham et al., 2014; McKean-Cowdin et al., 2008).

Glaucoma is a progressive neurodegenerative disorder of heterogeneous aetiology. There are many schools of thoughts when it comes to the primary site of onset for glaucoma; is it in the eye or in the brain? Multiple theories have been put forward to explain the pathophysiology of glaucoma. They ultimately sum up that glaucoma leads to Retinal Ganglion Cell (RGC) axonal degeneration, which includes progressive loss of axonal transport (Quigley et al., 2000; Farkas & Grosskreutz, 2001). This progressive axonopathy of RGC's eventually leads to the death of retinal ganglion cells which in turn results in visual field defects. Until recently, intraocular pressure (IOP) was believed to be the major factor causing RGC death. The intraocular

pressure is regulated by the balance between aqueous humour secretion and drainage. In glaucoma treatment, IOP is the only modifiable risk factor in glaucoma (Sommer A, 1989). Treating elevated IOP often helps in slowing down the progression of glaucomatous degenerative changes. Since there are approx. 30-40% of patients who presents with visual field defects even with normal IOP [normal tension glaucoma] (Hendrickx et al., 1994), elevated IOP is now believed to be one of the multiple factors which trigger the degenerative changes. A new paradigm to explain glaucoma is emerging which is generating the possibilities of glaucoma as primarily a disease of the brain rather than an eye disease or a combination of both (Johnson, 2016). The heterogeneous nature of glaucoma has not been well understood and possibly there are subsets of the disease which show greater sensitivity to IOP and others where non-IOP factors impact neuronal degeneration.

The death or apoptosis of RGCs continues to be a major focus for the underlying causes of glaucomatous degeneration. Various theories have been proposed to explain the apoptosis of RGC's including vascular, biochemical, and mechanical factors that cause the deformation of the lamina cribrosa and ganglion cell axons (Jonas et al., 2017). These changes result in the apoptosis of ganglion cells secondary to blockage of axonal transport. Because the axons of RGCs stretch from the retina through the optic nerve to the brain, their neighbouring amacrine cells also become damaged by glaucomatous axonopathy. Additional theories suggest that the glaucomatous axonopathy extends along the entire visual pathway and not just RGCs axons (Frezzotti et al., 2014).

The retina is the major sensory membrane of the eye where the retinal ganglion cells transmit visual information from the photoreceptors to the optic nerve head. They are distributed across the entire retina (Fig 1.4). The glaucoma driven apoptosis of RGC's results in the form of structural changes that include thinning of the retinal nerve fibre layer and the neuroretinal rim along with degenerative changes in the optic nerve head which manifest functionally as defects [also known as scotomas] in the field of vision.

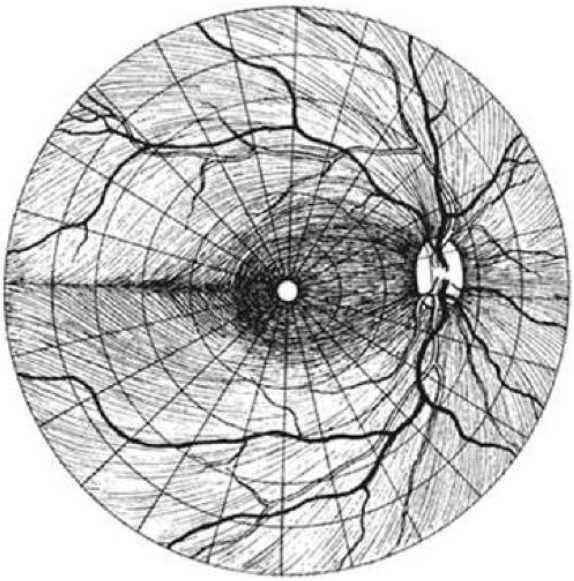

Figure 1.4: The retinal nerve fibre layer in the right eye. Damage to localized bundles of nerve fibres results in characteristic patterns of visual field loss in glaucoma. *(Harrington DO, Drake MV: The Visual Fields: Textbook and Atlas of Clinical Perimetry. St Louis, MO: Mosby, 1990.)*

Thus, any visual field defect due to glaucoma is secondary to structural changes in the retina. As mentioned, these defects are not very apparent at the early stages of glaucoma. Typical glaucomatous visual field defects often start to present with localised visual field loss and as the disease progresses the defects become deeper and enlarge, a process if left untreated could eventually lead to blindness. Assessing a patient's visual field provides essential information for diagnosing, staging, and monitoring the progression of glaucoma.

Visual field: Island of vision and measurement

The visual field is defined as the area in which objects can be detected while the eye is fixating on a point. The normal boundary of the visual field extends from 60 degrees nasally to approx. 100 degrees temporally, 60 degrees superiorly and 75 degrees inferiorly as depicted in fig.1.5 (Anderson & Patella, 1992).

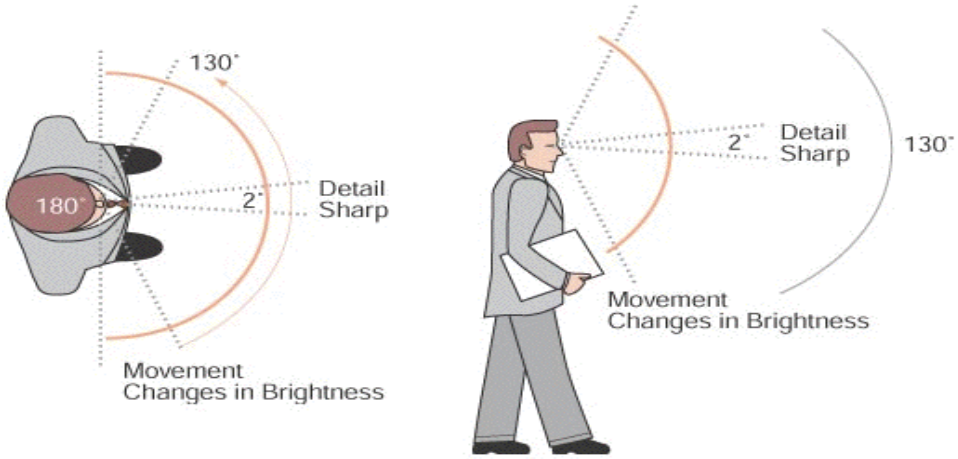

Figure 1.5: Diagram of horizontal and vertical visual field extents.

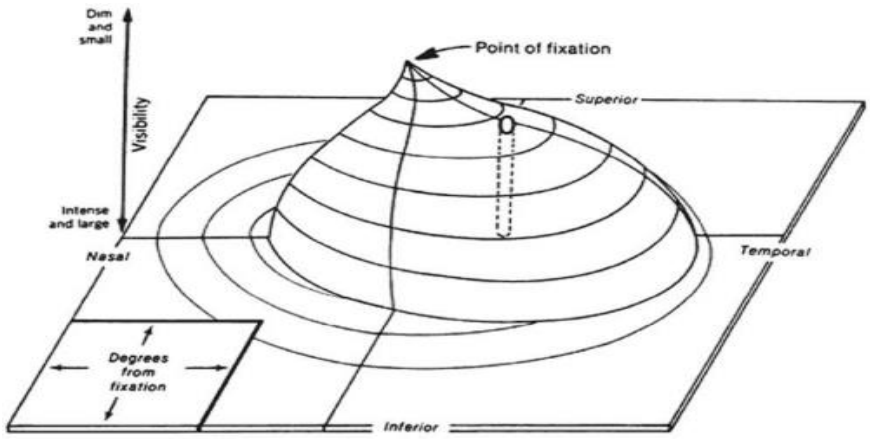

Figure 1.6: The normal island of vision. The hill is highest at fixation, where visual sensitivity is greatest. The height of the hill of vision declines toward the periphery as visual sensitivity diminishes. *(Anderson DR: Perimetry with and without Automation. 2nd ed. St Louis, MO: Mosby, 1987.)*

Traquair's analogy of the "island of vision" described the characteristics of the human visual field, where the central visual field has the highest visibility, and it decreases to the periphery (fig 1.6). The optic disc is approximately off centre by 15 degrees nasally for each eye when the eye is fixating on a point and this area corresponds to a physiological blind spot (Anderson & Patella, 1992). Neurodegenerative conditions like glaucoma, which affects the retina and other parts of the primary visual sensory pathway (which includes optic nerve, chiasm, optic tract, lateral geniculate bodies, geniculocalcrine radiations and the occipital cortex) alter the appearance of the 'island of vision'.

The importance of evaluating the visual field was understood a long time ago and it was around the late fifth century Before Common Era where the first recorded qualitative estimation of the visual field was found from Hippocrates. Though descriptions of the extent and the shape of the visual field were reported, it was in 1856 when the first measurements of the quantitative visual field were reported by Albrecht von Graefe. The technique of systematically assessing the visual field is known as 'perimetry'. The techniques of performing perimetry have been continually refined over the decades. The time consuming and highly operator dependent measurements of visual fields were revolutionised around 1970 with the automation of perimetry techniques (Johnson, Wall, and Thompson 2011).

The conventional approach of measuring a visual field and its limitations:

The Standard Automated Perimetry (SAP) is considered as the clinical standard of testing a visual field. This method is incorporated in a range of perimeters such as Humphrey (Zeiss Meditec, Dublin, California, USA), Octopus (Interzeag, Koeniz, Switzerland), Henson (Elektron, Cambridge, UK) field analyser and numerous other automated perimetry devices. At present times, the most used perimeters in the ophthalmology clinics across the globe are the Humphrey Field Analyzer (HFA) and Octopus. SAP measures the differential light sensitivity either by using a static or kinetic stimulus depending on the testing strategy used. Static SAP is the most used strategy in

ophthalmic clinics for diagnosing and monitoring visual field defect progression. In static testing, the SAP displays a series of achromatic light stimuli on a white background (white–on–white) in different standard test coordinates in the visual field. These established SAPs offer different testing strategies with different combinations for the number of test locations, stimulus size and extent of the tested visual field. Even though the perimeter has evolved over the past 200 decades, the traditional approach of testing the visual field has remained onerous and demanding. Conventional perimetry test requires a steady fixation throughout the course of testing by pressing a button on the perception of a stimulus (fig 1.7).

Figure 1.7: Patient performing visual field test in SAP (Humphrey field analyser). The head is stabilised using the forehead and chin rest of the machine to strictly control any head movements. The response button is held in the hand to press the button as soon as any stimulus is seen. An eye patch is visible which is used to occlude the non-tested eye. The patient's response and eye position can be viewed in real-time in the display.

Maintaining a steady central fixation for long durations with one eye can result in Ganzfeld blank out or Troxler's fading effect due to neural adaptation (Toepfer et al., 2008). This is experienced as disappearing

or fading of peripheral stimuli while fixating at a particular point for more than 20 seconds. It often leads to complaints by patients such as blurred vision, diplopia, inattention, discomfort, hallucination, and fatigue. This fixation requirement also suppresses the natural urge of the subject to look at new peripheral stimuli, further complicating an SAP measurement. Apart from the test procedure, the SAP also requires a skilled test instructor (perimetrist) for administering the test. This method of measuring the visual field has certain unavoidable limitations. Nevertheless, from a clinician's perspective, SAP is one of the important functional diagnostic tests which provides key information about a patient's visual field status as well as for monitoring the progression of any glaucomatous damage. Still, even experienced patients have reported that the visual field test is onerous and needs to be made easier (Glen, Baker, and Crabb 2014).

Current clinical diagnostics using SAP

The SAP by Humphrey Visual field Analyzer (HFA) is one of the most used perimeters in clinics worldwide. When a measurement is completed, the HFA provides different options for generating a clinical report. The 'Single field analysis' report (fig 1.8) is mostly used and consists of 8 different zones to systematically evaluate the outcome of the visual field test (Thomas & George 2001).

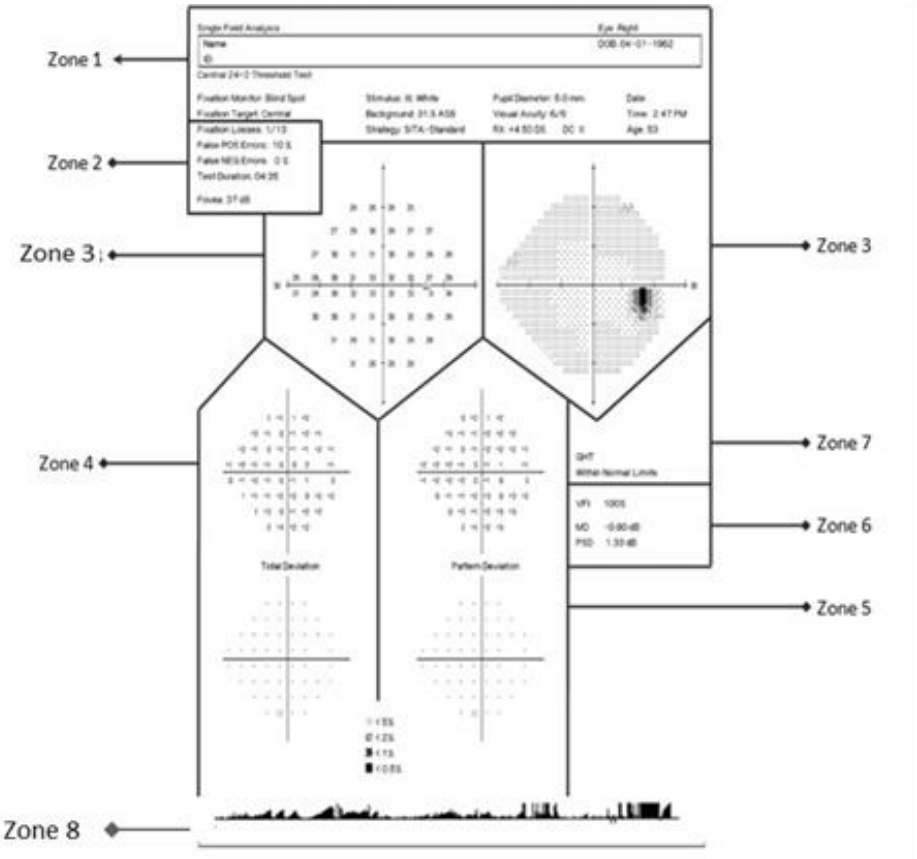

Figure 1.8: 'Single field analysis' report from HFA with marked zones within for systematic clinical interpretation

The zones contain the following information:

Zone 1: This zone documents the patient's demographic details i.e., name, date of birth, date of examination, pupil diameter, refractive error. Additionally, the test details such as test strategy and stimulus types are also mentioned here.

Zone 2: This zone includes information regarding the test reliability indices such as fixation losses, false positive and false negative responses, and test duration. In addition to these, it provides information about the foveal threshold (which is the sensitivity of the central part of the macula, this correlates with the visual acuity).

Zone 3: This zone represents the actual threshold value of the patient and the graphical representation of recorded threshold sensitivities, known as Greyscale plot. The areas of decreased sensitivities are displayed in darker tones. This plot is useful for educating a patient about her or his visual field status but not advisable to use for clinical interpretation.

Zone 4: The top panel in this zone represents the point-by-point deviation of the patient's threshold from those expected in age-matched normal subjects (from the machine's normative database). The bottom panel shows the flagged points that are depressed to a level seen in less than 5% of the normal age-matched population.

Zone 5: This zone represents the focal depression pertinent to glaucoma after adjusting the overall depression in the hill of vision that might be due to any diffuse medial opacities like cataract.

Zone 6: The values in this zone summarize the visual field when compared with normative limits. It includes Mean deviation of the overall visual field, pattern standard deviation (indicates the degree to which the numbers differ from each other) and visual field index (the global and staging index by aggregating the weighted percentage of visual function) are mentioned here, these are also known as global indices.

Zone 7: This index was added to the visual field report to be more precise about the focal visual field defect, which is pertaining to glaucoma. The visual field test grid was partitioned into ten sectors (five in the superior and five mirror sectors in the inferior hemi-field) as per the Retinal Nerve Fibre Layer anatomy. If the corresponding superior and inferior hemi-fields shows any difference compared with the normal population the field is flagged as outside normal limits.

Zone 8: This feature was introduced almost a decade back as an additional fixation monitor from the HFA II (model 740i-750i). Low-resolution real-time image analysis to verify the patient is looking at the fixation target and not looking around. This zone is optional. When the machine has a "gaze tracker', the trace shows whether the patient is fixating properly while the stimuli are presented. The deviation above

or below the horizontal line depicts the exact instances of saccadic deviation from the fixation. This approach is nowadays an advanced index monitoring fixation reliability. For older machines without the gaze tracking function, the fixation reliability was solely assessed using the Heijl-Krakau blind spot test. In this method, the test program would periodically present a stimulus in a patient's blind spot. With Reliable fixation we would not receive any response on blind spot projection if otherwise is calculated as fixation error.

Especially the information plotted in zones 4 and 5 provide important clinical details about the visual field status in terms of "depth" and "location" of the defect under monocular conditions. The depth of the defect tells us the clinical significance of the measured deviation from the normal population. This functional report aids clinical decision making for an ophthalmologist in deciding on the adequacy of treatment and the need for further investigations. This monocular approach is adequate for decision making on glaucoma progression. However, from a patient's perspective, a growing restriction of the visual field will also impact the actual field of view when performing activities of daily living (ADL), such as household tasks, reading and the ability to drive, take part in road traffic. Since these tasks involve binocular interactions, it is difficult for the ophthalmologist to address the impact of changes on these monocular tests on questions related to daily living activities. This remains a major limitation in current clinical visual field-testing strategies. To date, Humphrey's Esterman visual field test (HEVF) test is the most common binocular visual field test used to estimate functional visual field, but the main drawback of this test is its binary outcome (Esterman, 1982). The HEVF estimates visual field only as 'seen' and 'unseen' whereas the information on the depth of defect for binocular visual field remains unanswered. It is possible to construct a binocular visual field based on two monocular visual field reports, either on visual inspection or with the help of simulation software to calculate the total field of view of both eyes (Crabb & Viswanathan, 2005). Although this approach is quick to provide the view of functional binocular visual field testing its clinical validity remains impossible. None of these techniques are clinically successful and thus the gap in estimating the real-life functional binocular visual

field of a patient with glaucomatous visual field defect remains unanswered to date.

Demand for alternative perimetry approaches

Over the years, many attempts have been made towards modernising the perimetry test with the main emphasis on simplifying test administration and performance strategies. A few notable attempts for modernising visual field test include Pupil perimetry, Damato multifixation campimetry and Rarebit Perimetry (Kardon, 1992; Chen et al., 2008; Olsen et al., 2016; Brusini, P., et al., 2005). Even though these non-conventional devices were constructed with the aim of making the visual field test less onerous either by reducing the test duration or reduced involvement of the subject's perceptual performance, yet these have not become a part of routine clinical diagnostics. Eliminating the reason behind the major discomfort of performing the visual field test i.e., maintaining constant accurate fixation and suppressing the reflexive eye movement while performing the test would improve patient comfort. The making of an eye movement to a newly appearing object is part of the natural oculomotor response of the visual system. Restricting the reflexive eye movement to such "triggers" contradicts the innate oculomotor response and therefore requires a higher level of attention. The unnatural set-up of controlling reflexive eye movements and pressing a button on perceiving a new peripheral target sets is not physiological and eventually leads to inattention and fatigue of the subject thus indirectly affecting the reliability of the test results. The reason these non-conventional perimetry techniques cannot provide a solution can be due to the complexity of the test strategy, the inability to provide quantitative assessment and above all the precision of the test report for clinical interpretation.

In the modern era of perimetry, despite being onerous to perform SAPs (HFA & Octopus) provide adequate information about the test results for clinical interpretation (for e.g., Fig 1.8) without which the management of glaucoma is almost impossible. Combination of ease

of performance with a quantitative precise perimetry result might be able to address the current limitations associated with the SAPs.

An eye-tracking based approach to measure the extent of the visual field

The approach of testing the visual field in this thesis is based on eye movement responses. This approach was introduced during the 1980s by Jernigan where the eye movement responses were used as an index of perception of visual field testing (Jernigan 1980). Jernigan customised an eye movement monitor to record the horizontal and vertical responses during the test. Later, the integration of eye tracking as a method to record eye movement responses improved the method's objectivity. With the increased availability of accessible remote eye-tracking systems, this perimetric procedure of permitting eye movements has been explored in both children and adults (Pel et al., 2013; Murray et al., 2009; Satgunam et al., 2017). Application of high-resolution video-based eye trackers in synchronisation with HFA was reported by Kim et al., (1995) to test the visual field. This was coined as an Eye Movement Perimetry (EMP). The EMP by Kim et al., generated results using a decision algorithm and classified each response as 'seen' or 'unseen'. The visual field reports with eye movement responses were comparable to that of SAP for detecting visual field defects. Computer Assisted Moving Eye Perimeter (CAMEC) reported by Toepfer et al., (2008) is one among the approaches of visual field testing with moving fixation stimuli which showed comparable test results with SAP. Promising eye movement perimetry results were also reported in both children and adults by Murray et al., (2009), using Saccadic Vector Optokinetic Perimetry (SVOP). The reflexive saccadic eye movements were used by SVOP as an index for plotting the extent of the visual field. Visual field-testing using eye movements was reported to be consistent in discriminating normal and abnormal visual fields based on binary responses from subjects, i.e., seen, or unseen (Murray et al., 2017). Despite these promising results, no effort was made in the quantification of a visual field test report to assist clinical diagnosis and/or disease monitoring.

Towards an accessible, adaptable, and intuitive solution in visual field testing

The eye-tracking based approach to measure the extent of the visual field based on eye movements was adopted in 2011 by the vestibular and oculomotor research group (Dept. of Neuroscience, Erasmus MC) with a focus on clinical applicability. Here, a start was made to determine the timing of the Saccadic Eye Movement towards a seen stimulus, also known as the Saccadic Reaction Time (SRT). In a first publication, the authors showed good repeatability within healthy subjects and an average difference between measurements of 100 ms (Pel et al., 2013). Next, they integrated an SAP grid. In this paradigm, stimuli were plotted at 54 locations analogous to that of 24-2 test co-ordinates of Humphrey Field Analyser (HFA) at four levels of varying stimulus intensity. The peripheral stimulus of ~0.5 degrees (Goldman size III) was projected at random grid locations for a fixed duration of 1200 milliseconds with a gap of 0.2 seconds between stimulus presentations, with the fixation stimulus lit, i.e., an overlap paradigm. Subjects were encouraged to look at the visual stimulus detected peripherally and then re-fixate the fixation stimulus. Hence, the detected peripheral stimuli in the visual field resulted in normal reflexive eye movements. These eye movement responses were recorded using a remote non-invasive infra-red based eye-tracking system. Using a decision algorithm based on previously reported structural eye movement analysis the gaze data was classified as ‘seen’, ‘unseen’ or ‘invalid’. Additionally, for each of the ‘seen’ stimulus, the eye movement responses were quantified as Saccadic Reaction Time (SRT). The SRT was calculated as the time difference between stimulus presentation and the onset of the saccadic eye movements towards the presented stimulus. This approach of testing visual fields was published in 2013 (Pel et al., 2013). These findings served as the basis for extending its use to detect the areas of the visual fields at risk that can be the result of degenerative conditions.

The work described in this thesis is based on an international collaboration project on the application of affordable health between India and The Netherlands (the Netherlands Organization for Health

Research and Development (ZonMW), grant no.116310001 and the Department of Science and Technology, Government of India' [DST/INT/NL/Biomed/P (2)/2011(G)]). The collaborating institutes were: Medical Research Foundation Sankara Nethralaya, Chennai, India and Rotterdam Eye Hospital and Vestibular and Oculomotor research group, Department of Neuroscience, Erasmus MC, Rotterdam, The Netherlands.

Aim of this thesis

The aim of this thesis was to evaluate the clinical applicability of assessing the extent and the responsiveness of the visual field in glaucoma patients using Eye Movement Perimetry.

The study population and study design

The clinical measurements reported in this thesis were mainly executed at the Sankara Nethralaya, Chennai, a tertiary eye care centre in India. The study population comprised of volunteers (students/employees/family members of patients) and glaucoma patients from the outpatient clinic. Each participant underwent a complete ophthalmic examination and those who met the following eligibility criteria were included in the study:

a) Spherical ametropia less than ±5.00Dsph and cylindrical ametropia of less than -2.00Dsph,

b) Best Corrected Visual Acuity more than 20/40, 0.8M,

c) Intra Ocular Pressure less than 21mmHg,

d) Presence of sign of Retinal Nerve Fibre Layer changes or any abnormality on Optic Nerve Head, any history of ocular surgery or any retinal pathology were excluded.

e) Presence of ophthalmic conditions (e.g., oculomotor nerve palsy, corneal opacity, and ptosis) which might affect the eye-tracking were excluded.

Glaucoma patients were clinically classified based on the International Society of Geographical and Epidemiologic Ophthalmology (ISGEO) (Foster et al., 2002). The diagnosis of glaucoma was confirmed if the individuals were presented with specific glaucoma related damages such as:

a) An increased vertical Cup – Disc Ratio (VCDR) asymmetry > 0.2,

b) Focal or diffuse thinning of the Neuro Retinal Rim (NRR), Localized notching, disc haemorrhages, Retinal Nerve Fibre Layer (RNFL) defect with corresponding visual field changes on SITA standard HVF 24-2 protocol.

c) Glaucoma patients were defined and classified into mild, moderate, and severe glaucoma based on disease severity assessed using visual field reports based on Hodapp, Parrish and Anderson's classification (Brusini & Johnson, 2007).

Eligible subjects were informed about the test and requested to participate after informed consent. Each participant (both healthy controls and glaucoma) underwent visual field testing on the HFA [II 750, Carl Zeiss Meditec Inc, Dublin, CA, USA] and subjects with reliable normal visual field were included. The reliability of the visual field test was assessed following the recommendation of the STATPAC algorithm by Anderson & Patella (1999). Data from the healthy controls were used to generate normal reference values for visual field test locations. Data of the glaucoma patients were used to explore the diagnostic and clinical applicability. This study had a cross-sectional descriptive design and the study adhered to the Declaration of Helsinki for research involving human subjects (2003).

Main objective and research questions

There are certain mandatory features that need to be considered while investigating the clinical applicability of a perimetry device. Here, for this research, we have used conventional SAP as the clinical standard.

First, the following two research questions were addressed in chapter 2 , 3 and 4:

- What is the effect of the severity of glaucoma on Saccadic Reaction Time?
- What factors influence the Saccadic Reaction Time in a normal ageing population?

- Does Saccadic Reaction Time in Eye Movement Perimetry different between Dutch and Indian counterparts

To further explore the diagnostic basis of EMP, a quantitative comparison of an individual's test result with those of a population with the normal visual function must be provided. SAP uses indices such as Mean deviation and Total deviation (see, fig 8, Zone 4 & 6) to interpret the visual field defect severity against an age-matched normative group. To obtain a similar approach in EMP, the results of chapter 3 were adopted to construct a normative database of SRT that allowed me to answer these two research questions addressed in chapter 5:

- Are delays in SRT values significantly different between patients with glaucoma and healthy controls when corrected for age?
- What is the validity of Eye movement Perimetry compared to the conventional SAP?

Unlike glaucoma, visual field sensitivity losses produced by ocular or neurologic pathology can be diffuse, localised or a combination of both. SAP provides an extra diagnostic criterion to confirm that the visual field loss is the result of glaucomatous damage and not of another ocular or neurological pathology. This criterion is called the GHT index (see fig 8, zone 7), and this index is based on the retinal nerve fibre layer arrangements. To test whether a similar approach would be feasible in EMP, the following question was addressed in chapter 6:

- How sensitive are SRTs of Hemi field sectors in detecting glaucomatous visual field defects on Eye Movement Perimetry?

As mentioned, the use of Eye Movement Perimetry opens the possibility of assessing monocular as well as binocular visual fields, in terms of the extent of the tested field as well as its responsiveness. The impact that glaucoma has on binocular vision is still not well explored. The functional binocular visual field deficits may provide clinicians with useful diagnostic clues used for helping patients with ADLs and monitoring of visual field deficits. Here, we addressed the final two fundamental questions in chapter 7:

- What is the difference between monocular and binocular SRT values?
- What are the differences in SRTs between glaucoma patients and healthy controls assessed under binocular viewing conditions?

CHAPTER 2

COMPARISON OF SRT BETWEEN NORMAL AND GLAUCOMA USING AN EYE MOVEMENT PERIMETER

Deepmala Mazumdar[1,2,3], JJM Pel[4], Manish Panday[1], Rashima Asokan[1,2,3], L Vijaya[1], B Shantha [1], Ronnie George[1], J van der Steen[4]

[1]Department of Glaucoma, Medical and Vision Research Foundation, Chennai, India
[2]Elite School of Optometry, Chennai, India
[3]Birla Institute of Technology and Science, Pilani, Rajasthan, India
[4]Erasmus MC, dept. Neuroscience

Adapted from: Indian Journal of Ophthalmology, 2014, Jan;62(1):55-9.
DOI: 10.4103/0301-4738.126182

Abstract:

Aim: To compare the saccadic reaction time (SRT) in both the central and peripheral visual field in normal and glaucomatous eyes using eye movement perimetry (EMP).

Materials and Methods: Fifty-four normal and 25 glaucoma subjects underwent EMP and visual field testing on the Humphrey Field Analyser (HFA) 24-2 program. The EMP is based on infrared tracking of the corneal reflex. Fifty-four test locations corresponding to the locations on the 24-2 HFA program were tested. SRTs at different eccentricities and for different severities of glaucoma were compared between normal and glaucoma subjects.

Results: Mean SRT was calculated for both normal and glaucoma subjects. Mann-Whitney U test showed statistically significant ($P < 0.001$) differences in SRT's between normal and glaucoma subjects in all zones.

Conclusion: SRT was prolonged in eyes with glaucoma across different eccentricities.

Introduction

Glaucoma is the second leading cause of blindness worldwide (George, Ve, and Vijaya 2010; Quigley and Broman, 2006). It is a progressive optic neuropathy that starts with damage to the retinal ganglion cell (Quigley et al., 2000; Foster et al., 2002). Ganglion cell damage or loss is clinically assessed by measuring visual thresholds (Foster et al., 2002). Standard automated perimetry (SAP) is currently the most common and frequently used diagnostic procedure to assess visual field damage. SAP is based on human perceptual performance. During SAP, the subject is required to maintain fixation on the central fixation stimulus while visual stimuli of varying light intensities are presented for a brief period of time in the peripheral visual field. The subject is required to acknowledge seeing the stimulus by pressing a button. The weakest intensities perceived are used to produce the visual sensitivity threshold plot. SAP requires a high level of cooperation, attention, and effort from the subject to maintain central fixation throughout the test and suppress the tendency to make reflexive eye movements each time a new peripheral visual stimulus is presented. Since the test result is based on human performance discomfort, anxiety, fatigue can compromise the reliability of the result (Heijl, Lindgren, and Olsson, 1989; Wild et al., 1989; Toepfer et al., 2008).

Eye Movement Perimetry (EMP) measures saccadic eye movement towards the presented target, using these responses to map the visual field, without inhibiting the reflexive response of oculomotor control system (Jernigan et al., 1989; Kim et al., 1995).

The EMP algorithm measures a saccade as “seen or not seen. In addition, the Saccadic Reaction Time (SRT), the time taken to process visual information and to activate the ocular motor system, is also measured. The SRT is used to plot the visual threshold on the visual field (Jernigan et al., 1989; Kim et al., 1995; Trope, Eizenman, and Coyle 1989).

Saccades are affected in various optic nerve diseases (Brigell, Goodwiaf, and Lorance, 1998; Reulen, 1984). Delayed saccadic latency has been reported in optic nerve conditions such as optic

neuritis and glaucoma (Trope, Eizenman, and Coyle 1989). Kanjee et al., (2012) and Lamirel et al., (2014) have reported that there is a delay in saccadic eye movement initiation in glaucomatous optic neuropathy. In both mild and advanced glaucoma there is an increase in saccadic reaction time compared to normal (Kanjee et al., 2012; Lamirel et al., 2014). Most existing studies have shown the behaviour of saccades in the central visual field. There is little published literature on peripheral saccades.

We report the SRTs in both the central and peripheral field in normal and glaucomatous eyes using EMP.

Materials and Methods

Participants

Normal subjects aged between 30 and 70 years were recruited for the study. The participants were recruited from the patients seen in the outpatient clinic of our hospital and volunteers. Written informed consent was obtained from each participant. Each subject underwent a complete ophthalmic eye examination and subjects with spherical ametropia greater than ±5.00 dioptre sphere (Dsph) and / or cylindrical ametropia of more than -2.00Dsph, best-corrected visual acuity less than 20/40, N6, presence of strabismus, amblyopia, any oculomotor restriction, nystagmus, nerve palsy, pupil size less than 3mm, lens opacities more than N2, C1, P1 based on LOCS II, (Chylack et.al., 1989) any history of ocular surgery or any retinal pathology were excluded.

Subjects with glaucoma were recruited from the outpatient glaucoma clinic of the same hospital. Subjects with Primary open-angle or angle-closure glaucoma who had glaucomatous optic disc changes and corresponding reliable, repeatable visual field defects on SAP (Humphrey Field Analyzer (HFA)) (model 750; Carl Zeiss Meditec) were included. Reliability criteria were as recommended by the instrument's algorithm (fixation loss, <20%; false-positive and false-negative, <33%). Subjects with glaucoma were also classified into early, moderate, and severe defects based on visual field defect meeting Hodapp, Parrish and Anderson's classification (Brusini and Johnson,

2007). The experimental procedures were reviewed and approved by the Institutional Review Board and Medical Ethics Committee of Vision Research Foundation, Chennai.

Instrument description and procedure

The EMP setup comprised of a laptop, a 17-inch monitor with an in-built eye-tracking device with a refresh rate of 120Hz (Tobii120, ELO Intellitouch system). The eye tracking device works on the principle of corneal-reflection tracking. Fig. 2.1 shows EMP display screen showing the tracking status.

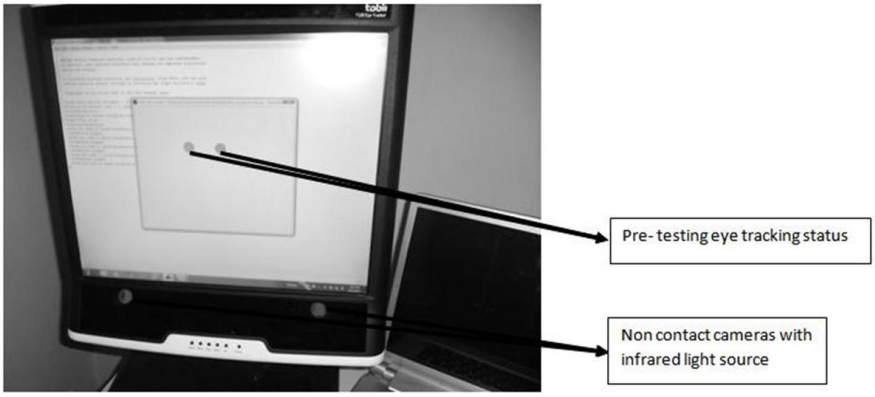

Figure 2.1: Eye movement perimeter display screen showing the tracking status for both eyes

Subjects were instructed to place their chin on a chinrest placed at a 60 cm distance from the monitor. No refractive correction was used while performing the test. The test was performed monocularly. However, since it is necessary for the eye tracker to perceive both the eyes in order to maintain accurate gaze, the non-tested eye was covered with a polymethyl methacrylate (PMMA) blocker which allows only infrared rays to be transmitted. This allows monitoring of both eyes simultaneously by the gaze tracker without the stimuli on the screen being visible. Figure 2.2 shows the testing setup of EMP.

Each measurement started with a nine-point calibration procedure, which involves following a circular blue coloured stimulus that moves at 15-degree angle up, down, left, and right from the centre of the

display screen. This procedure is necessary to obtain accurate gaze data.

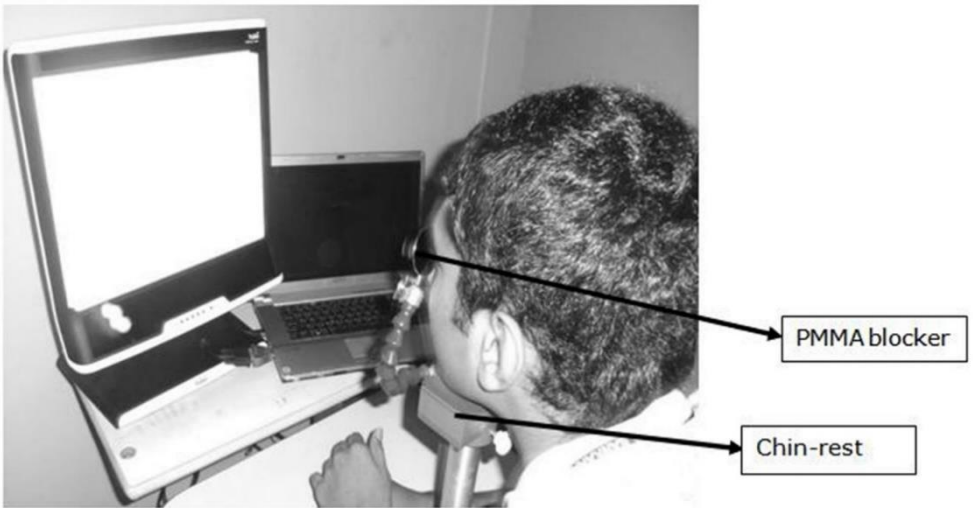

Figure 2.2: Eye movement perimeter setup used for the study

After calibration, the test began with a central fixation stimulus displayed on the centre of the screen. Fifty-four points were tested in the visual field at four different contrast levels against the background illumination of 140cd/m^2. Thus, the total number of points tested was 216. By using eccentric positions of the central target, the maximum visual angles were extended up to 27 degrees in horizontal and 21 degrees in the vertical direction. Overall, a visual field of a total of 54 x 42 degrees (horizontal x vertical) was tested.
At each location, four similar stimuli varying in brightness levels were plotted: 70% brightness (150cd/m^2), 80% brightness (162cd/m^2), 90% brightness (175cd/m^2) and 100% brightness (190cd/m^2). These different levels are denoted as increasing contrast levels 0.7, 0.8, 0.9 and 1.0. The locations tested in EMP exactly resemble the visual location tested in the 24-2 SITA standard strategy of automated HFA. Visual targets used during the test were of Goldmann size III (0.43 degrees angular diameter).

Subjects were asked to fixate on the central stimulus. Next, the peripheral stimuli were randomly presented one by one for a maximum

duration of 1.2 s with a gap of 0.2 s between stimuli. The subjects were encouraged to look at each visual target on detection and then return to the fixation target. Instructions were given to avoid searching for stimuli. Saccadic response at each of the 216 gaze data points of each subject were visually inspected and analysed using customised software.

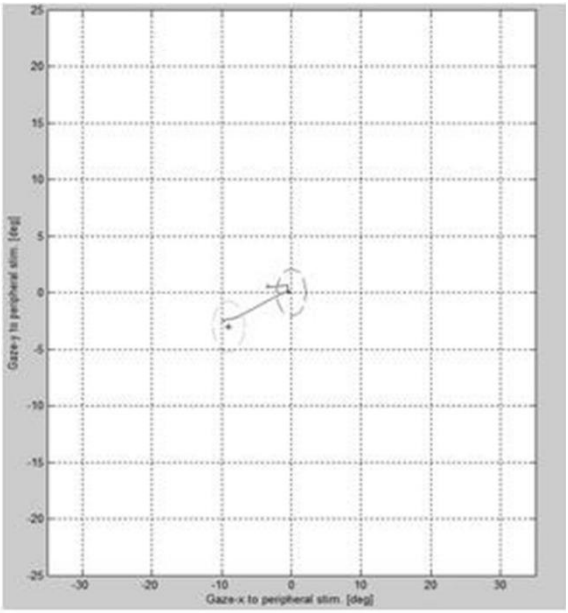

Figure 2.3: Eye movement pattern in a Matlab window where a saccadic eye movement was made from the centre towards a peripheral target in the lower left field

To analyse gaze data a decision algorithm was developed which classified each stimulus as ‘seen’ or ‘not seen’ depending on the eye movement pattern. This decision algorithm was based on a previously reported study on structural eye movement analysis (Jernigan 1980; Pel et al., 2013) An event was classified as ‘unseen’ if, during the presentation of the peripheral target, no eye movements were made towards the target, or the first saccade was not in the direction of the target. The event was labelled as ‘unknown’ when no eye movement data were available due to blinking or pupil detection failure. Events where clear saccadic movements were made towards the presented

visual target were considered as ‘seen’. Fig. 2.3 shows the eye movement pattern in the Matlab window where eye movement starting in the centre was made towards the peripheral target in the lower left field. For each ‘seen’ target the SRT was calculated as the time difference between stimulus presentation and the onset of the saccadic eye movement to the target. Fig. 2.4 illustrates the calculation of SRT corresponding gaze velocity.

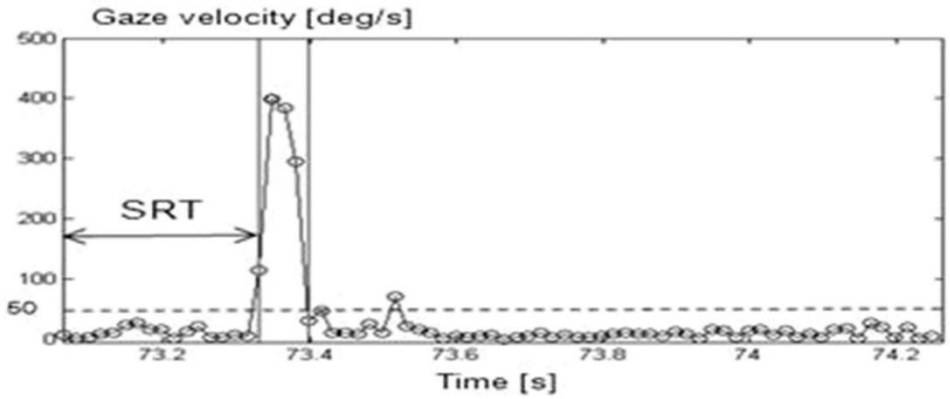

Figure 2.4: Measurement of saccadic reaction time from tracking data

Statistical analysis was carried out with SPSS 15.0 version (Statistical Package for Social Sciences Inc.) and MS Excel 2007. We used responses at Contrast Level 0.8 (162cd/m^2) and only the right eye for statistical analyses. SRT was converted to milliseconds. Since the SRT data was of wide range therefore for ease of analysis the data were transformed to Log_{10}. Tests for Normality were carried out for each quantitative variable and appropriate parametric/non-parametric analyses were utilized. Type I error was kept at a 5% level.

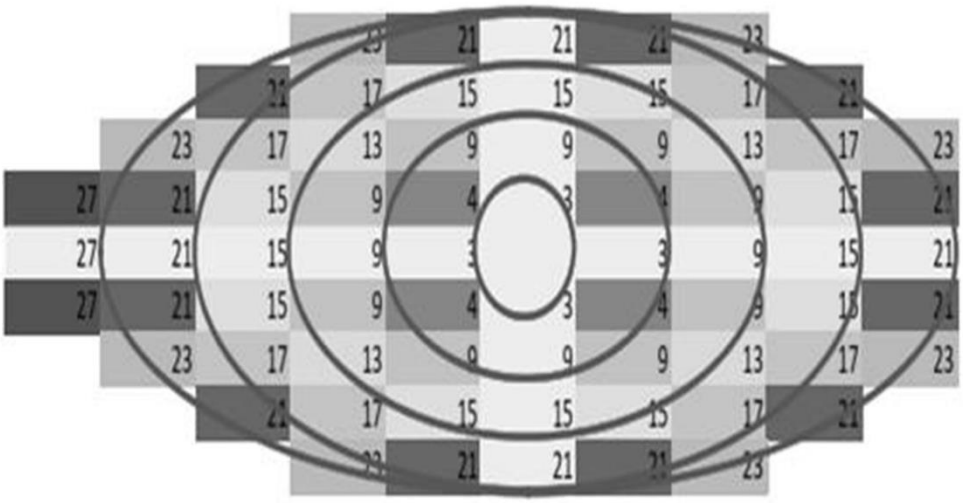

Figure 2.5: Division of tested points into eight zones equidistant from the centre

The stimulus locations were clustered and divided into different zones considering equal distances from the central stimulus. Calculating stimulus locations that are equidistant from the central fixation point eight zones were identified. Fig. 2.5 represents the zonal divisions of the tested field of vision.

Results

A total of 79 subjects were recruited in the study which included 54 normal and 25 glaucoma subjects. The demographic details of the subjects recruited are given in Table 2.1. Mean SRTs was found significantly longer in the glaucomatous eye in each age cohort (Table 2.2).

Table2.1: Demographics of the study population

Subject characteristics	**Normal (n=54)**	**Glaucoma (n=25)**
Age range (in years)	30-70	30-70
Mean age (SD)	42.0±13.3	54.2±11.6
Gender (in percentage)	Male-53.52%, Female- 46.48%	Male-66.7%, Female-33.30%

Table 2.2: Global mean SRT between normal and glaucoma

SRT* (Mean ± Std deviation) (in milliseconds)			
Age (in years)	**Normal**	**Glaucoma**	**p value**
30-39	597±200	767±246	0.01
40-49	606±249	834±279	0.04
50 and above	674±288	934±307	0.02

*SRT, Saccadic Reaction Time

When SRTs were compared across each of the eight zones classified based on eccentricity the difference between the normal and glaucoma was significant (Table 2.3 and Fig.2.6) with glaucomatous eyes having longer SRT as compared to normal.

Table 2.3: Mean SRT in normal and Glaucoma in all eight zones for contrast level 0.8

Eccentricity	SRT* (in milliseconds) in Normal			SRT* (in milliseconds) in Glaucoma		
	Mean ± SD	95 % CI¥		Mean ± SD	95 % CI¥	
		Lower limit	Upper limit		Lower limit	Upper limit
zone1	380±282	336	426	480±378	408	553
zone2	420±269	395	445	546±377	496	597
zone3	467±268	436	500	656±361	608	705
zone4	480±287	448	513	781±346	719	844
zone5	520±238	492	549	816±345	770	862
zone6	598±268	573	624	874±339	834	914
zone7	641±259	612	672	937±330	892	983
zone8	756±288	692	822	1100±242	1053	1147

*SRT, Saccadic Reaction Time; ¥CI, Confidence Interval

A trend towards increasing SRTs with increasing disease severity was also noted when SRT was compared with mild, moderate, and severe glaucoma. This difference with the increasing severity of glaucoma was also apparent for the different eccentricities (Fig. 2.7).

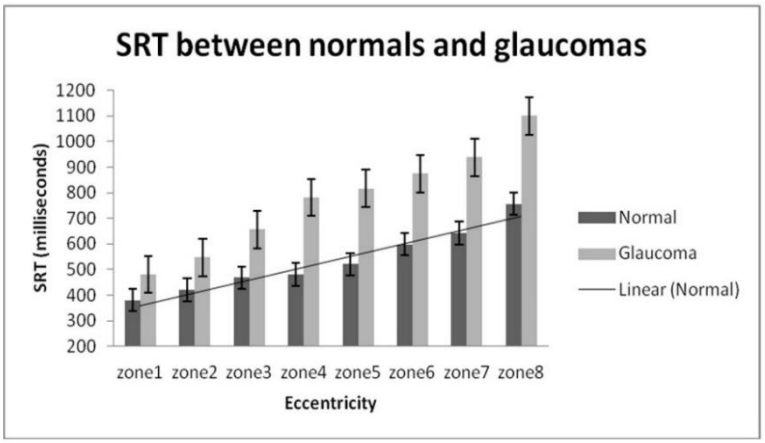

Figure 2.6: Comparison of saccadic reaction times between normal and glaucoma at varying eccentricities (mean, error bars show standard errors)

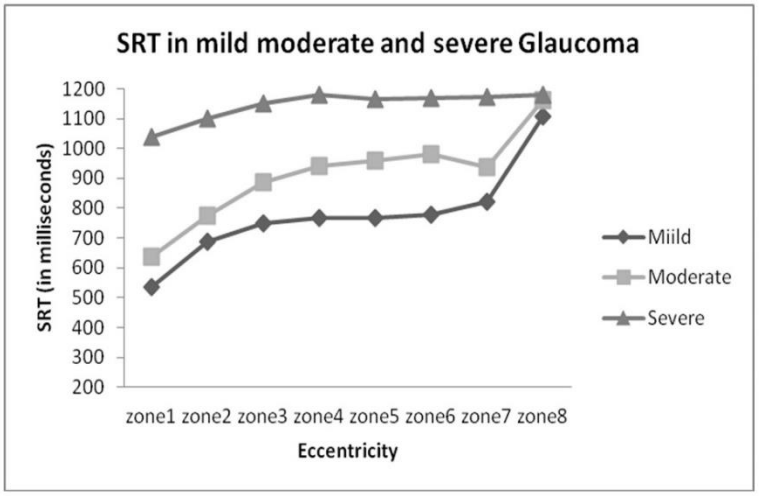

Figure 2.7: Mean SRT in mild, moderate, and severe glaucoma at different eccentricities

Discussion

The EMP has been evaluated as a potential device to test for glaucomatous visual field damage in the past. Kim *et al.,* (1995) had reported consistency of seen/unseen responses on EMP compared with SAP. They reported good concordance in a group of nine subjects with glaucomatous field damage and 10 normal. Murray *et al.,* (2009)

studied the ability of EMP to detect visual field defects. They tested locations based on the HFA C-40 test using a suprathreshold test strategy and reported excellent concordance with SAP suprathreshold results with the percentages of points in agreement ranged between 90 and 99%. In a pilot study Pel *et al*., (ARVO 2012, abstract no. 4812) showed that visual field sensitivity assessed with SAP correlated with visual field responsiveness assessed with EMP.

SRTs have been reported to be altered in glaucoma. Lamirel *et al*., (2014) compared eight Primary open-angle glaucoma (POAG) and four normal controls. They reported increased SRT values in glaucomatous eyes. However, points till only 7 degrees of eccentricity were tested. Kanjee *et al*., (2012) tested 16 glaucomatous and 21 normal eyes up to 10 degrees of eccentricity. Median SRT values were significantly increased in glaucomatous eyes as well as a decrease in the number of express saccades in this group. In this report, we found significantly increased SRT values compared to normal eyes. This was consistent across different eccentricities based on the HFA 24-2 test locations. This has important implications for EMP testing in glaucoma since detection of peripherally affected points is important for any perimetric test in glaucoma. SRT values also showed differences across different severity of glaucoma with increasing SRTs being seen with worsening glaucomatous severity. This is again consistent with Lamirel *et al.,* (2014) who reported that SRT values were increased among moderate glaucoma as compared to those with pre-perimetric disease.

EMP allows natural ocular motor eye movements on perceiving of a stimulus and continuous monitoring of eye movements, which eliminates false-positive calls and hence improving test precision. Kim *et al*., (1995) reported that subjects reported alleviation of some of the stress and tedium associated with SAP. Our own (anecdotal) experience was the same with most subjects being more comfortable with EMP testing despite the increased testing times.

Since the entire range of thresholds on SAP cannot be reproduced using a single contrast level on EMP we tested at four contrast levels. For this analysis only the 0.8 contrast level was used. While using all four contrast levels may help discriminate between small threshold

variations even testing at a single contrast level could help discriminate between different severities of glaucoma.

Our study demonstrates that SRT values show significant differences in glaucomatous eyes. However, the creation of age-specific normative databases will be required to classify individual locations as diseased. In addition, test duration would have to be shortened and a wider threshold would need to be tested for full comparison with SAP. While the test eliminates the need for testing for false positives an algorithm for testing false negatives would be required. Plotting visual field using reflexive eye movement might reduce the factors affecting visual field test results. SRTs in glaucoma provides one more parameter that can be suggestive of glaucomatous damage on perimetry.

Conclusion

SRTs are significantly increased in glaucoma subjects across the tested field of vision. This combined with the technique of test administration makes EMP a promising candidate for assessing visual field defects in glaucomatous eyes. Further studies are needed to collect a normative database for the test and to investigate the influence of contrast levels of the presented stimulus on saccadic reaction time.

Acknowledgment

Authors thank the 'Department of Science and Technology, Government of India' [DST/INT/NL/Biomed/P (2)/2011(G)] and 'Netherlands Organization for Scientific Research' (NOW) for their financial support.

CHAPTER 3

EFFECT OF AGE, SEX, STIMULUS INTENSITY, AND ECCENTRICITY ON SACCADIC REACTION TIME IN EYE MOVEMENT PERIMETRY

Deepmala Mazumdar[1,2], Najiya S. Kadavath Meethal[1,2], Manish Panday[2], Rashima Asokan[2,3], Gijs Thepass[1], Ronnie J. George[2], Johannes van der Steen[1,4], JJM Pel[1]

[1] Vestibular and Ocular Motor Research Group, Department of Neuroscience, Erasmus MC, the Netherlands
[2] Medical and Vision Research Foundation, Chennai, India
[3] Elite School of Optometry, Chennai, India
[4] Royal Dutch Visio, Huizen, the Netherlands

Adapted from: Translational Vision Science & Technology. 2019 Jul 30;8(4):13. DOI: 10.1167/tvst.8.4.13

Abstract

Purpose: In an eye movement perimetry (EMP), the extent of the visual field is tested by assessing the saccades using an eye tracker. The aim of the present study was to determine the effects of age and sex of the subjects, the eccentricity and intensity of the peripheral stimuli on saccadic reaction time (SRT), and the interaction between these parameters in healthy participants.

Methods: Healthy participants aged between 20 to 70 years underwent a complete ophthalmic examination and an EMP test. SRT was determined from detected peripheral stimuli of four intensity levels. A multilevel mixed-model analysis was used to verify the influence of subject and stimulus characteristics on SRT within the tested visual field.

Results: Ninety-five subjects (mean age 43.0 [15.0] years) were included. Age, stimulus intensity, and eccentricity had a statistically significant effect on SRT, not sex. SRTs were significantly faster with increasing stimulus intensity and decreasing eccentricity ($P<0.001$). At the lowest stimulus intensity of 192 cd/m^2, a significant interaction was found between age and eccentricity.

Conclusions: The current study demonstrated significant SRT dependence across the visual field measured up to 27^0, irrespective of sex. The presented SRT values may serve as the first normative guide for EMP.

Translational Relevance: This report of SRT interaction can aid in refining its use as a measure of visual field responsiveness.

Introduction

The sudden appearance of visual targets or any other features of interest in the peripheral visual field stimulates a cascade of events starting with a change in retinal activity. If not suppressed, this can eventually lead to ballistic eye movements known as saccadic eye movements (SEM) (Bahill & Troost, 1979). Parasol cells, which are a subset of retinal ganglion cells (RGCs), provide input for this cascade of events (Darrien et al., 2001). Spatial information from the retina is subsequently encoded in a saccade generation network located in the cerebral cortex, thalamus, basal ganglia, cerebellum, superior colliculus (SC), and brainstem areas that maintain the spatial coding of the target with respect to the fovea (Wurtz & Optican, 1994). This complex circuit then activates extraocular motor neurons to break fixation of the current target of interest and to make adequate SEM to align the fovea with the new visual target of interest (Fleuriet & Goffart, 2012).

Eye-tracking technology offers several methods for the qualitative (i.e., visual inspection) and quantitative evaluation (i.e., calculate saccadic properties) of SEM. Important parameters are saccadic reaction time (SRT), saccade velocity, amplitude, and duration (Kanjee et al., 2012). Various studies have reported alterations in SEM parameters in patients on psychotropic drugs and in various neurologic diseases, such as Parkinson's disease, Alzheimer's disease, as well as in optic nerve pathologies and glaucoma (Kanjee et al., 2012; Lamriel et al., 2014; Smith, Glen, and Crabb, 2012; Asfaw et al., 2018; Crabb et al., 2010; Kim et al., 1995; Murray et al., 2009). This change in ocular dynamics led to the use of saccadic parameters as a marker for evaluating the integrity of saccade generating neural network and in the diagnosis of neurodegenerative conditions (Kanjee et al., 2012; Lamirel et al., 2014).

In previous studies, SEM parameters and the extent of saccade disruption were evaluated in patients with glaucomatous optic neuropathy. Kanjee et al. (2012) evaluated glaucoma patients using a prosaccade step task, whereas Lamirel et al. (2014) investigated patients with primary open-angle glaucoma (POAG) using static and

kinetic targets. These studies reported significantly prolonged SRT and decreased eye movement precision in glaucoma patients. Smith, Glen, and Crabb, (2012) and Asfaw et al., (2018) found that the saccades and the spread of fixation during visual search processes were reduced in glaucoma patients when compared with their age-matched controls. Crabb et al., (2010) observed characteristic eye movement patterns in glaucoma patients when viewing a driving scene in a hazard perception test (HPT). Their results showed that saccadic behaviour was related to visual function and that patients with severe visual field defects showed fewer saccades per second than age-matched controls.

Investigators have also included SEM in visual field testing, so-called eye movement perimetry (EMP). During conventional visual field testing, such as in standard automated perimetry (SAP), a steady fixation throughout the course of testing is required. Especially the necessity to suppress reflexive eye movements compromises the test reliability (Kim et al., 1995; Murray et al., 2009). Kim et al., (1995) proposed an EMP system for visual field plotting based on eye movements as an alternative for SAP by presenting stimuli of various intensity levels (minimum of 15 dB). The visual field was reported on the basis of the minimum stimulus intensity seen (in dB). When compared between EMP and SAP, they reported less than 4 dB of sensitivity threshold difference in 92.8% of healthy subjects and 81.1% of glaucoma subjects (Kim et al., 1995). The eye movements, however, were observed by the investigator using a video-based eye tracker and a decision algorithm that classified each response as seen or not seen. Murray et al., (2009) included remote eye tracking technology to quantify visual fields on the basis of primary eye movement responses toward the peripheral stimuli named ‘saccadic vector optokinetic perimetry’ (SVOP) in both children and adults. They reported good agreement in discriminating normal eyes (adults: 99.2%, children: 99.1%) and eyes with glaucomatous visual field defects (adults 89.8%) when compared between the SVOP 41 test points and the C-40 screening test of Humphrey Field Analyser (HFA) (Murray et al., 2009). The EMP and SVOP were reported to be consistent in discriminating between normal and glaucoma when compared with the SAP. It showed the potential for assessing the extent of the visual field, even

though it was only based on binary responses from the subjects (i.e., seen or unseen) (Kim et al., 1995; Murray et al., 2009). Previous investigations conducted by the current study group attempted to quantify some of the SEM characteristics obtained from a similar remote eye tracking EMP system. A decision algorithm to classify an eye movement response as seen or unseen was included along with determining SRT for each seen point. This was denoted as a quantitative measure of visual field responsiveness (Mazumdar et al., 2014; Pel et al., 2013; Kadavath Meethal et al., 2018; Thepass et al., 2015). A significant delay in SRT was found in mild, moderate, and severe glaucoma patients when compared with their age-matched controls, indicating the potential importance of altered SEM values in glaucoma (Mazumdar et al., 2014).

Several studies have examined the effects of factors, such as stimulus eccentricity, contrast, luminance, size, and age on SEM in isolation. Munoz et al., (1998) reported age-related changes in the performance of healthy human subjects during pro- and anti-saccade task by projecting eccentric targets at 208 to either side of the fixation. They described the presence of delayed SRT and longer saccade duration in elderly subjects (60–79 years of age) in comparison to the younger age groups (Munoz et al., 1998). However, the effect of eccentricity and contrast was not explored. In another study, Pel et al., (2013) investigated the repeatability and variability of SRT at locations that covered 60 degrees horizontal and 40 degrees vertical visual field. They reported good repeatability across three measurement series (on average the differences were within 100 ms) and significantly delayed SRT with lower stimulus contrast and increasing stimulus eccentricity, but the subject's age was not included as a factor in the mixed linear analysis (Pel et al., 2013). Although the dependency of SRT on several factors, such as the age of the subject, stimulus intensities, and locations, are well documented in the literature, their interactions (including sex) and the combined effect on SRT obtained at locations in a visual field test have not been reported. To use SRT as a functional marker in visual field testing, it is essential to address its variability in healthy subjects. Therefore, the current study aims to assess the interaction of age, sex, intensity, and eccentricity on SRT in healthy

subjects using a mixed-model statistical analysis. The obtained data may serve as a first normative guide for EMP.

Materials and Methods

Participants

A total of 107 healthy adult subjects aged between 20 to 70 years were enrolled from the outpatient clinic of Sankara Nethralaya, a tertiary eye care hospital in India. Each subject underwent a complete ophthalmic examination and subjects with spherical ametropia greater than ±5.00 Dsph and cylindrical ametropia of more than -2.00 Dsph, best-corrected visual acuity less than 20/40, 0.8 M, ophthalmic conditions (e.g., oculomotor nerve palsy, corneal opacity, and ptosis), which might affect the eye-tracking, intraocular pressure more than 21 mm Hg, any sign of retinal nerve fibre layer changes or any abnormality on optic nerve head, any history of ocular surgery, or any retinal pathology were excluded. Only the eligible subjects were informed about the test and asked to participate. Twelve participants were excluded after recruitment due to eye tracking issues. Written informed consent was obtained prior to the clinical examination. The participant in Figure 1 provided informed consent to use the photograph for publication. Each subject underwent visual field testing in HFA (HFA model 750; Carl Zeiss Meditec, Dublin) and subjects with reliable normal visual field were included. The reliability of the visual field test was assessed as per the recommendation of the STATPAC algorithm by Anderson & Patella, (1999). The study was approved by the institutional review board and Ethics Committee of Vision Research Foundation, Chennai, India. The study adhered to the Declaration of Helsinki for research involving human subjects.

Instrument Description and Procedure Eye Movement Perimeter (EMP) The customized EMP testing setup comprised a laptop and a 17 inches thin film transistor (TFT) display of screen resolution 128031024 pixels with an inbuilt eye-tracking device with a refresh rate of 120 Hz (accuracy 0.5°; Tobii 120, Tobii, Sweden). The display unit was placed at a distance of 55 cm, allowing a visual angle toward the monitor of

34° x 23° (1280 x 1024 pixels), from the subjects (Fig. 3.1). A chin rest was provided to maintain a constant distance and minimize head movement during the test. No refractive correction was provided while performing the test. The test was performed under monocular viewing conditions by covering the left eye with a black polymethyl methacrylate plate (PMMA; see also Fig. 1 showing this lens holder including the PMMA glass). This plate permitted the passage of infrared light allowing the eye tracker to track both eyes for stable gaze tracking. Only the data of the right eye was used to prevent miscalculation of gaze positions due to any misalignment of the non-tested eye. The tests were performed in a clinical testing room. The background luminance was kept constant, and no talking was allowed during the test to avoid any distraction. The testing protocol began with an inbuilt nine-point calibration procedure to obtain good gaze accuracy. A red circular target was presented to align the subject's gaze with the calibration dots. The calibration procedure was repeated for locations that had insufficient sample points. In the main test, a central fixation stimulus was displayed at the centre of the screen (Mazumdar et al., 2014; Kadavath Meethal et al., 2018). The EMP visual field grid included all the 54 locations tested on the 24-2 SITA standard of HFA. The projected stimuli resembled the Goldmann size III stimuli and were point-wise projected at four different stimulus intensities against a background illumination of 152 cd/m^2. The following stimulus intensities were used: 192, 214, 249, and 276 cd/m^2. A total of 216 stimuli were presented and the total duration per exam was on average 12 minutes, including subject positioning, instruction, calibration, and an 11-minute test duration. The central target was not only projected into the central position on the screen but also in different eccentric positions to expand the tested visual field up to a visual angle of maximally 27° horizontally and 21° vertically. Stimuli were presented on the screen using an overlap paradigm (i.e., the central stimulus remained lit when a peripheral stimulus appeared). Subjects were asked to fixate the central stimulus. A central stimulus fixation of at least 0.2 seconds was followed by a random foretime between 1 and 2 seconds to prevent the predictability of presenting the next peripheral stimulus. Next, a peripheral stimulus was presented for a fixed duration of 1.2 seconds.

Subjects were instructed to look at each of the visual stimuli detected in the periphery and then fixate again on the central fixation stimulus.

EMP Data Analysis All 216 gaze data points of each subject were analysed using the customized software developed in MATLAB version 7.11 (MathWorks, Natick, MA). A previously published decision algorithm was used for automated offline processing of the data (Mazumdar et al., 2014; Pel et al., 2013; Meethal et al., 2018; Thepass et al., 2015).

Figure 3.1. EMP test set up comprising of a 17-in TFT monitor with an inbuilt infrared-based eye-tracking camera at the bottom panel. The chin rest placed at a distance of 55 cm was used for each measurement including a PMMA blocker holder positioned in a standard lens holder.

For all trials, a post-hoc check was done at the start of each trial to confirm a correct central stimulus fixation and to ensure that the correct location of the visual field was tested. Next, the gaze path from the central stimulus to the peripheral stimulus was visually inspected. Events were labelled as ‘seen’ when a SEM was initiated toward the presented visual target and covered more than 50% of the total central to peripheral stimulus distance. An event was classified as ‘unseen’ as follows when: (1) during the presentation of the peripheral target, no eye movements were made toward the target, (2) the first saccade was

not in the direction of the target, and (3) the angular disparity between the direction of the primary SEM and the peripheral stimulus location was larger than 45^0, indicating searching behaviour. An event where no eye movement data were available due to blinking or pupil detection failure was labelled as 'invalid' and was excluded from the analysis. For each 'seen' target the SRT was calculated as the time difference between stimulus presentation and the onset of the SEM in the direction of the target (Fig. 3.2) (Mazumdar et al., 2014; Pel et al., 2013; Meethal et al., 2018; Thepass et al., 2015). Calculation of SRT was done based on the gaze velocity criterion by calculating the reaction time at which the eye velocity crossed 50°/sec (Pel et al., 2013; Meethal et al., 2018). Special notice was given to the near central stimuli. Here, the eye velocity not always exceeded this limit.

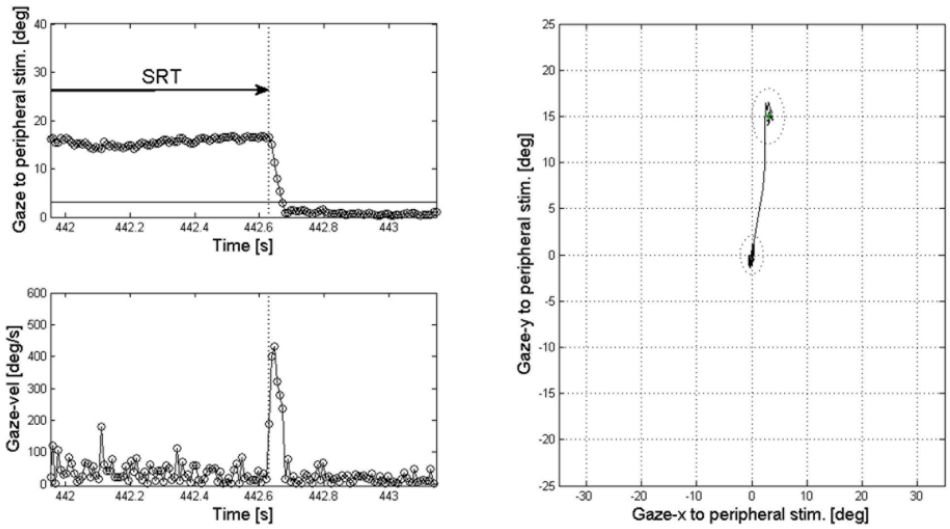

Figure 3.2. Illustration of an eye movement from the central fixation to a peripheral stimulus (right panel). The top left panel shows the relative gaze position with respect to the stimulus location and the left bottom panel shows the gaze velocity.

Statistical Analysis

To assess the influence of age on SRT the subjects were divided into the following five age groups: 20 to 29, 30 to 39, 40 to 49, 50 to 59, and 60 years and above. All four stimulus intensities (192, 214, 249, 276 cd/m^2) used in the testing algorithm were considered for analysing their influence on SRT. To assess SRT dependence on stimulus eccentricity four distinct eccentricities were determined by considering equidistance from the central fixation location which was termed as eccentricity 1 (4°), 2 (11°), 3 (16°), and 4 (22°) (Fig. 3.3). This approach was preferred over-analysing each location pointwise, because it improved the statistical power of the test. The two most nasal test locations were combined and denoted as eccentricity 5 (27°). From eccentricity 3, one location corresponding to the blind spot region was eliminated (Fig. 3.3). In addition, we also segregated the tested visual field into hemifields around the horizontal and vertical midline (superior and inferior as well as nasal and temporal) to assess visual area dependence of SRT behaviour. Data obtained from the right eye were considered for the analysis. SRT values were denoted in milliseconds. Tests for normality were carried out for each quantitative variable. Type I error was kept at the 5% level.

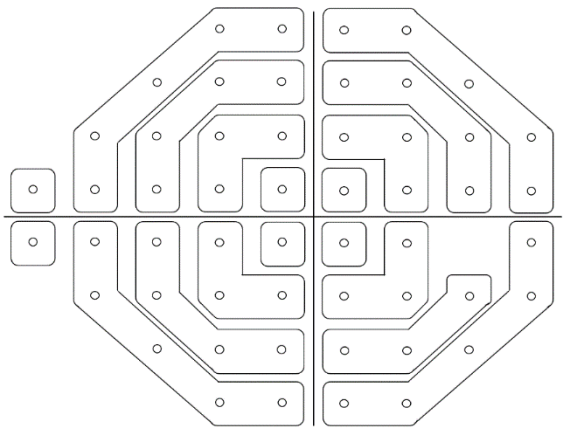

Figure 3.3. Illustration of stimulus grid (right eye) with distinctive eccentricities made by placing the concentric grid lines (not visible in the actual test) at different stimulus eccentricities. Stimulus locations were grouped by considering different sectors within each quadrant (i.e., 4 sectors per quadrant). Two nasal test locations were considered as eccentricity 5.

To determine the influence of the factors on the dependent variable SRT, a multilevel mixed model (generalized linear mixed model [GLMM]; SPSS, IBM, Armonk, NY) was used. GLMMs are an extension of linear mixed models to allow response variables from different distributions. The output of a GLMM is estimates of the mean SRT values and their corresponding confidence intervals. This method adjusts the SRTs for each factor, and as a result, only provides the estimated SRTs per factor. The individual factors included in the model were as follows: the age groups, sex, stimulus intensity levels, and stimulus eccentricity as categorical variables. The linear regression model allowed a levelled structure to look for SRT variability within each factor as follows: five age groups, two sex groups, four stimulus intensities, and four eccentricity-wise. Eccentricity 5 was not considered for the GLMM analysis as it consisted of only two test locations. The within factor levels were tested using pairwise contrast estimates as post hoc test. The interaction of different factors with SRT was added to the model using the following equation: gender x age group x stimulus intensity x eccentricity. The output reference categories were male, age group older than 60 years, stimulus intensity 276 cd/m^2 and eccentricity 4.

Results

A total of 95 healthy subjects were included in the study. The demographic details and the frequency of subjects in each age group are presented in Table 3.1.

Table 3.1. Demographics of the Study Population Subject Characteristics

Age range (in years)	20-70
Mean age in years (SD)	43.0±15.0
Age Groups (Number of subjects)	20-29 (22) 30-39 (18) 40-49 (21) 50-59 (17) 60 & above (17)
Gender – Number of subjects (%)	Male 50(53%) Female- 45 (47%)

Table 3.2 summarizes the total percentage of seen and unseen gaze data for each age group at the four stimulus intensities. The proportion of 'seen' was equally distributed between age groups at stimulus intensities 276 to 214 cd/m^2. However, for stimulus intensity 192 cd/m^2, the percentage of seen drops with approximately 15% to 25% in each age group. The percentage of invalid points remained low (<5%) and was consistent across all age groups.

Table 3.2 The total percentage of Seen and Unseen points for all age groups in all stimulus intensities

Eye Movement Responses (%)

Stimulus Intensity	20-29 years		30-39 years		40-49 years		50-59 years		60 years & above	
	Seen	Unseen	Seen	Unseen	Seen	Unseen	Seen	Unseen	Seen	Unseen
192 cd/m²	69	31	67	33	63	37	50	50	46	54
214 cd/m²	83	17	81	19	80	20	75	25	71	29
249 cd/m²	75	25	74	26	72	28	68	32	73	27
276 cd/m²	83	17	79	21	80	20	76	24	78	22

A fixed-effect model with the dependent variable SRT and predictors as sex, age group, stimulus intensity, and eccentricity are presented in Table 3.3. Overall, a statistically significant effect ($P < 0.001$) was found for SRT with age, stimulus intensity, and stimulus eccentricity, not for sex ($P = 0.74$).

Table 3.3. The fixed effect model of the individual factors on Saccadic Reaction Time

Tests of Fixed Effects [a]				
Source	**F**	**Numerator df**	**Denominator df**	**Sig.**
Intercept	17.99	80	12412	<0.001
Gender	0.110	1	12412	0.740
Age-group	7.94	4	12412	<0.001
Stimulus Intensity	223.73	3	12412	<0.001
Eccentricity	59.46	3	12412	<0.001

[a] Dependent variable: Saccadic Reaction Time

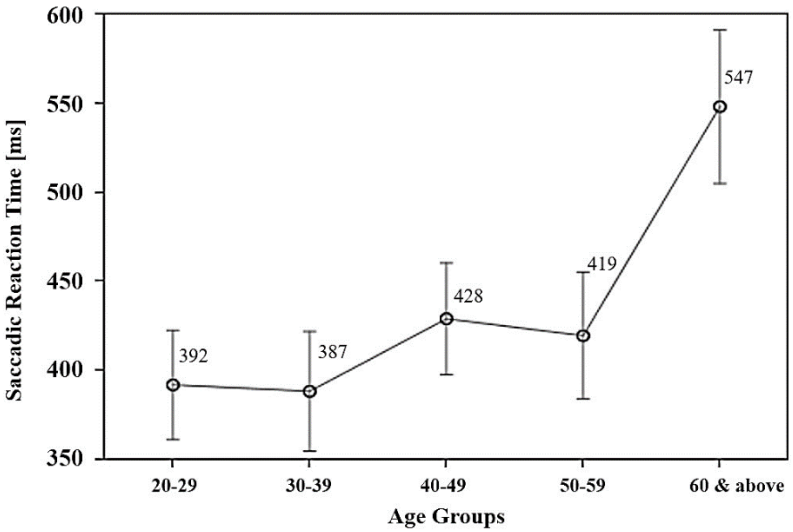

Figure 3.4. Estimated mean SRT and their 95% confidence intervals plotted as a function of age.

Next, a comprehensive overview of the model for the main effects of the factor levels (including age, stimulus intensity and eccentricity) with SRT are presented in Table 3.4. Estimated mean SRTs with corresponding 95% confidence intervals are presented in Figures 3.4-

3.6. SRTs were significantly faster with increasing stimulus intensity and decreasing eccentricity ($p < 0.001$).

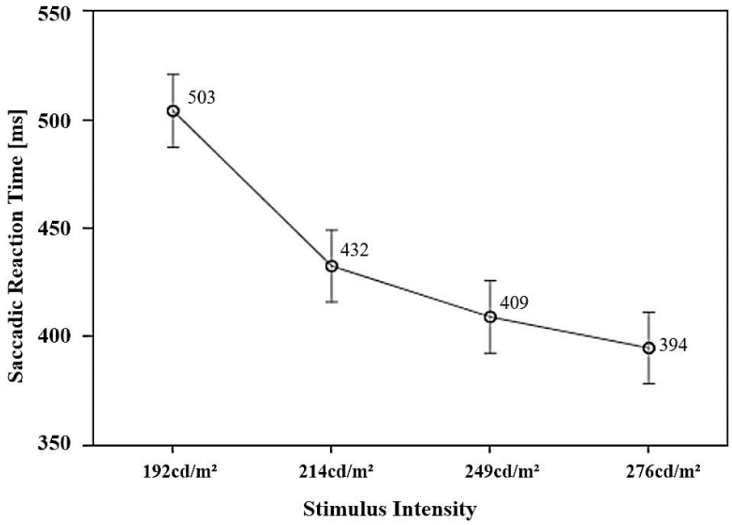

Figure 3.5. Estimated mean SRT and corresponding 95% confidence intervals plotted as a function of stimulus intensity.

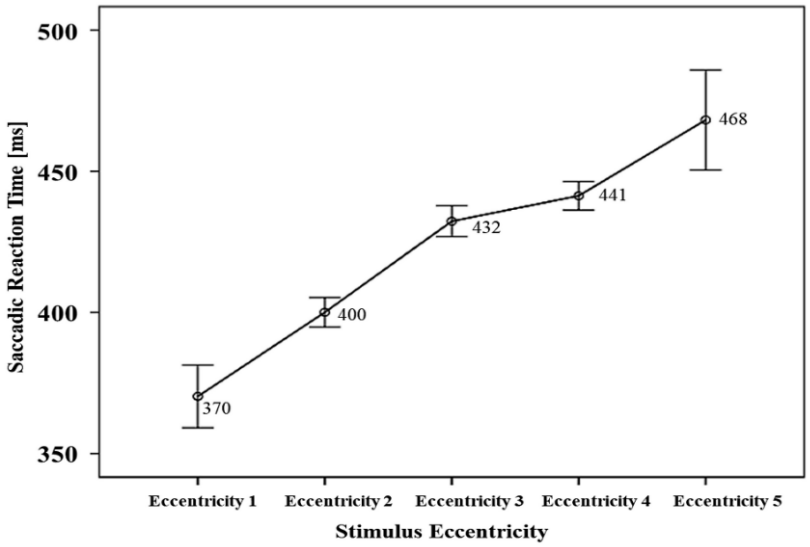

Figure 3.6. Estimated mean SRT and corresponding 95% confidence intervals plotted as a function of stimulus eccentricity.

Table 3.4. The results of the multilevel model of the individual factors and their levels

Saccadic Reaction Time [ms]			
Main Effect	**Parameter estimate**	**95% CI**	**p-value**
Intercept	481	439 to 523	**< 0.001**
Age			
20-29 years	-92	-144 to -39	**< 0.001**
30-39 years	-94	-149 to -40	**< 0.001**
40-49 years	-69	-122 to -16	**0.01**
50-59 years	-77	-135 to -20	**0.008**
60 years & above	Reference		
Stimulus intensity			
192 cd/m^2	141	109 to 174	**< 0.001**
214 cd/m^2	69	43 to 954	**< 0.001**
249 cd/m^2	17	-9 to 43	**0.196**
276 cd/m^2	Reference		
Stimulus eccentricity			
Eccentricity 1(4^o)	-58	-106 to -11	**0.016**
Eccentricity 2(11^o)	-36	-69 to -3	**0.034**
Eccentricity 3(16^o)	-14	-44 to -17	**0.387**
Eccentricity 4(22^o)	Reference		

The interaction of different factors on SRT is presented in Table 3.5. At the lowest stimulus intensity of 192 cd/m^2, a significant interaction was found between age and eccentricity. At eccentricity 4 and 22 degrees, the oldest age group was significantly delayed compared to the younger subjects. At the intermediate eccentricities (11 and 16 degrees), a significant difference was found between the different age groups, with the fastest SRTs assessed in 20-40 years old subjects.

Significant delays in SRT were also found at stimulus intensity 214 cd/m^2 at eccentricity 4 degrees in the oldest age group.

Visual response map

To visualize the SRT behaviour, the age specific mean SRT values per sector within each of the five eccentricities were calculated for the four stimulus intensities, see figure 3.7. For each sector, the average SRT value was calculated and plotted using a grey-scale map: SRT ranging from 130 ms – 1200 ms corresponded with red-green-blue (RGB) values ranging from (230 – 25). In that way, the fastest SRT were plotted in light grey and the most delayed SRTs were dark grey. The blind spot was plotted in black [RGB: 0-0-0]. These plots illustrate the delay in SRT with increasing age and decreasing stimulus intensity. Supplementary Figure 1 presents the age specific mean SRT values within each eccentricity with respect to stimulus intensity.

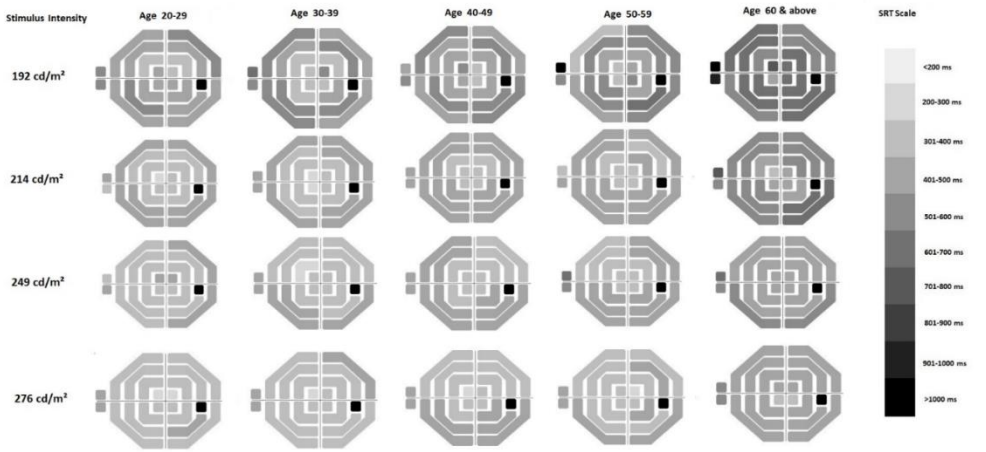

Figure 3.7. Illustration of Visual Response maps (Right eye) created using mean SRT for each sector in the tested visual field for all age groups at four stimulus intensities. The SRT scale shows the grey scale corresponding to the SRT range.

Table 3.5. Pairwise contrast estimates between the levels of factors

Pairwise Comparison										
									95% CI	
Stimulus intensity	**Eccentricity**	**Age groups**		**Contrast Estimate**	**Std Error**	**T**	**df**	**Adj. Sig.**	**Lower**	**Upper**
192 cd/m²	4°	≥60 years	20-29	133.86	43.98	3.04	12412	0.02	47.64	220.07
			30-39	168.77	45.76	3.69	12412	<0.001	79.07	258.48
			40-49	166.09	44.95	3.7	12412	<0.001	77.98	254.2
			50-59	133.23	50.37	2.65	12412	0.008	34.49	231.97
	11°	20-29	40-49	-62.65	27.52	-2.27	12412	0.02	-116.5	-8.71
			50-59	-91.79	29.66	-3.09	12412	0.002	-149.93	-33.65
		30-39	40-49	-78.87	29.11	-2.71	12412	0.007	-135.93	-21.81
			50-59	-108.01	31.32	-3.45	12412	0.001	-169.4	-46.61
		≥60 years	20-29	198.18	29.94	6.62	12412	<0.001	139.49	256.87
			30-39	214.4	31.41	6.83	12412	<0.001	152.83	275.96
			40-49	135.53	30.54	4.44	12412	<0.001	75.66	195.39
			50-59	106.39	32.61	3.26	12412	<0.001	42.47	170.31
	16°	20-29	40-49	-55.99	27.65	-2.03	12412	0.043	-110.19	-1.8
			50-59	-79.19	30.34	-2.61	12412	0.009	-138.66	-19.71
		≥60 years	20-29	207.04	30.7	6.74	12412	<0.001	146.86	267.23
			30-39	187.13	31.53	5.94	12412	<0.001	125.33	248.92
			40-49	151.05	31.08	4.86	12412	<0.001	90.13	211.96
			50-59	127.86	33.63	3.8	12412	<0.001	61.93	193.77
	22°	≥60 years	20-29	120.56	29.06	4.15	12412	<0.001	63.6	177.52
			30-39	121.82	29.89	4.08	12412	<0.001	63.23	180.41
			40-49	97.44	29.29	3.33	12412	0.01	40.04	154.85
			50-59	129.26	32.36	3.99	12412	<0.001	65.82	192.69
214 cd/m²	4°	≥60 years	20-29	90.19	36.24	2.49	12412	0.013	19.15	161.23
			30-39	119.71	38.44	3.11	12412	0.002	44.36	195.05
			40-49	88.3	37.55	2.35	12412	0.019	14.69	161.91

Discussion

The current study systematically investigated the interaction of the subject's age, sex, stimulus intensity and eccentricity on SRT behaviour using a remote eye tracker based EMP system. All the factors except sex were found to have a statistically significant effect on the SRT. A significant interaction was found between the lowest intensity and age. Here, the delayed SRTs were found in the 60 years and above group at all tested eccentricities. These findings provide essential information needed for better understanding the natural behaviour of SRT with ageing.

Interacting Factors

A significant delay in SRT was found with increasing age, where approximately a 40% delay in response time was found in subjects above 60 years of age compared with the youngest age group (20–29 years). Irving et al., (2006) reported the age-dependency of horizontal saccade dynamics, especially on SRT, accuracy, and peak velocity. Each parameter followed a distinct pattern of development and decline in relation to the complex network of brain structures accountable for the processing and generation of saccades. Saccades are found to be characterized by fast reaction times and high-peak velocities throughout the course of childhood and early adolescence, which stabilizes in the middle decades of life. Reaction time, peak velocity, and accuracy followed a significant decline with increasing age (Irving et al., 2006). Fischer et al., Munoz et al., and Pratt et al. evaluated the impact of age on SRT values. They demonstrated strong age-related effects on SRT (Fischer, Biscaldi, and Gezeck, 1997; Munoz et al., 1998; Pratt, Abrams, and Chasteen;1997), and our study results were consistent with these previous findings. Kenward et al., (2017) reported faster SRT (mean difference 28 ms) in baby girls (between 9 and 15 months) compared with age-matched boys when stimuli were projected at 14.2^0, whereas no such difference was found in adults. In the current study, we have also not found any significant difference in SRT between adult females and males in different age groups.

In addition, our results showed a delay in mean SRT (ranging from 394 – 503 ms) with decreasing stimulus intensity. A similar pattern was observed in previous studies (Pel et al., 2013; Bell et al., 2006; Carpenter et al., 2004). Bell et al., (2006) registered the commencement of neural activity in the intermediate layers of SC when saccades were generated in response to high- and low-intensity stimuli. They observed faster response onset for high-stimulus intensity in comparison with the lower- intensity stimuli (Bell et al., 2006). It was suggested that most of the age-related decline in visual functions cannot be credited to changes in the optical properties of the eye. Presumably, this decline is due to the alterations in the quality of the neural networks of the central nervous system (Munoz et al., 1998; Gella, Nittala, and Raman, 2014). It might include a decline in visual acuity, contrast sensitivity, binocular processing, and motion sensitivity. The delay found in SRT with respect to increasing age can also be attributed to the decline in visual abilities due to neurophysiologic changes during various stages of the degeneration process that include gradual atrophy of the grey and white matter of the cerebral cortex (Creasey and Stanley, 1985).

To investigate the SRT behaviour with stimulus eccentricity, we created five eccentricities based on their distance from the centre. We found SRT was dependent on stimulus eccentricity up to 27°. Hodgson investigated eye movements on a set of six subjects tested with a stimulus with and without location markers (Hodgson TL., 2002). The eccentricities used were 3° and 9° on either side of the fixation along the horizontal axis. The target without location marker subtended 0.26° and those with location marker subtended 0.43° in diameter. He reported a delay in reaction time at 9° eccentricity when location markers were used. Our study confirmed this finding of SRT dependency on eccentricity (Weber et al., 1992; Fuller et al., 1996); yet other studies contradict the eccentricity effects on SRT (Dafoe, Armstrong, and Munoz, 2007). Dafoe et al., (2007) reported that SRT was independent of eccentricity; however, their eccentricity was limited to 8°. We found that the effect was stronger when the targets were presented in eccentricities 3, 4, and 5, which extended to 27° eccentricity (fig 3.7). This effect could be attributed to the variation in

photoreceptor stimulation with respect to retinal eccentricity (Warren et al., 2013).

The differences in SRT between nasal and temporal hemifields were not significantly different as reported by J´ohannesson et al, (2012). A comparison in SRT between superior and inferior visual field did reveal significantly faster SRT in the superior field (~24 ms). This might be the result of the anatomic asymmetry of the human retina, such as differences in cone and ganglion cell density (Williams, Azzopardi, and Cowey 1995). The visual response maps introduced in the current study made the quantitative and qualitative visualization of SRT variability throughout the visual field visible. Based on the interactions, we conclude that at the lowest stimulus intensity of 192 cd/m^2 a significant interaction was found between age and eccentricity. Especially the SRT values in the oldest age group (≥60 years) showed significant delays. Such a general reduction in this age group is also found for the sensitivity thresholds in SAP. As a result, when interpreting SRT values, it is important to take the normative values as a reference to correctly distinguish abnormal from normal SEM behaviour.

Stimulus Conditions

An important question is whether there are systematic differences between the SRT values reported in the present study and the wide range of SRT values that have been reported in the literature (Darrient et al., 2001; Pel et al., 2013; Thepass et al., 2015; Warren et al., 2013). In general, the SRT values seem to mostly depend on stimulus intensity and stimulus eccentricity. Warren et al., (2013) reported similar SRT values between 400 and 500 ms in healthy subjects of 18 to 30 and 60 years and older. Their stimuli with an intensity of 250 cd/m^2 were projected on a comparable background intensity (150 cd/m^2) and eccentricity (Warren et al., 2013). In the present study, stimuli with higher intensity (e.g., 276 cd/m^2) indeed triggered slightly faster SRT values, whereas the stimuli with the lowest intensity of 192 cd/m^2 resulted in SRT values up to 700 ms in subjects of comparable age. In one of our previous EMP studies to test the effect of cataract on SRT,

we were able to project peripheral stimuli with much higher intensities of 210, 300, 385, 475 cd/m2 at a background luminance of 160 cd/m^2 due to a better-quality monitor (Thepass et al., 2015). Indeed, on average faster SRT values (~380 ms; ~16° eccentricity; age group ≥60 years) were found compared with the present study (~550 ms; ~16° eccentricity; age group ≥60 years).

The above comparisons seem to suggest that stimulus intensity dictates SRT. However, we cannot rule out the influence of background luminance on SRT. Darien et al., (2001) measured SRT by conducting a test that used a white background, a black fixation target, and red peripheral targets. Instead of SRT dependence, they reported SRT values (mean SRT ~250 ms) to be invariant with respect to eccentricity (10°, 15°, 20°, 24°, 28°) when stationary red targets were presented along the horizontal meridian at 10° to 30° (Darien et al., 2001). Their results might be explained by the bleaching desensitization of the photoreceptors when exposed to a very bright background. This might reduce visual field responsiveness at the retinal level (Pepperberg 2003). When stimuli were plotted on a black background, however, much faster SRT values were reported, not only in adults (~200–250 ms; >10 years of age) but also in children (~180 ms) (J.J M Pel, Manders, and van der Steen 2010; Fukushima, Hatta, and Fukushima 2000; Yang, Bucci, and Kapoula 2002). We think that the influence of the background luminance could be very delicate. This might be best illustrated by a previous study also conducted within our group, where we kept background luminance lower (~140 cd/m^2) than we did in this study. We found slightly faster SRT values even when the intensities of the plotted stimuli were lower than the stimuli used in the present study (~190 cd/m^2) in subjects between 20 and 30 years of age. The variability in SRT was equally small (Pel et al., 2013).

Finally, the test paradigm can also have an influence on SRT values. A gap paradigm may trigger eye movement responses (Saslow 1967). In a gap paradigm, the fixation target disappears on the appearance of the peripheral stimulus and may trigger (1) the initiation of express saccades characterized by faster SRT (~100 ms), or (2) searching of the fixation target when the peripheral target is plotted in an affected part of the visual field. To prevent searching behaviour during the test,

we used an overlap paradigm in which the fixation target was kept illuminated while a new stimulus appeared in the periphery. This approach also resembles testing the visual field using the SAP technique.

Study Limitations

The current study has some limitations to be addressed. Twelve of 107 participants had failure in eye tracking during the calibration procedure because of an error in pupil detection. From the 12 dropouts, eight were 60 years and above, one from the group 20 to 29, one from the group 40 to 49, and 2 from the group 50 to 59 years. Enrolling healthy subjects with age 60 years and above from a population (southern India) is challenging given the high rate of un-operated cataract (53%) patients, especially when meeting the stringent inclusion criteria set for age-related changes in the optical media and ocular surface (Vashist et al., 2011). Despite these stringent criteria, some of the patients that met the cataract criteria could have had reduced contrast acuity due to other media opacity, such as (invisible) corneal and vitreous changes. Previously, we have shown that the eye-tracker has good gaze tracking performance even in patients with cataract up to Lens Opacity Classification System III (LOCS III), grade 4 (Thepass et al., 2015). In addition, prior to be enrolled in this study, the subjects first underwent an HFA measurement. Even here, we had a similar number of dropouts, 13 healthy subjects (4 from the group 20–29, 2 from 50–59, and 7 from the group ≥60 years) were unable to produce reliable HVF test results. Hence, these subjects were not selected for this study. Table 3.2 described the pattern of eye movement responses (proportion seen/unseen) obtained from the subjects where the percentage of seen responses was found to decline with increasing age and decreasing stimulus intensity. In the elderly age group ≥60 years) the percentage of unseen responses was much lower for stimuli intensities, such as 276, 249, and 214 cd/m^2 when compared with 192 cd/m^2. This confirmed that the subjects did understand the task, and their reaction times, even to these low-intensity stimuli, were well within the 1200-ms projection time.

Even though the selected stimulus intensities are well within the visible range, yet the poor performance for the stimulus intensity 192 cd/m^2 was alarming. On further inspection of the data, it was found that the maximum percentage of unseen responses were most obtained at eccentricity 5 (27°) followed by eccentricity 1 (4°). Eccentricity 5 is the extreme periphery and it involved 2 testing locations that were excluded from the GLMM analysis. For eccentricity 1, the central four locations, unseen responses were highest for the lowest stimulus intensity of 192 cd/m^2 for the age group 60 and above. Maybe these stimuli were perceived even without making an eye movement or the eye movements were so small in amplitude, that neither the software nor visual inspection identified these saccades. This limits the application of EMP in testing for central visual field losses, as done, for example, in the HFA 10-2 protocol. The aim of the present study was to explore SRT as an outcome measure for plotting the visual field. It gave us the insight to modify the testing strategy by reducing testing points and stimulus intensities. As it is evident that the reliable response percentage is minimal with the lowest stimulus intensity (192 cd/m^2), the inclusion of the same might not add any clinical value.

Clinical Application

Eye-tracking technology has been recently used in several studies as a new method to eliminate drawbacks of traditional visual field plotting techniques, such as the requirement to maintain steady fixation while suppressing a reflexive eye movement or pressing a button on perceiving a stimulus (Kim et al., 1995; Murray et al., 2009; Murray et al., 2017). Mc Trusty et al., (2017) reported that a visual field test in combination with eye movements was preferred by subjects over conventional methods, especially with respect to the testing procedure as well as ergonomics. Even though EMP requires a central target fixation, subjects are encouraged to make eye movements toward detected stimuli. It thus incorporates the natural oculomotor response to new visual features and at the same time, it avoids the continuous and conscious decision of whether to press a button or not. Natural reflexive eye movements were used to quantify visual field isopters in infants and patients with special needs, showing the potential of

plotting visual fields on the basis of eye movements (Satgunam et al., 2017). The further development of EMP may hopefully result in a reliable tool for implementation in the community, especially in rural parts of countries like India to screen the visual field status of many people in order to detect the high percentage of visual impairment due to glaucoma (George, Ve, and Vijaya 2010; Flaxman et al., 2017). In a previously published study, we have introduced an EMP screening grid (Kadavatah Meethal et al., 2018). This grid consisted of 26 locations that resulted in an average test duration of 2 minutes (test points at 214 and 276 cd/m^2). These data presented in this study may be a good normative guide for implementing EMP as a screening tool.

Conclusion

The current study provides the age specific SRT characteristics in healthy subjects. Within the tested visual field, the interaction of age, sex, stimulus intensity, and eccentricity on SRT provided insight in age-dependent SEM behaviour. The analysis of SRT interaction can help in refining its use as an index for plotting visual field responsiveness in patients with glaucoma and other neurologic disorders.

Acknowledgements

Supported by Grant Number 116310001 from the Netherlands Organization for Health Research and Development (ZonMw) and the Department of Science and Technology, Government of India [DST/INT/NL/Biomed/P (2)/2011(G)].

Supplementary Figure

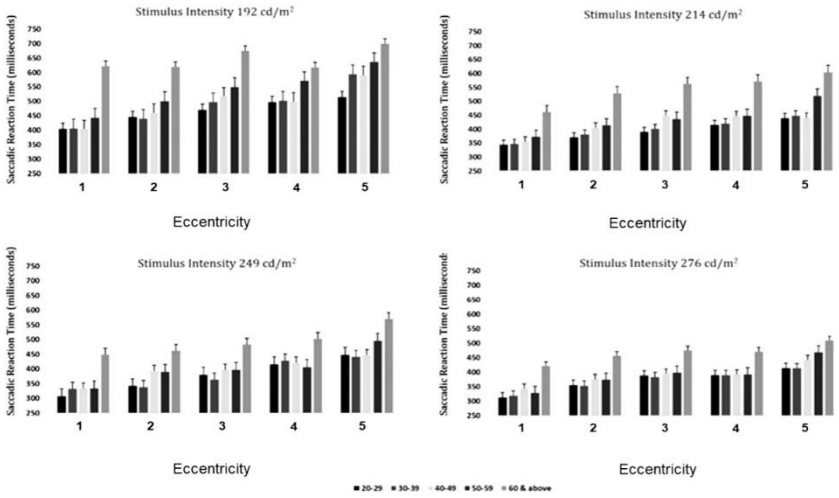

Supplementary Figure 1. Age-specific Saccadic Reaction Time behaviour with respect to stimulus eccentricity for all the intensity levels. Error bars represents the standard error (SE)

CHAPTER 4

Manuscript in preparation

CHAPTER 5

VISUAL FIELD PLOTS: A COMPARISON STUDY BETWEEN STANDARD AUTOMATED PERIMETRY AND EYE MOVEMENT PERIMETRY

Deepmala Mazumdar[1, 2], Johan J. M. Pel[1], Najiya Sundus Kadavath Meethal[1, 2], Rashima Asokan[2], Manish Panday[2], Johannes van der Steen[1,3], Ronnie George[2]

[1] Department of Neuroscience, Vestibular and ocular Motor Research Group, Erasmus MC, 2040, 3000, CA Rotterdam, The Netherlands
[2] Medical and Vision Research Foundation, Chennai, India
[3] Royal Dutch Visio, Huizen, The Netherlands

Adapted from: Journal of Glaucoma. 2020 May;29(5):351-361.
DOI: 10.1097/IJG.0000000000001477

Précis

This Eye movement Perimetry (EMP) study describes the development of Saccadic Reaction Time (SRT) based visual field plots which could effectively display the presence, location and extent of glaucomatous defects and support clinical decision making.

Abstract

Purpose: EMP can discriminate normal from glaucomatous visual field defects on the basis of average delays in SRTs. To classify the presence and extent of age-corrected visual field defects, it is required to create SRT-based probability maps.

Aim: The aim of this study was to create visual field probability plots based on SRTs and to evaluate their clinical applicability by two glaucoma specialists.

Methods: The development phase included 95 controls segregated into 5 age bins to estimate normative limits of SRT. Next, for the testing phase, a set of 28 healthy subjects & 24 glaucoma patients were recruited who underwent Standard Automated Perimetry (SAP) and EMP visual field testing. Fifty-two SAP and EMP plots were presented to two glaucoma specialists to classify them as normal/abnormal and to identify the defect location and pattern as 1 or more of seven predefined categories.

Results: The glaucoma specialists showed a sensitivity of 100% and a specificity of 93% and 96% for identifying normal versus the abnormal visual field. For specialist 1 & 2, 85% & 92%, respectively, of EMP reports were assigned to the same category as SAP. The reports that did not agree with SAP were graded to a higher defect pattern. The inter-method agreement for specialist 1 and 2 was κ 0.92 & 0.96, respectively.

Conclusions: SRT-based visual field probability plots provided a comprehensive summary of an individual's visual field status and showed comparable clinical applicability to that of SAP plots.

Introduction

Standard Automated Perimetry (SAP) is considered to be the clinical standard for visual field testing. It has been widely used for several decades for the diagnosis and management of different diseases presenting with visual field defects, such as glaucoma, optic neuritis, and Retinitis Pigmentosa (Johnson, Wall, and Thompson 2011). SAP uses differential light sensitivity to map the visual field threshold at each location. The extent of the damage is displayed on probability maps, which shows the difference in visual field thresholds compared with the age-corrected normative values (Heijl, Lindgren, and Olsson 1989). SAP demands considerable patient co-operation as it requires a steady fixation during the test and a response to the perception of a stimulus. The necessity to suppress reflex eye movements is reported to compromise the test reliability (Toepfer et al., 2008; Warren et al., 2013; Kim et al., 1995). A recently published survey on participant test experience of conventional visual field testing revealed that the test induced discomfort and anxiety, even in experienced patients (Chew et al., 2016). Others found that patients reported SAP as onerous and suggested to modernise the visual field test (Glen, Baker, and Crabb 2014).

Eye Movement Perimetry (EMP) uses reflexive human eye movement responses to map the visual field. The test includes goal-directed saccades to peripherally shown stimuli (Damato, 1985; Murray et al., 2009; Pel et al., 2013; Mazumdar et al., 2014; Kadavath Meethal et al., 2018). We have previously investigated the possibility of using the Saccadic Reaction Time (SRT) of eye movements in 'seen' peripheral stimuli as a measure for visual field responsiveness (Pel et al., 2013; Mazumdar et al., 2014; Kadavath Meethal et al., 2018). In the past, several studies have investigated the dependence of SRTs on age (Munoz et al., 1998) and sex (Irving et al., 2006) and stimulus factors, such as eccentricity, intensity, and size, in isolation or combined (Pel et al., 2013; Irving et al., 2006; Bell et al., 2006; Fuller, 1996) in healthy subjects. Most studies consistently showed that age, stimulus intensity and eccentricity have a significant effect on SRT. We recently showed that at low stimulus intensities, significant interactions exist between

age and eccentricity (Mazumdar et al., 2019). This suggests that normative SRT values are required when patients with visual field defects are compared with healthy subjects.

Comparable and consistent findings between SAP and EMP have been reported on the extent of the visual fields, including the locations of the defects (Kim et al, 1995; Murray et al., 2009; Kadavath Meethal et al., 2018; Mctrusty et al., 2017). Kim et al., (1995) and McTrusty et al., (2017) have reported the possibilities of plotting the extent of the visual field on the basis of binary responses from subjects, i.e., seen or unseen. Previous investigations by the current group attempted to quantify the measure of visual field responsiveness as SRT (Kadavath Meethal et al., 2018). In terms of eye movement behaviours, it was found that glaucoma patients showed delayed SRTs during a static pro-saccade test (Kanjee et al., 2012) and a static and kinetic test to targets at horizontal meridian locations (Lamirel et al., 2014). We showed in glaucoma patients, that their mean SRT was significantly delayed compared with age-matched controls at locations comparable to the 24-2 test locations in SAP using an overlap paradigm (Mazumdar et al., 2014; Kadavath Meethal et al., 2018 2019). Even though the findings support the potential use of SRT as a measure of functional integrity especially in glaucoma, yet a comprehensive visual field response map that summarises a patient's visual field status is still lacking. Such a map could support clinical decision making by identifying the presence, extent, and depth of the visual field defect. For the clinical implementation of a new perimetry approach, the visual field defect patterns should be comparable with the conventional SAP [clinical standard]. Hence, we aimed to create probability plots based on SRTs and to test their applicability in a clinical setting.

First, we analysed the collected eye movement data for healthy subjects to estimate the location-wise SRTs for different stimulus intensities. After the construction of the probability values for different age groups, we recruited glaucoma patients with varying disease severity in EMP and healthy subjects to plot their probability plots using the estimated limits. We presented the probability plots from both SAP and EMP to two glaucoma specialists to grade each visual field. Finally,

the agreement between both the measurement methods was assessed.

Materials & Methods

This study comprised of two parts a development and testing phase. For the development phase, we analysed the collected eye movement data for healthy subjects to estimate location-wise SRTs for different stimulus intensities. For the testing phase we recruited glaucoma patients with varying disease severity and a new group of healthy subjects.

Subjects

A total of 66 normal subjects and patients diagnosed to have glaucoma aged between 20-70 years were recruited from the outpatient department of the glaucoma clinic of Sankara Nethralaya, a tertiary eye care hospital situated in southern India. The study adhered to the tenets of the declaration of Helsinki (2013) and the experimental measures were reviewed and accepted by the Institutional Review Board and Ethics Committee of Vision Research Foundation, Chennai. Exclusion criteria were spherical ametropia greater than ±5.00 DSph and cylindrical ametropia of more than -2.00 Dcyl, best-corrected Visual Acuity worse than 20/40, 0.8M and ophthalmic conditions that are known to affect eye-tracking, such as ptosis, corneal opacity, and oculomotor apraxia (Pel et al., 2013). After obtaining informed consent, all subjects underwent a complete ophthalmic examination including a visual field examination. The visual field was assessed using the Humphrey Visual Field Analyser (HFA) II 750 (Carl Zeiss Meditec Inc, Dublin, CA, USA), program 24-2, with Swedish Interactive Threshold Algorithm (SITA) standard strategy. The participants, who were unable to perform SAP reliably, were not included in the study. Reliability criteria for HFA tests included fixation loss, <20%; false positive and false negative, <33% according to the recommendations of the manufacturer. The International Society of Geographical and Epidemiologic Ophthalmology (ISGEO) classification was used to define subjects with glaucoma (Foster et al., 2002). Glaucomatous

eyes had to have definite structural changes whereas a relatively lenient criterion was used for functional changes with visual fields meeting at least one of Anderson's criteria (Foster et al., 2002; Anderson & Patella, 1999). Further, the visual fields were classified into mild, moderate, and severe based on their SAP reports using Hodapp, Parrish and Anderson's classification (Brusini & Johnson, 2007).

Normal subjects were defined as those with an Intra Ocular Pressure (IOP) less than 21mmHg, with no family history of glaucoma or any other ocular pathologies, a healthy anterior and posterior segment along with a normal visual field.

Eye Movement Perimetry

Next, each subject underwent an EMP measurement (Mazumdar et al., 2014; Meethal et al., 2018). In brief, the EMP test was performed on a 17'' Thin Film Transistor (TFT) display of screen resolution 1280x1024 pixels with an inbuilt eye-tracking device with a refresh rate of 120 Hz (accuracy 0.5 degrees) (Tobii T120 Eye Tracker) at a viewing distance of 60 centimetres. The test was run in a dimly illuminated room and the noise was kept at a minimum level. The visual field test started with an inbuilt nine-point calibration, which uses an internal anatomic 3D eye model to calculate the gaze data by the device. Upon passing the calibration test, the main test was initiated. The visual field grid coordinates were kept equivalent to the 24-2 SITA standard of HFA, where 54 locations were tested in four stimulus intensities (192, 214, 249 and 276 cd/m^2) against a background of 152 cd/m^2. The luminance levels of the background, and of the peripheral stimuli were assessed using Gossen M504G MAVO-MONITOR USB. To expand the tested visual field, the fixation target was projected centrally as well as at eccentric positions to warrant a total visual angle of 54 degrees horizontally and 42 degrees vertically. The peripheral stimulus of Goldmann size III was projected randomly for a fixed duration of 1200 milliseconds with a gap of 0.2 seconds between stimuli presentations, with the fixation stimulus lit, that is, an overlap paradigm. Subjects were encouraged to look at the visual stimulus detected peripherally and then re-fixate the fixation stimulus.

The eye movement responses were first visually inspected and next analysed using a previously published decision algorithm developed in Matlab Version 7.11 (Math Works, Natick, MA) (Jernigan, 1980; Pel et al., 2013; Mazumdar et al., 2014; Kadavath Meethal et al., 2018 2019). A total of 216 gaze data points of each subject were analysed by inspecting the gaze path from fixation stimulus to peripheral stimulus. The responses were labelled as seen, unseen and invalid. 'Seen' responses adhered to the following criteria: a) A Saccadic Eye Movement (SEM), initiated towards the presented visual target, b) SEM, at onset, was in the direction of the peripheral target and covered >50% of the total fixation to peripheral target distance, c) The angular disparity of less than 45 degrees between the direction of the primary SEM and the peripheral stimulus location. 'Unseen' responses adhered to the following (and they are): a) No eye movements were made on presentation of the peripheral target, b) SEM, at onset, was not in the direction of the peripheral target, c) The angular disparity between the peripheral and fixation target is larger than 45 degrees, which is indicative of searching behaviour. Finally, responses were labelled as 'invalid' when eye movement data were not available due to blinking or failure in pupil detection and was excluded from the analysis. SRT was calculated on the basis of the gaze velocity criterion by calculating the reaction time at which the eye velocity crossed 50 degrees per seconds. It was defined as the time difference between the stimulus presentation and the onset of the SEM toward the direction of the peripheral target.

Development phase: Normative EMP data

EMP data collected from normal subjects, which were previously reported (Mazumdar et al., 2019), were used to calculate the likelihood of SRT for five age groups: 20-29, 30-39, 40-49, 50-59 and 60 years & above. SRTs were available at 4 different stimulus intensities at each of the 54 tested locations. On the basis of these normative reference values of SRT, the percentile levels of 5%, 2.5%, 1% and 0.5% were determined separately for each point adopting the standard approach used by Heijl et al., (1989) to develop the probability maps for SAP.

EMP visual field and probability plots

As in SAP, a number of plots were made from each subject's EMP measurement:

Plot 1: A visual field plot was constructed that showed the response at each tested location as seen, unseen and invalid points to visualise the extent of the visual field and its defects. Of the 'seen' points, the lowest contrast at a particular location was plotted, here referred to as the SI plot (fig 5.1) on a red-green-blue (RGB) scale of 239-113, where 239 corresponded to the lowest stimulus intensity tested, that is, 192 and 113 to 276 cd/m^2. The unseen locations were plotted as black circles [RGB: 0-0-0], and the invalid points were plotted as smaller and empty circles.

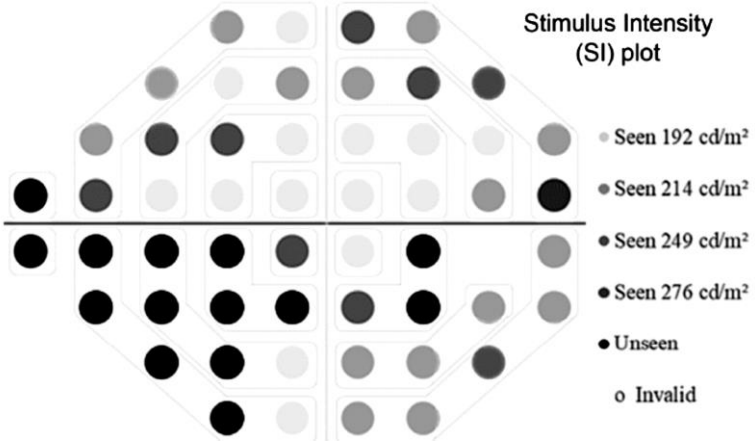

Figure 5.1. Illustration of Contrast plot (Right Eye) created by plotting the eye movement response for the lowest stimulus intensity seen on a RGB scale of [239-113]. The unseen locations were plotted in black [RGB: 0-0-0]. RGB indicates red, green, and blue.

Plot 2: At each location, SRT for the lowest stimulus intensity seen was plotted again using a greyscale plot. SRT ranging between 200ms-1200ms corresponded with RGB values ranging from [230-25]. Thus, the fastest SRTs were plotted in light grey and the most delayed SRTs were plotted in dark grey, see figure 5.2. This plot was called the SRT plot.

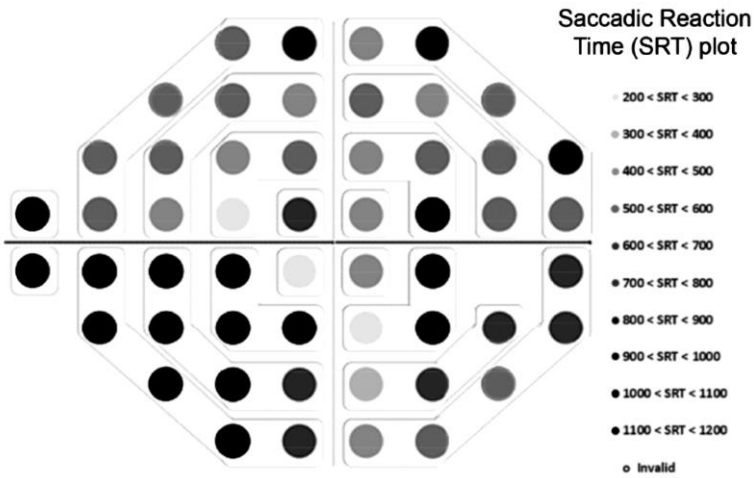

Figure 5.2. Illustration of latency plot (Right Eye) created by plotting SRT for the minimum stimulus intensity seen. The SRT ranging from 200ms-1200ms corresponded with RGB values to plot the greyscale. The blind spot [x= 15, y= -3] was kept blank. RGB indicates red, green, and blue; SRT, Saccadic reaction Time.

Plot 3: Each tested location was graded as normal or abnormal on the basis of the patient's SRT in comparison with the expected percentile levels corresponding to the age matched normal SRT values. The SRTs that were outside the 5% percentile limit were flagged. The probability levels were plotted [fig 5.3] on an RGB scale of 242-64, where 242 corresponds to level 5% and 64 to level 0.5%. The normal locations were represented by a white circle [RGB: 255-255-255]. This plot highlighted the presence of any overall delay in visual field responsiveness. The invalid responses, where eye movement data were not available, were plotted with a smaller and empty circle. The blind spot [x= 15, y= -3] was kept blank. Figure 3 shows an example of this probability plot for four stimulus intensities (PF plot).

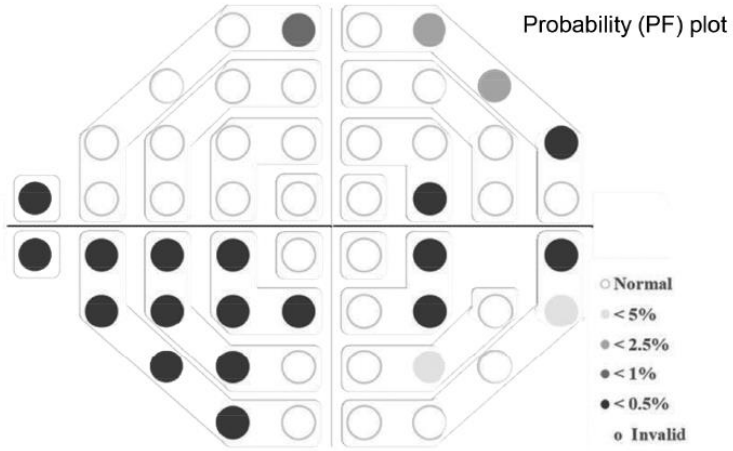

Figure 5.3. The illustration of an EMP probability plot (Right Eye) plotted levels of 5%, 2.5%, 1% and 0.5% corresponded with RGB scale [242-64]. The responses classified as normal were represented with a white circle [RGB: 255-255-255]. EMP indicates Eye Movement Perimetry.

Data preparation for testing phase:

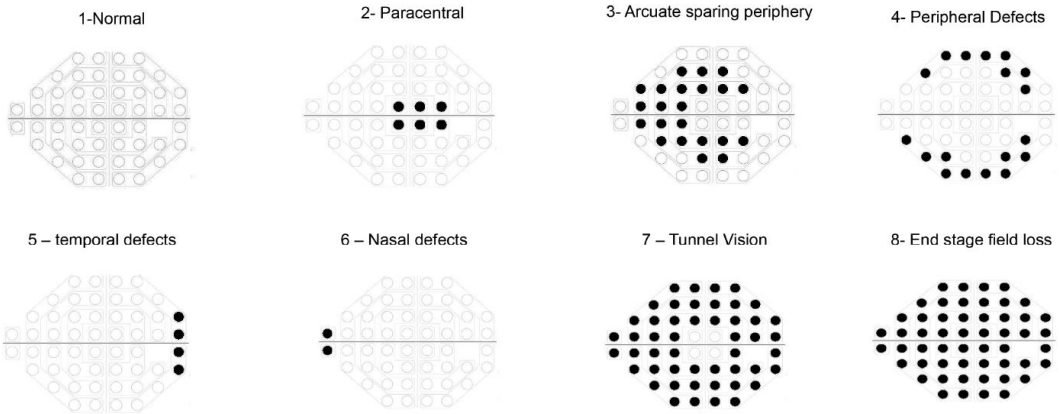

Figure 5.4. Schematic presentation of the patterns of visual field defect classification presented to the specialists. These patterns are adapted from the visual field segmentation of Garway-Heath et al., (1999)

For each subject, the SAP SITA-standard test report, (amongst others the total and pattern deviation plot) and the three customised EMP reports were collected. The modified Andersen's criteria (Anderson & Patella, 1999) were used to discriminate visual fields by SAP into normal and glaucomatous by the investigators. Care was taken to omit all the information from the SAP report that pointed towards a diagnosis of the patient, glaucoma Hemifield test (GHT) alert. The SAP and EMP results were assigned with a unique number to avoid the identification of the results from both devices from a single patient. Two specialists from the glaucoma clinic (one ophthalmologist & one optometrist), who had more than 10 years of experience in the field, were assigned to this study. They were provided with detailed instructions [Appendix I] on the custom generated EMP reports and how to systematically interpret and grade the SAP and EMP visual field reports. The specialists were blinded to the diagnosis and clinical findings. The first step was to discriminate the visual field reports as normal or abnormal. They were asked to further specify the characteristics of the defects of the visual field. For this, the specialists were asked to grade defects on the basis of visual field segments reported by Garway-Heath et al., (1999). These segments of the visual field were derived from the anatomic arrangements of the nerve fibre layers (Garway-Heath et al., 1999). On the basis of the pattern of visual field defect, the specialists had to classify this defect into 1 or more of the following eight groups: 1-normal, 2-paracentral, 3-Arcuate sparing periphery, 4- Peripheral defects, 5-Temporal defects, 6- Nasal defects, 7- Tunnel vision, 8-End-stage field loss inspired from the visual field segmentation of Garway et al., (1999), see also figure 5.4. The two specialists were instructed to mention the defects within the given categories (more than one category if necessary) of visual field defect. Finally, they were asked to note the orientation of the visual field defect as superior, inferior or both. The specialists performed the task independently in about 45 minutes. Both started with the set of SAP visual field plots.

Data Analysis & Statistics

The right eye of each participant was considered for the analysis. Descriptive analyses of the demographic details were carried out. Normality assumptions were assessed using the Kolmogorov-Smirnov test. Independent T-tests were used to compare between two groups. All tests used were 2-sided and type I error was kept at 5%.

The subjects were classified into normal and glaucomatous by the specialists based on the visual field reports generated by HFA and EMP. The sample counts were represented in 2x2 contingency tables. The diagnostic performance (sensitivity & specificity) for the specialists in both the visual field test methods were calculated on the basis of cell frequencies observed in each category. The agreement between the two methods (Inter-method) was assessed using weighted *kappa (*κ).

For the glaucomatous visual field defects, the specialists assigned the type of defect and orientation of the defect for each subject. The highest degree of a defect was considered where more than one pattern was assigned by the specialists. The inter-method agreement for the assigned visual field defect category was assessed qualitatively by cross-tabulation and bar graph was used for the graphical representation.

Results

Testing phase:

From the 66 included subjects, a total of 14 subjects (21%) were excluded. Eight subjects (12%) did not satisfy the SAP reliability criteria and another six subjects (9%) were excluded (>25% invalid responses in EMP) due to eye-tracking problems, that is, data loss due to blinking or loss of tracking. The final analysis included a total of 52 subjects comprising of 28 healthy subjects and 24 glaucoma patients. In the glaucoma group, 4 patients had mild glaucoma, 11 and 9 patients had moderate and severe glaucoma, respectively. Table 5.1 presents the demographic details and the summary of the data.

Table 5.1 Demographics and data summary of the study population

	Normal	Glaucoma	p-value
Age (years)	42 (14)	53 (13)	<0.001
Gender (%)	Male 57% Female 43%	Male 79% Female 21%	<0.001
Intra-Ocular Pressure (mmHg)	15 (3)	15 (5)	0.95
Cup-Disc ratio (-)	0.5 (0.14)	0.8 (0.2)	<0.001
Mean Deviation* (dB)	-1.6 (1.5)	-14.4 (9.4)	<0.001
Saccadic Reaction Time† (ms)	402 (22)	914 (35)	<0.001

*Mean Deviation from Standard Automated Perimetry in decibel (dB), †Saccadic Reaction Time (SRT) from Eye Movement Perimetry in milliseconds (ms).

Normal versus abnormal visual fields

The visual fields were classified into normal and glaucomatous by the specialists on the basis of visual field reports generated by SAP and EMP. The sensitivity and specificity values calculated for the specialists using SAP as the reference standard are shown in table 5.2. A sensitivity of 100% was found for both the investigators and specificity of 93% and 96.4% were shown for investigator 1 & 2 respectively. The inter-method agreement for specialists 1 & 2 was κ 0.92 & 0.96, respectively.

Next, to compare the diagnostic accuracy of EMP, the modified Andersen's criteria (Anderson & Patella, 1999) was used to discriminate visual fields by SAP into normal and glaucomatous by study investigators. The sensitivity and specificity were calculated for the two specialists for SAP as well as EMP and the results of the modified Andersen's criteria were used as a reference. For SAP, sensitivity was 100% for both the specialists and specificity 78% for specialist 1 and 86% for specialist 2 (Table 5.2). The inter-method agreement κ was 0.78 for specialist 1 and 0.84 for specialist 2. For EMP, sensitivity was 100% for both specialists and specificity of 93% for specialist 1 and 96% for specialist 2. Between EMP & modified Anderson's criteria the agreement was 0.92 & 0.96 for specialist 1 & 2, respectively.

Table 5.2. Contingency table for Inter-method Agreement

	Eye Movement Perimetry	Standard Automated Perimeter	
		Normal	Glaucoma
Specialist 1	Normal	26	0
	Glaucoma	2	24
Specialist 2	Normal	27	0
	Glaucoma	1	24
		Modified Anderson's criteria	
	Standard Automated Perimetry	Normal	Glaucoma
Specialist 1	Normal	22	0
	Glaucoma	6	24
Specialist 2	Normal	24	0
	Glaucoma	4	24
	Eye Movement Perimetry		
Specialist 1	Normal	26	0
	Glaucoma	2	24
Specialist 2	Normal	27	0
	Glaucoma	1	24

EMP indicates Eye Movement Perimetry; SAP, Standard Automated perimetry.

Visual field defects agreement based on defect pattern

Agreement between SAP and EMP defect patterns was assessed for both specialists using the patterns depicted in SAP as a reference. The most extensive degree of a defect was used for grading when more than one defect pattern was assigned by a specialist. Figure 5.5 shows the number of cases assigned for each pattern in SAP and EMP by the two specialists. Of the 22 subjects that were assigned to pattern 1 by specialist 1, 20 agreed on EMP as well. This specialist assigned 10 subjects to pattern 3 (Arcuate sparing periphery), while only 4 of them agreed in EMP. The 6 unmatched subjects were assigned to pattern 4 (peripheral defects). Furthermore, specialist 2 assigned more subjects

to pattern 3 in SAP than in EMP, 6 versus 2 respectively. Here, the 4 subjects were also assigned to pattern 4. Overall, for those patterns where SAP and EMP did not agree, the EMP visual field defect tended to be assigned to a higher pattern defect.

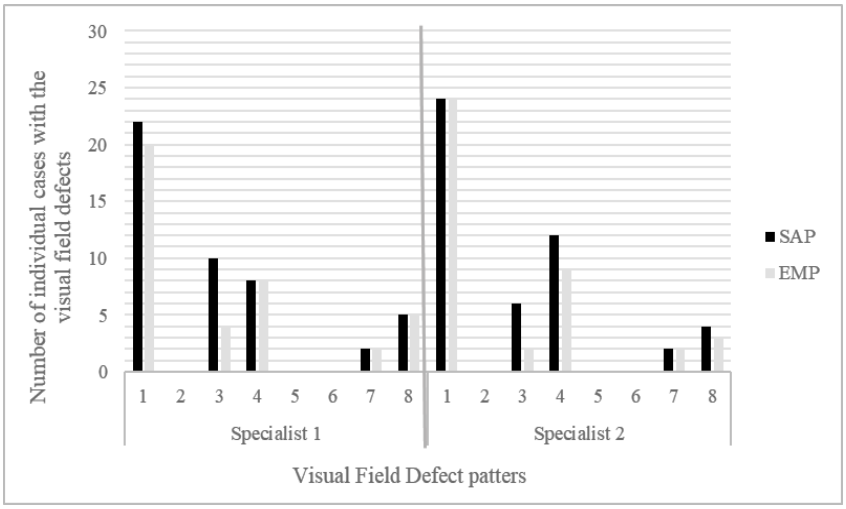

Figure 5.5 The pattern of visual field defects detected for each case by specialists for Standard Automated perimetry (SAP) and Eye Movement Perimetry (EMP)

The subjects were classified into normal, and mild, moderate, severe glaucoma based on their mean deviation (MD) in SAP by using Hodapp, Parrish & Anderson's classification (Brusini & Johnson, 2007). Irrespective of the level of depression, the number of depressed points were obtained from each HFA pattern deviation plot and the corresponding EMP probability plot for each subject. The mean deviation was plotted against the difference between the two (EMP – HFA) of that subject, see figure 5.6. For mild and moderate glaucoma subjects, more points seem to be depressed in EMP compared with SAP. In severe glaucoma, more points seem to be depressed in SAP compared to EMP. In the normal subjects, no shifts of depressed points are seen.

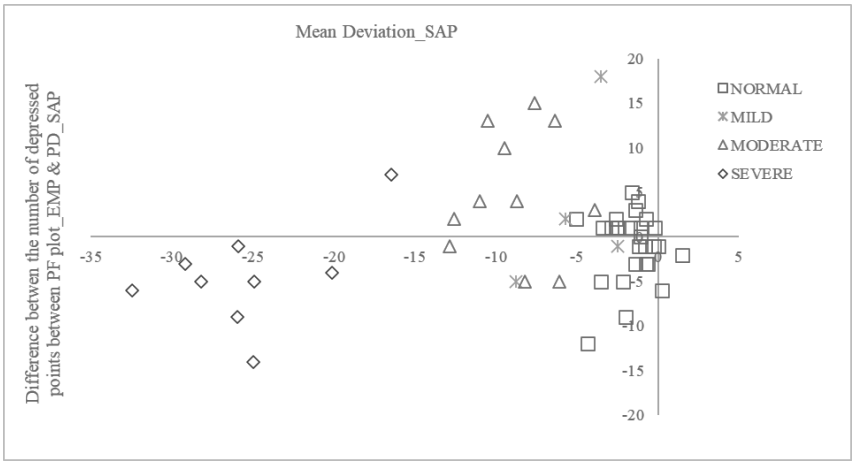

Figure 5.6 The Mean Deviation of SAP [the reference standard] plotted against the difference in the number of depressed points in the visual field by SAP and EMP. EMP indicates Eye Movement Perimetry; PD, Pattern Deviation; PF, Probability plot for four SIs; SAP, Standard Automated Perimetry.

Orientation of the visual field defect

The inter-method agreement for visual field defect orientation between SAP and EMP for specialist 1 and 2 is presented in table 3. The inter-method agreement (κ 0.91 & 0.86, $p<0.001$) was found to be good for both the specialists.

Table 5.3. The inter-method agreement for visual field defect orientation between SAP and EMP for specialist 1 and 2.

	Standard Automated Perimetry	Eye Movement Perimeter				
		Superior	Inferior	Both	kappa	p-value
Specialist 1	Superior	5	0	1	0.91	<0.001
	Inferior	0	2	0		
	Both	0	0	16		
Specialist 2	Superior	6	0	0	0.86	<0.001
	Inferior	0	2	0		
	Both	3	1	12		

EMP indicates Eye Movement Perimetry; SAP, Standard Automated Perimetry

Discussion

We have presented an agreement for visual field defects on probability plots on the basis of SRT values obtained from a large group of healthy volunteers who underwent EMP. The basis for this plot was a normative database that has been described in a previous study (Mazumdar et al., 2019). In the present study, SAP and EMP visual field reports obtained from a new group of healthy controls and glaucoma patients were carefully graded by two glaucoma specialists as normal or abnormal. To avoid decision bias the specialists were approached individually for sorting and grading the visual field reports instead of conducting a collective consensus as reported by McTrusty et al., (2017). This approach allowed us to compare the two independent grading responses. As the random presentation of visual field reports from two different perimetry methods would have bewildered the specialists, we chose to start the process with HFA reports followed by the EMP reports. This was accepted by the specialists as well due to their familiarity with the HFA reports in their routine clinics. Despite the fact of being new, both specialists indicated that the probability plots generated from EMP were easy to comprehend.

Overall, the grading from both the specialists revealed that the EMP probability plots exhibit excellent agreement, in comparison with SAP

while discriminating normal and glaucomatous visual field defects (κ 0.92 & 0.96).

Probability plot in EMP

The pragmatic view of a cut-off value is essential for a clinician to determine the true extent of an abnormally depressed area in the visual field. The empiric probability plots would enable to confirm the presence of the defect, its location, extent, and the statistical significance. The conventional SAP reports present probability plots as Total Deviation (TD) and Pattern Deviation (PD) plots, where TD projects the point-by-point difference in the subject's threshold from the expected in age-matched normal and PD probability plot presents the point-by-point significant deviation corrected for generalized depression in overall field sensitivity (Heijl et al., 1989; Thomas and George, 2001). Here, we have proposed the creation of EMP probability plots based on the SRT values and its comparison with the expected age-matched cut-offs which may offer considerable help to discriminate the physiological age-related delay in SRT from pathological defects. The visual field reports generated by SAP were given to the specialists after removing the details such as GHT alert message, which might influence their grading.

To grade the pattern of the visual field defect, we adopted the visual field segments reported by Garway-Heath et al., (1999) where the area of RNFL bundle loss was defined following the visual field segments that correspond to the predefined optic disc sectors. A similar approach of grading visual field defects pattern was reported by McTrusty et al., (2017) where they used the defect pattern grading (Broadway, 2012) typical to glaucomatous visual field defects. For the current study, we chose to categorize the defect pattern on the basis of the area of the RNFL bundle segmentations (Garway-Heath et al., 1999) as the visual field defects appear on the plots are more relatable if we go by the defect area rather than by typical schematic patterns (Broadway, 2012) used while depicting glaucomatous visual field defects.

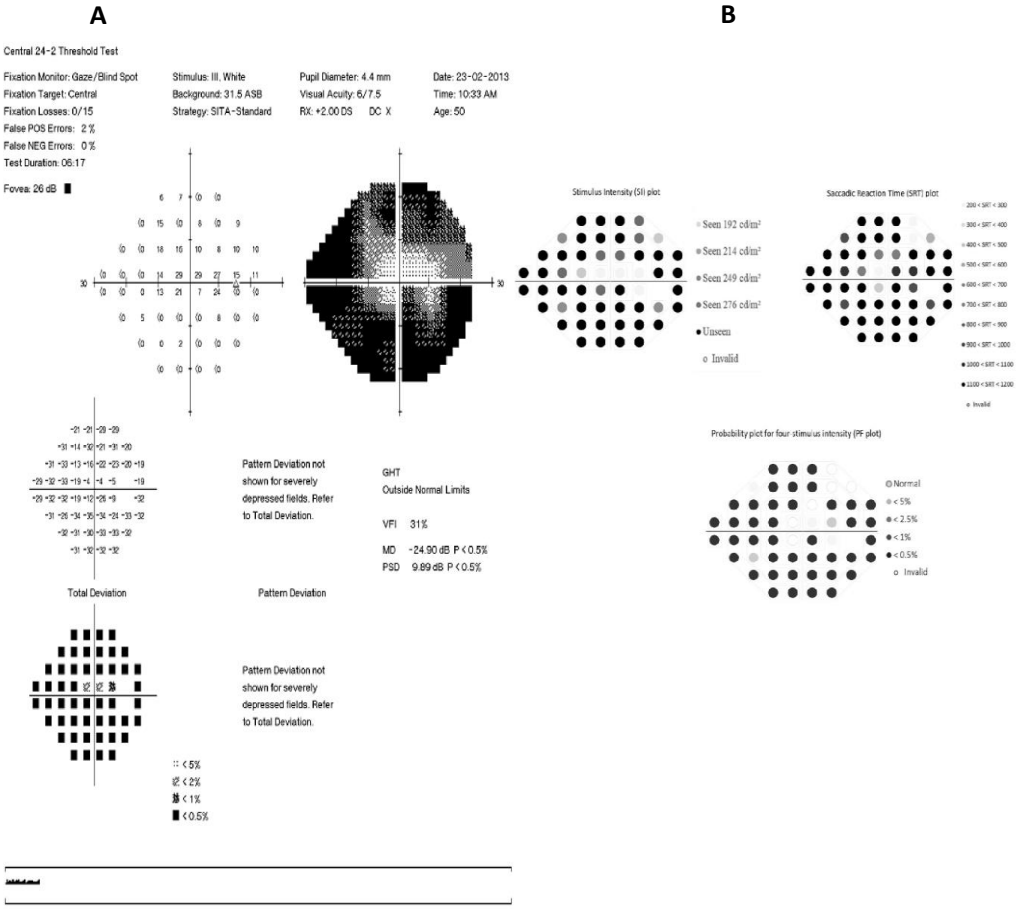

Figure 5.7. A, Presentation of visual field reports for a severe glaucoma subject showing the HFA 24-2 SITA-standard report with end-stage glaucoma or advanced field loss. **B**, The EMP plots for the same patient of (A), with defects corresponding to advanced field loss sparing a small central island of vision. EMP indicates eye movement perimetry; HFA, Humphrey Visual Field Analyser; SITA, Swedish Interactive Threshold Algorithm.

The defect pattern was graded for both SAP and EMP and figure 5.5 was plotted by cross tabulating the number of cases assigned for each category in SAP & EMP. The visual field defect patterns detected by SAP and EMP showed good agreement for both the specialist. For specialist 1 & 2, 85% & 92% of EMP reports were assigned to the same category as SAP. Only 8 reports for specialist 1 and 5 for specialist 2 were differed by more than one category. For these visual field reports,

where SAP and EMP did not agree, the EMP visual field defects found in mild and moderate glaucoma tended to be assigned to a higher defect pattern. For specialist 1, all the 8 reports which did not agree with SAP were graded higher, and, of 5 reports for specialist 2, only 1 was graded milder than SAP. The single visual field report that was graded milder on EMP was with a severe field defect on SAP (fig 5.7A) That did not generate a pattern deviation which probably made the specialist grade the defect for End-stage field loss, whereas in EMP PF plot a small central island (“tunnel”) of vision is remaining when tested in the same patient (fig 5.7B).

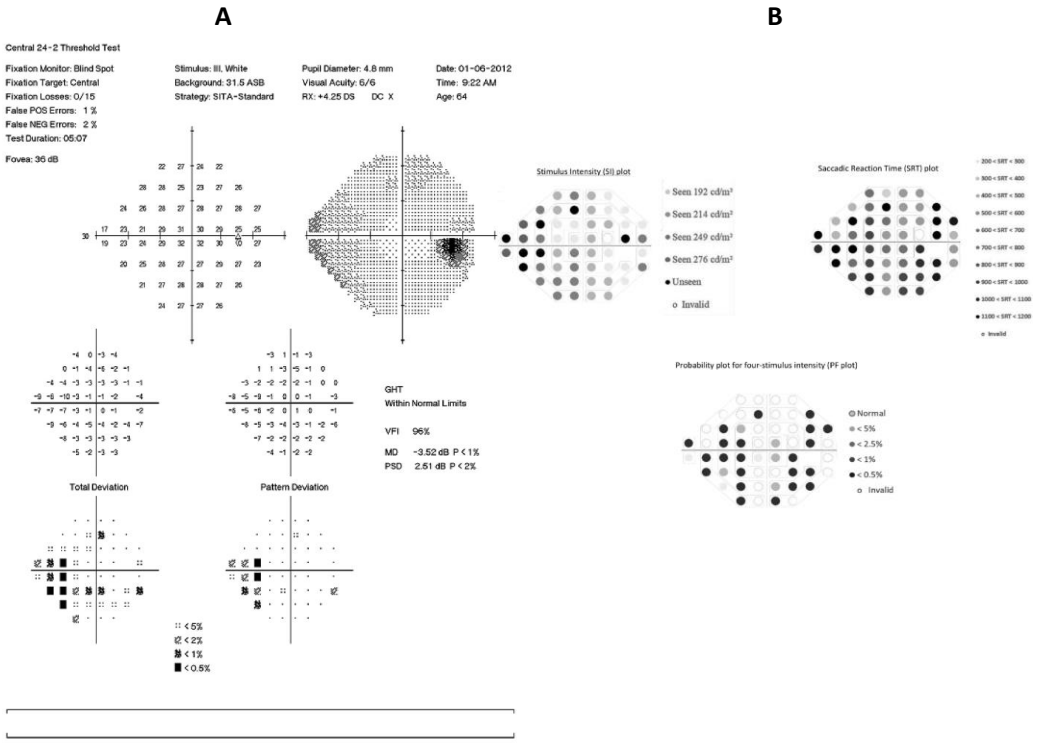

Figure 5.8. **A** Presentation of HFA 24-2 SITA-standard visual field report for a mild glaucoma subject with shallow nasal step. **B**, The EMP plots for the same patient showed in (A) presents nasal defects with additional scattered areas of delayed SRT. EMP indicates eye movement perimetry; GHT, glaucoma Hemifield test; HFA, Humphrey Visual Field Analyser; MD, mean deviation; PSD, pattern standard deviation; SITA, Swedish Interactive Threshold Algorithm; SRT, saccadic reaction time; VFI, visual field index.

In an alternative attempt of comparing the visual field defect between SAP and EMP, irrespective of the level of depression figure 5.4 was plotted considering the difference (EMP – HFA) in the number of depressed points obtained from HFA (pattern deviation) and EMP (probability plot) against the mean deviation (HFA). Analogous to the results found in defect pattern agreement, these results also suggest that the number of depressed points are more in EMP for mild and moderate glaucoma whereas in severe glaucoma SAP showed a greater number of depressed points. The visual field report from HFA in fig 5.8A, showing a shallow nasal step and the structural clinical evaluation is suggestive of definite glaucomatous changes. The EMP PF plot of the same individual is presented in fig 5.8B, showing the same defect pattern nasally with additional scattered areas of delayed SRT.

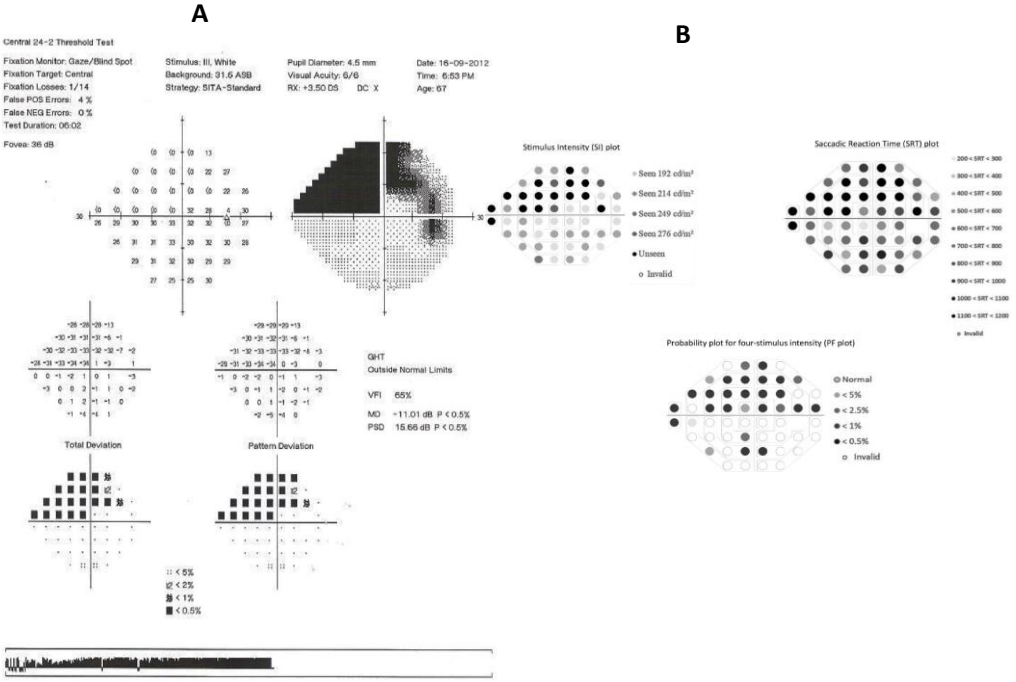

Figure 5.9. A, Presentation of HFA visual field reports for a moderate glaucoma patient showing the superior arcuate defect. **B**, The EMP plots for the same patient in (A) present superior arcuate with additional areas of delayed SRT inferiorly. EMP indicates eye movement perimetry; GHT, glaucoma Hemifield test; HFA, Humphrey Visual Field Analyser; MD, mean deviation; PSD, pattern standard deviation; SRT, saccadic reaction time; VFI, visual field index.

An SAP field with superior defect is presented in fig 5.9A. The PF plot in EMP for the same individual showed superior defects analogous to the HFA report, again with additional scattered areas of delayed SRT (fig 5.9B). Consistent with the findings reported by McTrusty et.al., (2017) on Saccadic Vector Optokinetic Perimeter (SVOP), EMP is also inclined towards producing visual field reports depressed to a higher degree than that of SAP. Even in our previous study (Kadavath Meethal et al., 2019), which evaluated the clinical performance of EMP as a screening method for glaucomatous field defects, 17% of healthy individuals were reported to have delayed SRT values with which they were categorised into glaucoma subset and 43% of mild glaucoma patients were labelled as moderate category by EMP.

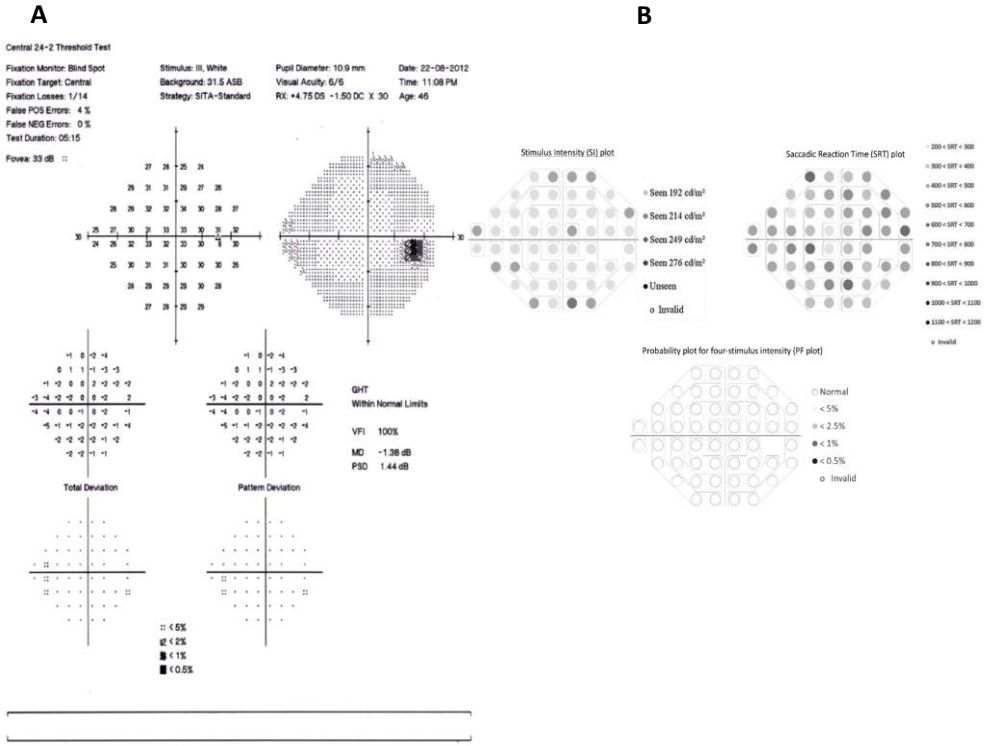

Figure 5.10. **A**, Presentation of HFA 24-2 SITA-standard visual field report for a healthy subject. **B**, The EMP plots for the same subject of (A) showed normal SRT. EMP indicates eye movement perimetry; GHT, glaucoma Hemifield test; HFA, Humphrey Visual Field Analyser; MD, mean deviation; PSD, pattern standard deviation SITA, Swedish Interactive Threshold Algorithm; SRT, saccadic reaction time; VFI, visual field index.

Healthy and glaucomatous subjects were categorized based on established clinical diagnosis [see materials and methods section for details]. Interestingly, we have found some disagreement in classifying healthy subjects based on SAP reports by the two specialists. Out of 28 healthy subjects (clinically), 22 were categorized as normal by specialist 1 and specialist 2 categorized 24 as normal. Using EMP reports 20 out of these 28 was categorized as normal by specialist 1 and 24 by specialist 2. The HFA reports from the healthy subjects being classified as abnormal by specialists could be due to the fact that the information from the HFA report essential to discriminate between 'normal' and 'abnormal' was omitted. To achieve comparable reports for both the test methods (SAP & EMP), the grading was done solely based on the plots. For example, fig 5.10A shows the HFA report from a healthy subject where the 'GHT' alert was omitted while presenting to the specialists. When looking only at the TD and PD plots, the specialist might misclassify the pattern as 'mild' instead of 'normal'. Figure 10B is the EMP report from the same healthy subject, though the PF plot shows an absolutely normal visual field for this particular subject. Overall, EMP tended to show few extra points with delays in SRT which led to the misclassification of normal as 'mild'.

In the current study, unlike SVOP (McTrusty et al., 2017), EMP showed good agreement with SAP for classifying normal by both the specialists. This finding can be justified by recapitulating the basis for the EMP plots creation. As the relation of SRT with age and other factors such as stimulus intensity and eccentricity are well documented, having an age-matched normative basis for defining the likelihood of SRT of a specific age group is necessary. The creation of empirical probability plots would be of considerable help to clearly define the grey zone between undeniably normal and evidently abnormal (delayed SRT) by reducing the ambiguity and thereby minimising the common false interpretations.

Study limitations & Recommendations:

Loss of eye-tracking gaze data, despite any visible abnormalities, was mostly observed in moderate to severe patients. This could be secondary to the adverse effects of anti-glaucoma medications such as

frequent blinking due to dry eyes or other corneal epithelium disorders, long eyelashes, pupillary constrictions caused by parasympathomimetic drugs (Inoue, 2014). Presence of any one of the mentioned conditions could hinder in capturing the pupil centre corneal reflection (PCCR) for eye-tracking cameras to calculate gaze direction.

The numbers of the cases with different disease severity were not equally distributed due to randomised selection criteria. The weight was more on moderate and severe instead of mild. Yet, when comparing the number of depressed points, the few mild cases also showed more depressed points in EMP plots.
Currently, EMP had a different outline of the visual field plots when compared to HFA reports, which presents with additional diagnostic indices (e.g., Glaucoma Hemi-field test and global indices) to consider for classifying visual field as abnormal (Brusini and Johnson, 2007; Thomas and George, 2001). In the current study we are presenting a first attempt to discriminate between a normal visual field from an abnormal on the basis of EMP. Further iterations such as exploring SRT behaviour in the hemi-field sectors, creation of global indices and development of algorithms adjusting the generalized delay in SRT due to high refractive error / dense cataract (>LOCSIII) (Thepass et al., 2015) may be implemented in an EMP visual field report to support clinical decision making.

In the present EMP test paradigm, the longer test duration is a major limitation that might restrain its clinical implementations. Hence, we further worked with the aim of developing a screening protocol where we have attempted to reduce the test duration to approximately 2-2.5 minutes [88 ± 19s for healthy and 151 ± 25s for glaucoma] without compromising the diagnostic ability (Kadavath Meethal et al., 2018 2019). We feel that such an approach is the next step in making EMP feasible in a busy clinical setting. In developing countries such as India, where the prevalence of glaucoma is 11.2 million, a high demand exists for fast screening tools. From a patient preference point of view, a questionnaire revealed that moderate–severe glaucoma patients had EMP preferences over SAP (Kadavath Meethal et al., 2019). The patients felt less anxious due to the fact that eye movements are

allowed during the course of the testing. With reduced testing times this approach may have clinical acceptance.

Conclusion

SRT based empiric probability plots generated by EMP could effectively display the presence, location, and extent of the defect along with the statistical significance. These plots can support clinical decision making by identifying glaucomatous visual field defects.

Appendix

Eye movement perimetry (EMP) report

The EMP visual field report consists of Patient demographics and test details along with the FOUR custom generated EMP plots. Each of the plots are created using grey scales and the corresponding numerical scales are provided adjacent to the plots for interpretation.

1. Stimulus Intensity (SI) plot
2. Saccadic Reaction Time (SRT) plot
3. Probability plot for a Single stimulus intensity (PS plot)
4. Probability plot for Four stimulus intensities (PF plot)

Plot description

1. Stimulus Intensity (SI) plot
Projects the minimum stimulus intensity to which the patient has responded reliably for each specified location while tested using the four stimulus intensities (192 cd/m^2, 214 cd/m^2, 249 cd/m^2 and 276 cd/m^2).

2. Saccadic Reaction Time (SRT) plot
Projects the Saccadic Reaction Time (SRT) corresponding to the minimal stimulus intensity detected by the patient for a particular location.

3. Probability plot for a single stimulus intensity (PS plot)
Categorises each location as ‘Normal’ or ‘depressed’ by comparing the per-location SRT values obtained for a single stimulus intensity (214 cd/m^2) with the expected age-matched values. Depressed locations are segregated to four probability levels based on the severity of delay in SRT. This serves as a quick screening plot for detecting the presence of any gross depression in visual field responsiveness.

4. Probability plot for four-stimulus intensity (PF plot)

Categorises each location as ‘Normal’ or ‘Abnormal’ by comparing the per-location SRT values obtained for all the stimulus intensities with the expected age-matched values. Locations are segregated to four probability levels based on the based on the severity of delay in SRT. This plot illustrates the presence of an overall depression in visual field responsiveness.

CHAPTER 6

SACCADIC REACTION TIME IN MIRROR IMAGE SECTORS ACROSS HORIZONTAL MERIDIAN IN EYE MOVEMENT PERIMETRY

Deepmala Mazumdar [1, 2], Najiya S. Kadavath Meethal [1, 2], Ronnie George [2], Johan J.M. Pel[1]

[1] Department of Neuroscience, Vestibular and ocular Motor Research Group, Erasmus MC, 2040, 3000, CA Rotterdam, The Netherlands
[2] Medical and Vision Research Foundation, Chennai, India

Adapted from: Scientific Reports. 2021 Jan 29;11(1):2630. DOI: 10.1038/s41598-021-81762-y.

Abstract

In Eye Movement Perimetry (EMP), the Saccadic Reaction Time (SRT) to ‘seen’ visual stimuli are delayed in glaucoma. Evaluating SRT behaviour in hemi-field sectors could refine its clinical implication. The development phase included 60 controls retrospectively and for the test cohort in the evaluation phase, another 30 healthy subjects and 30 glaucoma patients were recruited prospectively. The SRTs were used to calculate the normative limits within 5 predefined hemi-field sectors. Scores were assigned to probabilities for SRT at the level of 5%, 2.5% 1% and 0.5%. Per sector pair, a Probability Score Limit (PSL) was calculated at each of the four levels and were compared with the scores obtained from the test cohort. The classification accuracy ‘normal versus abnormal’ was assessed for PSL in EMP and compared with Glaucoma Hemi-field Test (GHT) in Standard Automated Perimetry (SAP). We found no statistically significant differences in SRTs between the mirror sectors in healthy subjects. The PSL at 2.5% had moderate classification accuracy with a specificity of 77% and sensitivity of 70%. This could be suggestive of an SRT delay in the overall visual field in glaucoma.

Introduction

Standard Automated Perimetry (SAP) is the most widely used and accepted functional test to determine the extent of the visual field. SAP uses differential light sensitivity threshold values, and it has been an integral part of the diagnosis and management of glaucoma (Johnson, Wall, and Thompson 2011; Heijl, Lindgren, and Olsson 1989). Eye Movement Perimetry (EMP) on the other hand is an unconventional approach to assess the extent of the visual field using saccadic eye movements (SEM). This technique of testing the visual field relies on reflexive SEM responses from a central fixation point presented in the middle of the screen to consecutively shown stimuli in the periphery. From all the goal-directed SEMs to the seen peripheral stimuli, the saccadic reaction time (SRT) is quantified. Here, a peripheral stimulus is labelled as seen when an SEM is initiated in the direction of the peripheral stimulus and covers >50% of the path (Mazumdar et al., 2019; Kim et al., 1995; Murray et al., 2009; Pel et al., 2013). Therefore, this method introduces the possibility to plot all obtained SRT values as a function of the tested locations as well as a measure of the subject's visual field responsiveness. It was demonstrated that analogous to light sensitivity threshold, SRT depends on subjects' age, and factors in the tested visual field such as stimulus intensity and eccentricity (Mazumdar et al., 2019; Pel et al., 2013; Munoz et al., 1998). Moreover, the SRTs were found to be significantly delayed in glaucoma patients when compared to their age-matched healthy subjects (Kanjee et al., 2012; Lamirel et al., 2014; Mazumdar et al., 2014; Kadavath Meethal et al., 2018; Meethal et al., 2019). In addition, the physiological variability of SRT was considered and empirical probability plots were created to display the presence and extent of the defect along with the statistical significance (Mazumdar et al., 2020). These plots can aid the interpretation of visual field report produced by EMP.

In the Humphrey Field analyser (HFA), global indices such as mean deviation (MD), Pattern deviation (PD) are sensitive to the reduction in light sensitivity as assessed in a population with healthy eyes. Since glaucomatous visual field defect was shown to be localised and

asymmetrical across the horizontal meridian, methods comparing the hemi-fields across the horizontal meridian for the additional diagnostic purpose have been reported in the literature (Enger and Sommer et al., 1987; Åsman and Heijl 1992a). To differentiate between typical glaucomatous defects from the diffuse loss in light sensitivity [caused by media opacities], further refinements of the basic approach were made and termed Glaucomatous Hemi-field Test (GHT). This modified approach, introducing new sector borders corresponding to normal nerve fibre layer arrangements, has been described by Asman & Heijl (1992a). The GHT comprises of 10 sectors [5 horizontal hemi-field sector pairs], where the superior hemi-field sectors are the mirror images of the inferior hemi-field.

Though SRT was found to be delayed in glaucoma, the nature of the glaucomatous visual field defect assessed by SRT is still unexplored. Since the construction of GHT sectors were based on retinal nerve fibre layer arrangements, the exploration of SRT behaviour in GHT sectors may add to a more concise approach of interpreting the EMP reports with respect to the glaucomatous visual field defect. In contemplation of investigating the behaviour of SRT in the GHT sectors, we first aimed to evaluate the SRT behaviour in the 5 superior and 5 mirrors inferior GHT sectors in healthy eyes. Next, the classification accuracy of EMP based on sector-wise comparison of SRTs within the hemi-fields was calculated in an additional group of healthy and glaucomatous eyes.

Materials and Methods

This study comprised of two phases. The first phase is the development of hemi-field sectors normative data. Here, estimation of point-wise normative limits based on SRT values are calculated for each of the five hemi-field sectors in healthy eyes. The second phase is the evaluation of its classification accuracy in a new set of healthy eyes and glaucomatous eyes.

Development of hemi-field sectors normative data

Participants:

Data obtained in the right eye of sixty healthy subjects between 20 and 70 years of age were (randomly) selected from our database to estimate the normative limit for each sector of the Hemi-field. These data were collected between 2012 -2015 and part of this data have been published (Mazumdar et al., 2019). The 60 eyes were grouped into five age groups: 20-29 years, 30-39 years, 40-49 years, 50-59 years and 60 years & above. Each subject had the measurement data available from the Humphrey Field Analyser (HFA) II 750 (Carl Zeiss Meditec Inc, Dublin, CA, USA), program 24-2, with Swedish Interactive Threshold Algorithm (SITA) standard strategy and EMP. The test grids (co-ordinates) in both methods were identical (Mazumdar et al., 2019).

Identifying Glaucoma Hemi-field Sectors in EMP: Analogous to 24-2 SITA Standard GHT sectors, ten sectors were identified and composed of five sectors in the superior hemi-field and their mirror images in the inferior hemi-field, see figure 6.1.

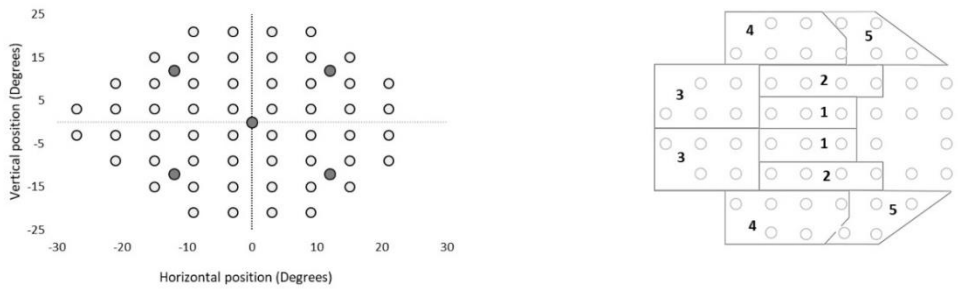

Figure 6.1. The Glaucoma Hemi-filed sectors in EMP test grid; Left panel: EMP 54 points test grid (depicted as circles) with the stimulus locations (blank circles) in degrees and illustrating the position of the fixation stimuli in filled circles (grey), Right panel: EMP test grid partitioned into 10 sectors corresponding to retinal nerve fibre layer anatomy [Åsman and Heijl (1992a)]. The 10 sectors include 5 demarcated sectors in the superior hemi-field and five mirrored sectors in the inferior hemi-field across the horizontal meridian. The five sector pairs are numbered from 1 to 5.

Estimation of normative limits: Limits of normality were estimated from a previously published EMP database, where SRT interaction was evaluated for different factors (Age, Stimulus intensity & eccentricity) within the tested visual field in healthy subjects (Mazumdar et al., 2019). The SRT interaction implies how different factors such as the age of the participant, presented stimulus intensity and eccentricity of the peripheral stimulus affect SRT in the healthy individuals in the EMP test. To estimate the likelihood of SRT for a specified age group, the probability for SRT at the level of 5%, 2.5%, 1% and 0.5% were calculated from this dataset (Mazumdar et al., 2020). The normal limits of the SRT were calculated based on the empirically determined deviations from the age corrected normal SRT. Thus, the 5%, 2.5%, 1%, 0.5% significance levels of SRT distributions were determined separately for each tested point in the visual field in each age group calculating the inverse of the cumulative standardised normal distribution. Any SRT outside the 5% percentile limit were flagged, which means that only 5% of the healthy population of that age group might exhibit such SRT value, whereas the other 95% would show faster SRTs.

Assigning Probability Score (PS) for delayed SRT

The SRTs obtained at all tested locations were checked if they were depressed to a probability level that was adapted from the point - by-point probability scores of Åsman and Heijl (1992a). In the healthy subjects, the raw SRT values were compared with the age-matched normative reference. Higher scores were assigned to the locations showing extreme delays in SRT compared with the age-corrected normal reference database. Instead of using the raw SRT values, these scores were used to calculate the normative limits for each of the 10 hemi-field sectors. A probability score (PS) was assigned against the probability levels, i.e., non-significant - PS= 0, 5% - PS= 1, 2.5% - PS= 2 & 1% - PS= 5. For the locations with extreme delay in SRT at the level of 0.5%, an individualised score was assigned based on the age corrected limit which corrected for the height of the normal reference visual field. This adjusted the overall ceiling effect of SRT delay in the visual field. Here, the scoring was based on the significant delay in SRT

from an age-matched normal value shown in EMP [PS = 10 x Delay in SRT (milliseconds) / 0.5% (SRT limit)], see table 6.1.

Table 6.1: The probability score (PS) assigned for SRT delayed at each probability levels

Probability scores	
The significant probability level for delay in SRT	Probability Score
Not significant	0
5%	1
2.5%	2
1%	5
0.5%	$\frac{\text{10 x Delay in SRT (milliseconds)}^{a}}{\text{0.5\% (SRT limit)}^{b}}$

[a]Delay in SRT is the residual SRT after subtracting the SRT raw value from the age matched normal reference value for that particular location. [b]SRT limit is the expected age corrected SRT value for that location at the probability level of 0.5%. SRT indicates saccadic reaction time in milliseconds.

Determination of Probability Score Limits (PSL) for hemi-field sectors

To estimate the limits for the hemi-field sectors, the PS of all points in each of the 10 sectors were calculated. The absolute difference between $PS_{upper} – PS_{lower}$ was calculated for each sector mirror image pair in 60 healthy eyes. This resulted in 5 Probability Score Limits (PSL) for each sector pair. This procedure was repeated to obtain the PSLs at the level of 5%, 2.5%, 1% and 0.5%, see table 6.2. Later these values were used to estimate the diagnostic accuracy of PSLs at different levels (see, Evaluation of SRT in hemi-field sectors results).

Table 6.2: The normative Probability Score Limits (PSL) in four levels were determined for each hemi-field sector pair from the absolute up-down differences in probability scores obtained from the SRT using Eye Movement Perimetry

Probability Score Limits (PSL)				
Hemi-field Sector Pair	**Levels (%)**			
	5%	**2.5%**	**1%**	**0.5%**
1	14	16	18	19
2	12	14	15	17
3	17	19	21	23
4	24	26	29	32
5	19	21	24	26

SRT, Saccadic Reaction Time

Evaluation of SRT in hemi-field sectors

Participants

A new group of thirty healthy subjects and thirty glaucoma patients between 20 and 70 years of age were recruited from the day-to-day glaucoma clinic in Sankara Nethralaya, Chennai, India. The post hoc power analysis for the sample size of the phase that dealt with the evaluation of SRT in hemi-field sectors revealed the power of 100% with an alpha error 0.05. The age of the subjects included here is representative of the populations reported in the clinic for mild and moderate glaucoma cases. These participants were recruited to estimate the classification ability of the modified Glaucomatous Hemi-field based on SRT values. Subjects with spherical ametropia greater than ±5.00 DSph and cylindrical ametropia of more than -2.00 DSph, best-corrected Visual Acuity less than 20/40, 0.8M and ophthalmic conditions that are known to affect eye tracking, such as ptosis, corneal

opacity and oculomotor nerve palsy, manifested strabismus with deviation > 6 prism dioptre, presence of nystagmus, any history of impaired cognitive status, mental illness or neurological disorders were excluded. Healthy subjects were defined as those with an Intra Ocular Pressure (IOP) less than 21mmHg, with no family history of glaucoma or any other ocular pathologies, a healthy anterior and posterior segment along with a normal visual field. The visual field was assessed using the 24-2 Humphrey Visual Field Analyser (HFA) consisting of 54 points and the Eye Movement Perimeter set-up using the same 54-point test grid in random order. The subjects, who were unable to perform SAP reliably, were not included in the study. Reliability criteria for HFA tests included fixation loss, <20%; false-positive, <15% according to the recommendations of the manufacturer. Subjects with primary glaucoma were defined according to the definition and classification by Foster *et al.* (2002). This classification was used to discriminate between healthy and glaucoma and was used as a reference for further comparisons. The disease severity of the glaucoma patients was classified into normal, mild, and moderate glaucoma using the SAP visual field reports based on Hodapp, Parrish and Anderson's (HAP) classification (Brusini and Johnson, 2007). The eligible subjects were informed about the test and written informed consent was obtained prior to the clinical examination. The study was approved by the institutional review board and Ethics committee of Vision Research Foundation, Chennai, India. The study adhered to the Declaration of Helsinki for research involving human subjects (2013).

Eye movement Perimetry (EMP)

The EMP measurement setup has been previously described (Mazumdar et al., 2019; Mazumdar et al., 2014; Kadavath Meethal et al., 2018; Kadavath Meethal et al., 2019; Mazumdar et al., 2020). Briefly, the test setting includes a 17" Thin Film Transistor (TFT) display with an inbuilt Tobii 120 eye tracking device of refresh rate 120Hz with an accuracy of 0.5 degrees at a testing distance of 60 centimetres. The test started with a nine-point calibration test provided in the eye tracker Software Development Kit inbuilt in the Tobii 120, where the subject needs to follow a red circular target and the calibration was repeated

for the locations that had insufficient gaze data sample. If one or more points were not correctly calibrated, these points were re-calibrated until all points met the criteria (within 0.5 deg. spatial accuracy). Only in a few cases in both healthy and glaucoma group, a re-calibration was needed irrespective of the subject group due to positional alignment or unable to comprehend the instruction in the first time. The test was performed under monocular viewing conditions by covering the non-tested eye with a black Polymethyl Methacrylate plate (PMMA), which permitted the passage of infrared light allowing stable binocular gaze tracking.

In EMP, stimuli with an intensity of 214 cd/m^2 were presented at 54 locations against a background of 152 cd/m^2. The test started with a fixation point presented at the centre of the screen, i.e., position (0°, 0°). After a consistent fixation of 0.5 seconds, a peripheral stimulus was presented for a maximum duration of 1200 milliseconds (ms) using an overlap paradigm. Upon detection, each subject was encouraged to fixate this peripheral stimulus. After a fixation duration of 200 ms, this stimulus disappeared and the subject re-fixated the central fixation point to repeat this sequence. In total, 54 peripheral stimuli were shown in a consecutive manner using the same visual field test co-ordinates used in the 24-2 SITA standard of HFA. To warrant a visual angle of ~60 degrees horizontally and ~45 degrees vertically, we altered the central fixation position (0°, 0°). When 14 peripheral stimuli had been presented, the central fixation stimulus was shifted to an eccentric position (-12°, -12°). Here, 10 peripheral stimuli were shown, and this was repeated another three times (-12°, 12°), (12°, 12°) and (12°, -12°), see also figure 1, left panel for an illustration of the 5 different fixation points used. On average, the test duration was ~7-8 minutes per eye.

The trajectory and time course of each Saccadic Eye Movement (SEM) towards a peripheral stimulus was first visually inspected and next analysed using a previously published decision algorithm developed in Matlab Version 7.11 (Math Works, Natick, MA, USA) (Mazumdar et al., 2019; Kadavath Meethal et al., 2018; Kadavath Meethal et al., 2019). A peripheral stimulus was labelled as ‘seen’ if the responses adhered to the following criteria: a) A SEM, initiated towards the presented

visual stimulus, b) SEM, at onset, was in the direction of the peripheral stimulus and covered >50% of the total fixation to peripheral stimulus distance, c) The angular disparity of less than 45 degrees between the direction of the primary SEM and the peripheral stimulus location. A stimulus was labelled as 'unseen' if the above criteria were not satisfied. 'Invalid' responses were labelled when eye movement data was not available due to blinking or failure in pupil detection and was excluded from the analysis. An EMP report with more than 25% of invalid responses was considered as 'unreliable'. SRT was defined as the time difference between the stimulus presentation and the onset of the SEM towards the direction of the peripheral stimulus based on the gaze velocity criterion by calculation the reaction time at which the eye velocity crossed 80 degrees /seconds.

Data preparation:

For each subject, the SAP 24-2 SITA standard test report was collected with a GHT notification '*with in normal limits'* and '*outside normal limits*. From the EMP measurement, the PSL was determined for each hemi-field sector pair for each subject of the test cohort belonging to the evaluation of SRT in hemi-field sectors. The PSL's of each subject was compared with the normal limits of PSL obtained in the controls. A visual field of a subject was classified as abnormal if the PSL of one or more of the five sector pairs were found outside the normal limits for PSL. This was calculated for all four levels (5%, 2.5%, 1% and 0.5%) of PSL.

Statistical analysis:

The right eye gaze data of each participant obtained at stimulus intensity 214 cd/m^2 was considered for analysis. Statistical analysis was performed using SPSS (Statistical Package for Social Sciences, Version 15, Chicago, IL, USA). Assumptions of normality was assessed using the Kolmogorov-Smirnov test.

A descriptive analysis of the demographic details was done for both phases. The Kolmogorov-Smirnov test was used to assess the normality assumptions of the quantitative variable and appropriate

parametric tests were chosen. Type I error was kept at a 5% level. A two-tailed independent t-test was used for comparison between the groups. Factorial ANOVA was used to assess the SRT behaviour in different hemi-field sectors in healthy subjects of different age groups; a significant interaction was interpreted by a subsequent post-hoc Student-Newman-Keuls test (SNK). Receiver Operating Characteristic (ROC) curves were plotted to evaluate the diagnostic ability of the 4 sets of limits (5%, 2.5%, 1% and 0.5%) using the PSLs obtained from the development phase (see, Table 2). The Area Under the Curve (AUC) values were considered as a measure to quantify the diagnostic accuracy of PSL. The subjects were first divided into healthy and glaucoma using Foster et al. classification (2002). Next, in order to evaluate the ability of PSL to detect glaucomatous visual field defects the glaucoma subjects were divided based on disease severity into mild and moderate glaucoma based on HAP criteria (Brusini and Johnson, 2007) of Standard Automated Perimetry. The number of subjects were represented in 2x2 contingency tables. The sensitivity and specificity were calculated based on the cell frequencies observed in each category keeping the Foster et al. (2002) and HAP (Brusini and Johnson, 2007) classification as a reference standard.

Results

A total of 90 healthy subjects and 30 glaucoma patients aged between 20-70 years were recruited in the study. Table 6.3 presents the demographic details [mean (SD)] and the summary of the data. The glaucoma group was divided into mild and moderate glaucoma with 15 patients in each group using HAP criteria (Brusini and Johnson, 2007) (table 6.4).

Table 6.3: Demographics and data summary of the Development of hemi-field sectors normative data in EMP and Evaluation of SRT in hemi-field sectors study population

	Development of hemi-field sectors normative data		**Evaluation of SRT in hemi-field sectors**		
	Healthy (n = 60)	**p-value**	**Healthy (n = 30)**	**Glaucoma (n=30)**	**p-value**
Age (years)	44(13)	0.94*	45(13)	53(13)	<0.001†
Gender (%)	Male 53%	0.47¤	Male 57%	Male 79%	<0.001‡
IOP[a] (mmHg)	16(3)	0.10*	15(3)	15(6)	0.95†
Cup-Disc ratio (-)	0.5(0.10)	0.21*	0.5(0.14)	0.7(0.2)	<0.001†
MD[b] (dB)	-1.5(1.5)	0.40*	-1.8(1.5)	-8.4(4.5)	<0.001†
SRT[c] (ms)	402(40)	0.20*	380(35)	615(56)	<0.001†

[a]IOP, Intra-ocular Pressure in mmHg; [b]MD, Mean Deviation from Standard Automated Perimetry in decibel (dB); [c]SRT, Saccadic Reaction Time from Eye Movement Perimetry in milliseconds (ms); Data expressed as mean (SD); Type I error was kept at 5% level and two-tailed tests were used. *Independent T-test between healthy eye from Development and Evaluation phase; ¤Chi-square test for proportion of male and female between the groups; †Independent T test for the Evaluation phase of the study population of Normal and glaucoma 30 in each group; ‡ Chi-square test for proportion of male and female between the groups.

Table 6.4: Demographics and data summary of the glaucoma group from Evaluation of SRT in hemi-field sectors phase study population

	Mild glaucoma (n = 15)	Moderate glaucoma (n=15)	p-value*
Age (years)	51(12)	57(11)	0.22
IOP[a] (mmHg)	14(5)	16(4)	0.95
Cup-Disc ratio (-)	0.5(0.2)	0.8(0.1)	<0.001
MD[b] (dB)	-3.5(2.4)	-9.5(2.5)	<0.001
SRT[c] (ms)	482(85)	587(84)	0.02

[a]IOP, Intra-ocular Pressure in mmHg; [b]MD, Mean Deviation from Standard Automated Perimetry in decibel (dB); [c]SRT, Saccadic Reaction Time from Eye Movement Perimetry in milliseconds (ms); Data expressed as mean (SD); Type I error was kept at 5% level and two-tailed tests were used. *Independent T-test

SRT behaviour in superior and inferior GHT sectors in healthy eyes

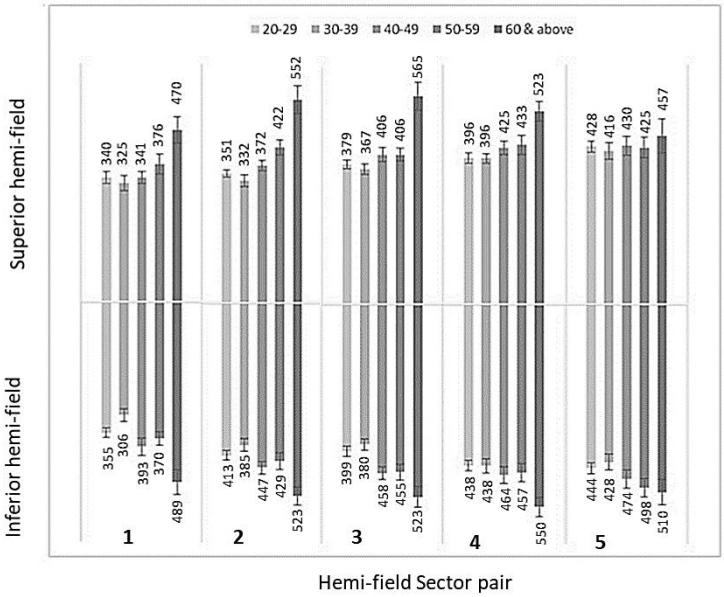

Figure 6.2. The SRT behaviour in Hemi-field sectors among healthy subjects; The mean SRTs with corresponding standard error was plotted among healthy eyes in different age groups between 20 to 60 years & above for stimulus intensity 214 cd/m^2. SRT showed symmetrical behaviour across the age groups in Eye movement perimetry.

SRTs were compared between superior and inferior sector pairs in all 5 age groups in healthy eyes. Overall, a statistically significant ($p<0.001$) interaction was found between the age groups and visual field sectors. The post-hoc SNK test showed that when compared between the mirror image hemi-field sector pairs (such as hemi-field superior sector 1 and inferior sector 1) the SRTs difference were not statistically significant ($p> 0.005$) for any hemi-field up-down sector pairs. Figure 6.2 was plotted using the mean SRT responses from healthy eyes in different age groups aged 20 - 70 for the stimulus intensity 214 cd/m2 in the five hemi-field sectors.

Evaluation of SRT in hemi-field sectors:

The PSLs in the healthy and glaucomatous eyes: The PSL (Probability Score Limits) scores were assessed in 30 healthy eyes and 30 glaucomatous eyes for each of the 5 hemi-field sector pairs. These per eye scores were compared with the normative PSLs obtained from the phase that dealt with the development of hemi-field sectors normative data (table 6.2).

GHT in SAP and PSL in EMP:

The Foster *et al.,* (2002) classification was used to discriminate eyes into normal and glaucomatous, see Table 6.5. The sensitivity and specificity were calculated PSL in EMP at all levels using the Foster *et al.* diagnosis as a reference, see table 6. Since 14 out of 30 of the glaucomatous eyes were misclassified as normal with PSL 0.5%, the sensitivity at this level was compromised to 53% with a promising specificity of 83%. PSL 2.5% showed a balanced sensitivity of 70% and specificity of 77%.

Table 6.5: Contingency table for PSL from Eye Movement Perimetry using the Foster et al*.,* (2002) classification for glaucoma as reference.

		Foster *et al.* classification	
Probability Score Limit in Eye Movement Perimetry		**Glaucoma[a]**	**Normal[a]**
PSL_5%	Glaucoma	21	10
	Normal	09	20
PSL_2.5%	Glaucoma	21	07
	Normal	09	23
PSL_1%	Glaucoma	18	06
	Normal	12	24
PSL_0.5%	Glaucoma	16	05
	Normal	14	25

PSL, Probability Score Limits; [a]All values represent number of subjects.

Table 6.6: Sensitivity and specificity with positive & negative predictive values of PSLs based on SRT at different levels

SRT based PSL[a]	**Sensitivity (%)**	**Specificity (%)**	**Positive Predictive value (%)**	**Negative Predictive value (%)**
PSL_5%	70	67	68	69
PSL_2.5%	70	77	75	72
PSL_1%	60	80	75	67
PSL_0.5%	53	83	76	64

[a] PSL indicates Probability Score Limits and SRT, Saccadic Reaction Time

The area under the ROC curves was plotted for the normative PSLs of EMP at a different level against the Foster *et al.* classification of glaucoma diagnosis, fig 6.3. The Area under the curve (AUC) for the PSLs at different level was ranging between 0.783-0.683, shown in table 6.7.

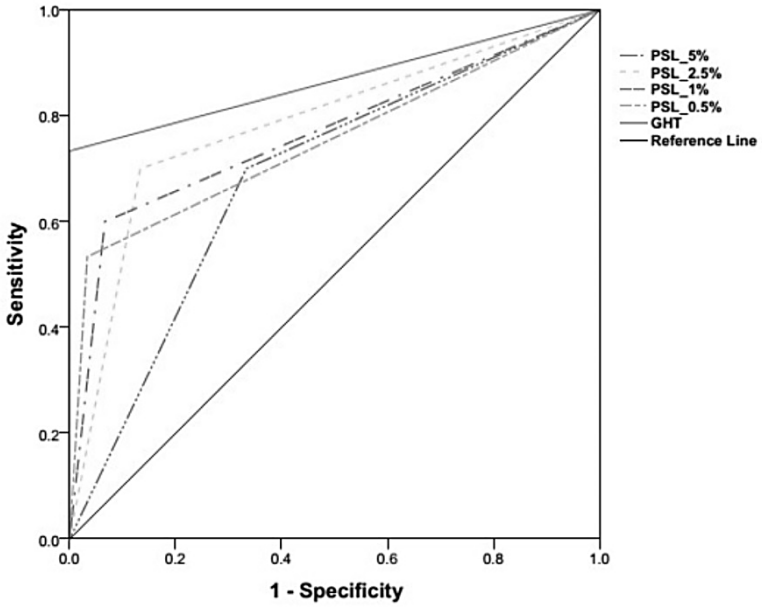

Figure 6.3. ROC curves plotted for the different levels of the normative PSLs of EMP; The PSL values were obtained from SRT estimated at the level of 5%, 2.5%, 1% and 0.5%.

Table 6.7: Area under the curve for the PSLs at the level of 5%, 2.5%, 1%, and 0.5%

Variables	Area under the curve*
PSL_5%	0.683
PSL_2.5%	0.783
PSL_1%	0.767
PSL_0.5%	0.750

* p-value<0.001, PSL: probability Score Limit in Eye Movement Perimetry

Figure 6.4, Left panel presents an SAP visual field report of a mild glaucoma patient as identified with the clinical evaluation (Foster *et al.* & HAP classification) and GHT showing 'outside normal limit'. The PSL of this patient obtained in EMP also showed an asymmetry across the hemi-field meridian when compared to the normative PSL and was labelled as 'abnormal' fig 6.4, Right panel.

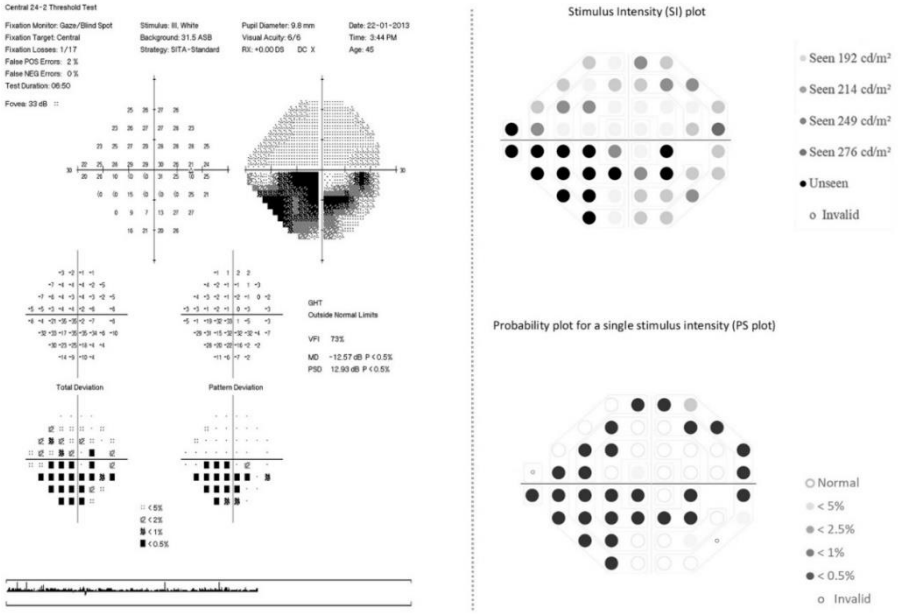

Figure 6.4. Illustration of HFA and EMP visual field report of a patient with mild glaucomatous visual field defect; Left Panel: Presentation of HFA 24-2 SITA-standard visual field report identified with mild glaucoma showing the shallow nasal defect. HFA indicates Humphrey Visual Field Analyser, SITA, Swedish Interactive Threshold Algorithm. Right panel: The EMP plots for the same patient in 4, left panel, Right top panel presenting Saccadic Reaction Time (SRT) plot at 54 points with corresponding numerical greyscale; Right bottom panel presenting probability plot corresponding to the SRT responses at the stimulus intensity 214 cd/m² presents visual field defect nasally with additional scattered areas of delayed SRT. EMP indicates Eye Movement perimetry**;** HFA, Humphrey Field Analyzer; SITA, Swedish interactive threshold algorithm.

Next, an SAP report of a moderate glaucoma patient is shown in fig 6.5, Left panel with an incomplete inferior arcuate defect and GHT indicating ‘outside normal limit’. Figure 6.5, Right panel presenting the EMP reports with comparable affected areas as detected with SAP, but here the PSL was labelled as ‘normal’ due to symmetry across the hemi-field meridian, thus the opposite of GHT in SAP.

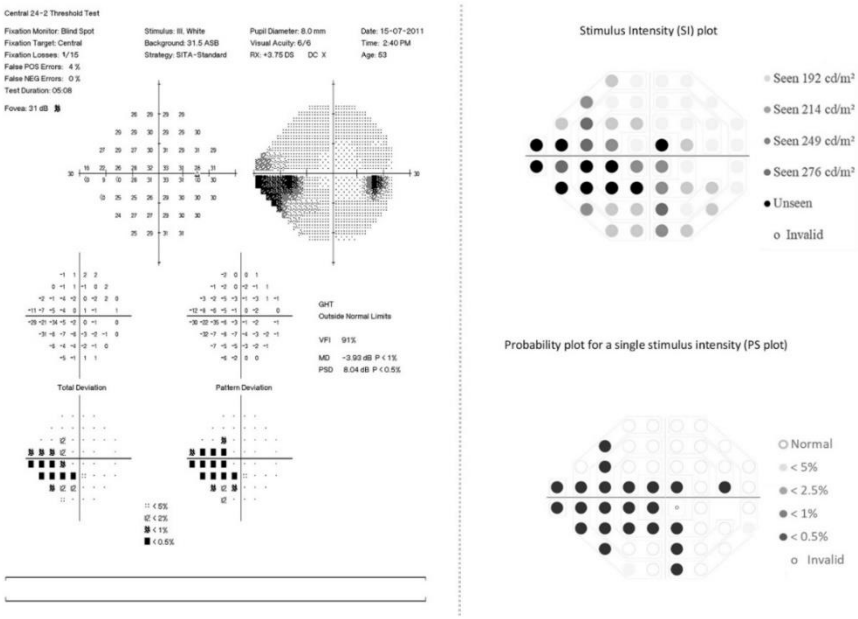

Figure 6.5. Illustration of HFA and EMP visual field report for a moderate glaucoma patient; Left panel: Presentation of HFA 24-2 SITA-standard visual field report showing the incomplete inferior arcuate defect. HFA indicates Humphrey Visual Field Analyser, SITA, Swedish Interactive Threshold Algorithm. Right panel: The EMP plots for the same patient in 5, left panel: top panel presenting Saccadic Reaction Time (SRT) plot at 54 points with corresponding numerical greyscale; Bottom panel presenting probability plot corresponding to the SRT responses at the stimulus intensity 214 cd/m² presents visual field defect inferiorly with additional areas of delayed SRT superiorly. EMP indicates Eye Movement perimetry**;** HFA, Humphrey Field Analyzer; SITA, Swedish interactive threshold algorithm.

The visual fields were further classified into three groups normal (n=30) and a combination of mild (n=15) and moderate (n=15) glaucomatous eyes using the HAP classification (Brusini et al., 2007). To estimate the diagnostic accuracy separately in mild and moderate glaucoma groups, they were compared between the HAP criteria of Humphrey Field Analyser (HFA) and PSL outcome of EMP. The comparison was done based on the PSL outcome ‘normal’ or ‘abnormal’, where 12 out of 15 mild (at PSL 2.5% and 5%) and 9 moderate (at PSL 2.5%) glaucoma

patients were presented with abnormal PSL outcome. The sensitivity and specificity along with positive and negative predictive values presented in table 6.7 were calculated for the PSL levels using HAP classification as the reference standard. The PSL at the level of 2.5% showed a sensitivity of 67% and 60% in detecting mild and moderate defects respectively (table 6.8).

Table 6.8: Diagnostic ability of PSLs from Eye Movement Perimetry in mild and moderate glaucoma using the HAP classification (Brusini et al., 2007) as reference.

Mild glaucoma (n=15)	**Sensitivity (%)**	**Specificity (%)**	**Positive Predictive value (%)**	**Negative Predictive value (%)**
SRT based PSL				
PSL_5%	80	67	55	87
PSL_2.5%	67	77	59	82
PSL_1%	67	80	63	83
PSL_0.5%	60	83	75	87
Moderate glaucoma (n=15)	**Sensitivity (%)**	**Specificity (%)**	**Positive Predictive value (%)**	**Negative Predictive value (%)**
SRT based PSL				
PSL_5%	60	67	47	73
PSL_2.5%	60	77	56	79
PSL_1%	53	80	57	77
PSL_0.5%	47	83	58	76

*HAP classification: Hodapp Parish and Anderson classification (2007)

Discussion

The current study investigated the SRT behaviour within the paired sectors of glaucomatous hemi-fields. Since the GHT approach was used with the aim to detect the localised functional loss commonly found in glaucomatous visual field defects, we used the same GHT

sectors (fig 6.1) as reported by Asman and Heijl (1992a). Here, SRTs showed symmetrical behaviour across superior-inferior hemi-field sectors of GHT when evaluated in healthy eyes. A contrasting pattern was observed in eyes with glaucomatous visual field defects indicating the presence of SRT variability between hemi-field sectors.

Sommer and co-workers reported the first approach of estimating the up-down threshold differences between the mirror image sectors with normative limits (Enger and Sommer, 1987). This approach was refined by Asman and Heijl (1992a), where they introduced the use of significant deviations from normal limits in the mirror image sector differences instead of actual threshold values. Asman and Heijl's approach of estimating normal limits showed improved sensitivity and specificity with the inclusion of only healthy eyes (1992a; 1992b). In the present study, we estimated the normal limits of PS (Probability Scores) in healthy eyes. Since the effect of age and stimulus eccentricity on SRT in EMP is well documented in the literature (Mazumdar et al., 2019), for this study we have derived PSLs (Probability Score Limits) from the significant deviations in location-specific SRT from age-corrected normal than actual SRT.

To estimate the classification accuracy on the basis of EMP, we recruited healthy subjects and patients with mild to moderate glaucoma based on the Foster *et al.* (2002) and HAP (Brusini and Johnson, 2007) classification and excluded those with advanced/severe visual field loss. Inclusion of advanced glaucomatous eyes would likely to have produced little or no asymmetry in the hemi-filed sectors while using SRTs as a measure of visual field responsiveness. However, as suggested by Asman and Heijl, the inclusion of such advanced cases would possibly have lowered the hemi-field test sensitivity (1992a). This could be explained by the fact that the subjects with advanced visual field loss are expected to have a few 'seen' test points and it is often impossible to separate the localised defects from the little or no remaining field of vision.

We decided to restrict our classification of the visual field as 'normal' and 'abnormal' on the basis of PSLs derived from SRT. In the current study, the classification ability for EMP was evaluated on the basis of

the PSL asymmetry across the hemi-field meridian only. The specificity ranged between 83% – 67% and sensitivity 70% - 53% at all the four levels of PSLs [5%, 2.5%, 1%, and 0.5%]. The PSL at the level of 2.5% presented with the optimum combination of specificity 77% and sensitivity 70%, AUC 0.78 (fig 6.3, table 6.7) with good Positive Predictive Value – 75% and Negative Predictive Value – 72% (table 6.6). Even though the PSL approach for classifying normal versus abnormal exhibited well enough diagnostic accuracy, it lacked the sensitivity when estimated separately for mild and moderate glaucoma. Here, the sensitivity dropped especially for the moderate cases [sensitivity 60% & Specificity 77%, at PSL 2.5%] (table 6.8). In mild glaucoma, PSL at 2.5% showed comparatively good discriminatory ability [sensitivity 67% & Specificity 77%] than the rest of the PSL levels.

The relatively lower sensitivity obtained on the basis of PSL, especially in the moderate group, maybe due to the fact that SRT tends to show generalised delay throughout the complete glaucomatous visual field. In several other approaches, EMP has shown a good ability to discriminate between normal and glaucoma when based on the average delay in SRT (Mazumdar et al., 2014; Kadavath Meethal et al., 2018; Kadavath Meethal et al., 2019; Mazumdar et al., 2020) and also on the basis of the binary responses, i.e., seen or unseen (Kim et al, 1995; McTrusty et al., 2017). However, for the current study the magnitude of SRT asymmetry in the mirrored sectors seemed not prominent enough when compared to the light sensitivity threshold in SAP. This is different in GHT. It is worth emphasizing that the approach of GHT was introduced to incorporate the information of retinal nerve fibre layer to enable the possibilities of differentiating localised field loss typical of glaucoma from the generalised one. Najjar et al. and Lamirel et al. reported marked disruptions in SEM in glaucoma patients who exhibited no detectable visual field loss on SAP (pre-perimetric glaucoma) (Najjar et al., 2017; Lamirel et al., 2014). Additionally, another SEM parameter termed saccadic gain is an important measure in order to describe saccade performance with regard to its accuracy and precision. Saccadic gain is calculated as the ratio between the amplitude of the saccade and the distance of the peripheral target from the fixation target. Lamirel et al. reported that saccadic gain was lower

in glaucoma when compared with age-matched healthy subjects (Lamirel et al., 2014). These abnormal eye movements were attributed to the altered neural signalling leading to the inhibition of reflexive saccades. The inclusion of saccadic gain combined with SRT in EMP could be effective in the early diagnosis of disrupted eye movement behaviour in glaucoma. In alternative methods of comparing the glaucomatous visual field defects between SAP and EMP based on SRT, delays in SRT tended to produce visual field reports depressed to a higher degree than that of SAP (Mazumdar et al., 2020) which is consistent with the findings of McTrusty et al., (2017) based on the 'seen or unseen' responses using Saccadic Vector Optokinetic Perimeter. Apparently, these delays are not localised in nature. Even after adjusting SRT for age and other factors in the visual field, i.e., eccentricity and stimulus intensity and exclusion of patients with any visible ocular media opacities, it still depicting an increase in SRTs in the overall glaucomatous visual fields. We conclude that the classification of normal versus abnormal based on PSL in EMP is limited.

Conclusion

The current study demonstrates moderate sensitivity and specificity for PSL at 2.5% in detecting abnormal visual fields using Foster *et al.,* (2002) and HAP (Brusini and Johnson, 2007) classification as a reference standard. The present data suggest an overall delay in SRT in the glaucomatous visual field. Further clarity on the pathophysiological delay in SRT for patients with glaucoma will aid in explaining the visual field defect pattern to be expected using EMP.

Acknowledgement

The authors thank Prof. J van der Steen from Vestibular and Ocular Motor Research group, Dept. of Neuroscience, Erasmus MC, The Netherlands, Dr. Rashima Asokan and Dr. B Shantha from Medical Research Foundation, Chennai, India for their advisory role during the initiation of this work. We also thank Dr. Manish Panday from Medical Research Foundation, Chennai, India for his relentless involvement in patient recruitment and for providing expert clinical opinions.

CHAPTER 7

Manuscript in preparation

CHAPTER 8

GENERAL DISCUSSION

In this thesis, I studied the applicability of Eye Movement Perimetry (EMP) in a clinical setting. In the last decade infrared video-based eye-tracking has become a widely used tool to quantify oculomotor responses to visual stimuli presented on a computer monitor (Larrazabal, Gracia Cena, and Martinez, 2019). One of the promising developments is the use of oculomotor responses in assessing the integrity of the visual field. In contrast to standard perimetry (e.g., Humphrey) oculomotor responses have the potential of providing not only binary responses (seen or not seen) but also quantitative data on response times expressed as saccadic reaction times.

My main aim was to evaluate Saccadic Reaction Time (SRT) in healthy subjects and in patients with glaucoma as an outcome measure of visual field responsiveness.

In this thesis work, I showed that SRT values provide a valid, quantifiable measure of visual field responsiveness and that prolonged or absent SRTs are a sensitive indicator of the presence of defects in the island of vision.

In the first part of my thesis, I focused on the methodological aspect of Eye movement perimetry. In particular, I investigated the relationship between prolonged SRTs and glaucomatous damage. Additionally, I evaluated the effect of eccentricity, stimulus intensity and age with SRT in healthy subjects when tested in a visual field-testing paradigm.

In the second part of my thesis, I focused on the clinical applicability of EMP, in particular, to explore the possibility of making new diagnostic classifications based on EMP. For this purpose, I compared normative SRTs in a cohort of healthy subjects with SRTs obtained from glaucoma patients across different age groups.

The main findings from my studies are:

1. EMP reliably detects glaucomatous visual field defects based on eye movement responses to seen peripheral stimuli.

2. The intact parts of the visual field of patients with glaucoma have delayed SRTs; the more severe the glaucomatous damage, the more prolonged the SRTs are.

3. Analogous to that of SAP, the SRT based probability plots are comparable to conventional clinical standards of visual field assessments.

4. In patients with glaucoma, SRT presents with more generalised suppression of visual field responsiveness compared to the localized threshold suppression in SAP.

5. The EMP method can be used to study monocular versus binocular visual field properties.

In the following sections, I will discuss the advantages and cautions of EMP as an alternative to standard perimetry based on the outcomes of my experiments.

Here, I will discuss the following topics of my research. First, I will discuss the in- and exclusion criteria as a guideline to recruit populations for future studies. Next, I will discuss how the visual field plots and probability plots based on eye movements and SRTs compare to plots used in HFA.

Thirdly, I will discuss the neural pathways involved in generating eye movement responses and the possible causes for the prolonged SRT in glaucomatous eyes.

Fourthly, because demographics may play an important role in EMP, I will discuss the impact that ethnicity may have on eye movement responses and on its normative characterization between Indian and Dutch populations.

Fifthly, I will discuss the possibilities that binocular visual field testing with EMP offers for predicting functional binocular visual field perception and rehabilitation especially in cases with advanced visual field loss.

Lastly, I will present ideas for further evaluation of the EMP method as visual field screening tool in the community.

The testing set-up and characteristics of the study population

In my experiments, the study population comprised of healthy subjects and glaucoma patients aged between 20-70 years. After consenting, the volunteers and patients underwent a complete comprehensive ophthalmic examination. Each subject underwent visual field testing first in SAP using Humphrey Field Analyser (HFA) and then EMP testing. Overall, subjects and patients reported that the strategy of testing visual field using reflexive eye movements without active instructions was easier to perform and was more reliable than other modes of visual field testing even with young children and older adults (Murray et al., 2009; Pel et al., 2010; Kadavath Meethal et al., 2019).

One of the difficulties we experienced was the reliability of the HFA outcomes. Performing HFA reliably requires proper comprehension of instructions and utmost effort from patients. Since most of the glaucoma patients were elderly the effort required to produce a reliable SAP report was challenging. Because SAP was used as our reference standard test to distinguish and confirm healthy from glaucoma subjects, individuals who could not perform SAP reliably even after repeated instructions could not be recruited for the EMP testing (in chapter 5, we had to exclude 12% (8 out of 66) subjects on this ground).

Another limiting factor of EMP was that each subject needed to successfully complete a calibration that involves the fixation of points presented on the test screen. From a technical point of view, a limiting factor when recording eye movements is the quality of the recorded data by the eye tracker. In my studies, I used a remote infra-red Tobii T120 infra-red tracker system which is based on pupil centre corneal reflections (PCCR) at a distance between 50-70 cms. It has a simple inbuilt 9-point calibration test and gaze tracking allows free head movement to some extent. Eye trackers that rely on PCCR may have difficulties with acquiring gaze data of patients with ocular media opacities such as corneal scar, cataracts (>LOCS III), pupillary miosis (<2mm) and blepharospasm. The requirement of vector plotting using the PCCR also hindered the use of EMP in patients with strabismus especially in large-angle strabismus (>6 prism dioptre) of any form. Apart from this, the mandatory calibration test was not successful in

cases where a patient had positional ailment or was unable to comprehend verbal instructions. A good calibration was mandatory for reliable testing. If one or more points out of the 9-points were not correctly calibrated these points were calibrated until all points met the criteria within 0.5 degrees of spatial accuracy.

One of the difficulties which we encountered during the study course is that despite any visible abnormalities, there were instances of poor gaze data quality or loss of data especially in glaucoma patients. This could be due to adverse effects such as dry eyes, long eyelashes, or pupillary constriction from prolong use of parasympathomimetic drugs used in anti-glaucoma medication (Inoue, K. 2014).

A further limitation of the setup we used was the difficulty in detecting small saccades to near central stimuli. The decision algorithm was programmed to include saccades above a velocity threshold of 80^0/sec. The small saccades were often below this threshold. With respect to accuracy: all the stimuli were projected for 1200 ms. Given SRTs varying from 200 – 1100 ms, a 60 Hz sample rate is sufficient for the quantification of delays between populations.

The initial EMP test paradigm had a fixed duration of 12 minutes per eye. The most used testing strategy in the clinics using HFA takes ~7-8 minutes per eye to test the visual field based on the patient's response. This long test duration of EMP was one of the major concerns for accurate testing of a subject's visual field. Hence, we further modified the fixed duration paradigm into an interactive paradigm (chapter 7). Here, the peripheral stimulus projection window was dynamically altered based on the eye movement response time. The test duration of this interactive EMP test program was reduced to an average of ~7-8 minutes per eye (including 4 different stimulus intensities) and thus comparable to that of an HFA measurement. Upon evaluating the patient preference between HFA, Frequency Doubling Perimeter (FDP) or EMP by our study group, 65% of the patients with severe glaucoma preferred EMP. Approximately 20% of the glaucoma patients had complained of claustrophobia (Kadavath Meethal et al., 2019) while performing SAPs. This could be due to its instrumental set up which necessitates the need for placing the head in the bowl in HFA

or in the viewing piece in FDP. The EMP setup is more flexible, allows regular inherent reflexes and has little postural restraints while doing the test. Overall, especially elderly participants with moderate to severe visual field defects reported to prefer EMP over other conventional visual field-testing methods (Kadavath Meethal et al., 2019).

Toward clinical implementation: Eye Movement Perimetry in glaucoma diagnostics

In the introduction of this thesis, I have described the current clinical diagnostics using the SAP report of Humphrey Visual field Analyzer (HFA) as a typical example. The HFA report (fig 8.1, left panel) contains zonal divisions which offer a systematic interpretation of the results. The EMP test paradigm contains the same test grid, and thus an EMP report can be displayed in a similar manner as an HFA report.

A customised EMP test report is presented in fig 8.1, right panel. It shows the same zones for systematic clinical interpretation, i.e., patient information, response plots, global indices, and deviation plots. Reliability indices, such as fixation losses and the number of false positives, are not included in this example. The patient response deviation maps are to evaluate SRTs in the visual field by differentiating between healthy and abnormal SRTs as well as highlighting the presence, extent, and depth of the depression in the field of vision. To illustrate the strategy used to estimate normative data, the location wise SRT deviations of three different co-ordinates are shown in figure 8.2.

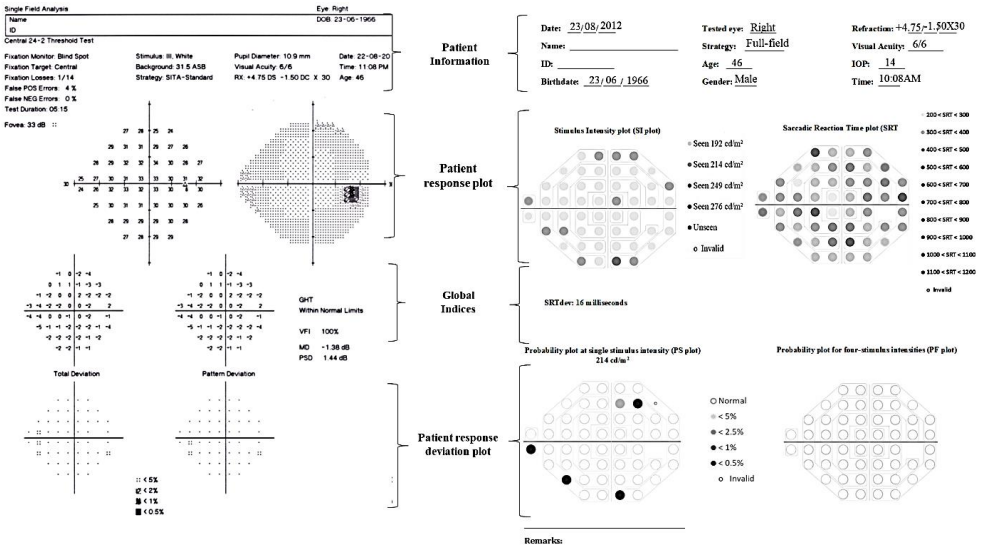

Figure 8.1: 'Single field analysis' report from HFA (left panel) and EMP (right panel) with marked zones within for systematic clinical interpretation.

Estimation of normative reference limits to differentiate normal and glaucomatous Saccadic Reaction Time

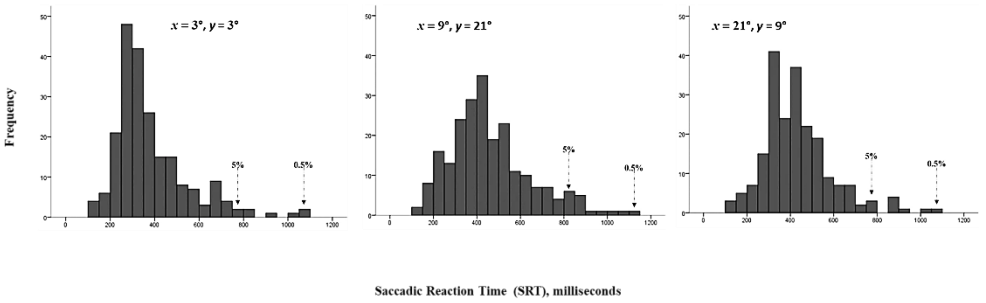

Figure 8.2: Three locations from the visual field test coordinates are presented here with the SRT deviations from age-corrected healthy subjects. The observed 5% and 0.5% percentiles are marked. This was done for all the tested locations at each stimulus intensity.

To differentiate between a 'normal' and an 'abnormal' visual field, the SRT cut-offs (5%, 2.5%, 1% and 0.5% percentiles) were estimated at each tested location and for each stimulus intensity obtained in healthy individuals. Because of the non-Gaussian nature of the distribution of

SRT, the normal limits were calculated based on empirically ascertained deviations at each tested location from the age corrected normal SRT. The age bins were chosen with 10 years interval between 20 years to 60 years and above. The normative limits were determined at the significance levels of 5%, 2.5%, 1% and 0.5% separately at each tested location in different age bins for all the stimulus intensities by calculating the inverse of the cumulative standardised normal distribution. To assemble the EMP probability plot, points that were delayed to a level of less than 5% of the normal age-matched population were flagged. Additionally, the EMP report contains the probabilities that are associated with the presence of any subtle depression in the tested field of vision. Additional to the visual field plots the HFA report contains auxiliary diagnostics indices known as global indices (see, page 23). As a global index, the EMP report contains SRT deviation information as 'SRTdev' of the overall visual field which summarizes the visual field when compared with normative limits.

Since SAP and EMP are entirely different modalities of testing the visual field, it was not possible to assess both outcome measures in the same measurement. The SAP was used as a reference standard to quantify the diagnostic ability of EMP (chapter 5). In this research, we reported a qualitative comparison of visual fields between EMP and HFA (like fig 8.1). In addition to the Total deviation plot (i.e., age-adjusted result), HFA also adjusts the visual field outcome for any overall depression in the hill of vision triggered by conditions (such as cataract, high refractive error) other than glaucoma. Unlike HFA, the empiric probability plots used in EMP are generated exclusively after adjusting for eccentricity, stimulus intensity and compared with the age-matched healthy subjects but not adjusted for overall depression in the visual field. In a previous study done in our lab, it was shown that cataract up to LOCS III does not alter SRT responses (Thepass et al., 2015). Further studies exploring SRT delays in relation to other factors such as high refractive error might add information necessary to construct a visual field report adjusting for the overall depression in the hill of vision.

Causes of prolonged delays: How Glaucoma affects preparation and initiation of eye movements in pro-saccade task

From a clinical point of view, glaucoma has long been associated with increased intraocular pressure (IOP). Since the last two decades, researchers and clinicians have been considering glaucoma as a primary optic neuropathy with highly characteristic changes in the optic nerve head (ONH) morphology, accompanied by thinning of the nerve fibre layer, and eventual loss of RGCs (Vrabec and Levin, 2007). Since the Lateral Geniculate Nucleus (LGN) within the thalamus and the superior colliculus are the main targets of RGCs (fig.8.3), glaucomatous changes are likely to affect these areas of the midbrain as well (Crish et al., 2010). The LGN is the link between the optic nerve and the occipital lobe, the primary cortical visual input station with projections to a wide range of visual cortical areas (see figure 8.3). At the motor execution side, it is the superior colliculus that receives its information from the prefrontal and parietal areas and is responsible for transforming the sensory input into motor commands to generate eye movements. Any structural changes in these areas might functionally manifest delays in processing visual information and in preparing and executing eye movements. This notion fits well with the observations and results described in this thesis. Although the effect of glaucoma on eye movements has been reported in the literature (Murray et al., 2009; Kanjee et al., 2012; Smith, Glen, and Crabb 2012; Asfaw et al., 2018), to date no quantitative method is available that enables clinicians to characterise glaucoma with the help of saccadic reaction times. Najjar et al., reported altered saccadic eye movement properties that included saccadic velocities, amplitudes, and gains in patients with primary open-angle glaucoma (in pre-perimetric glaucoma patients) (Najjar et al., 2017). In my thesis, I show that the average SRT is increased in glaucomatous eyes when compared to healthy eyes. An additional finding was that SRT's increased with disease severity, i.e., 'mild', 'moderate' and 'severe' stages of glaucoma (chapter 2). These findings underline the importance of EMP that not only allows the assessment

of the width / extent of the visual field but also its responsiveness to stimuli that are shown in the visual field.

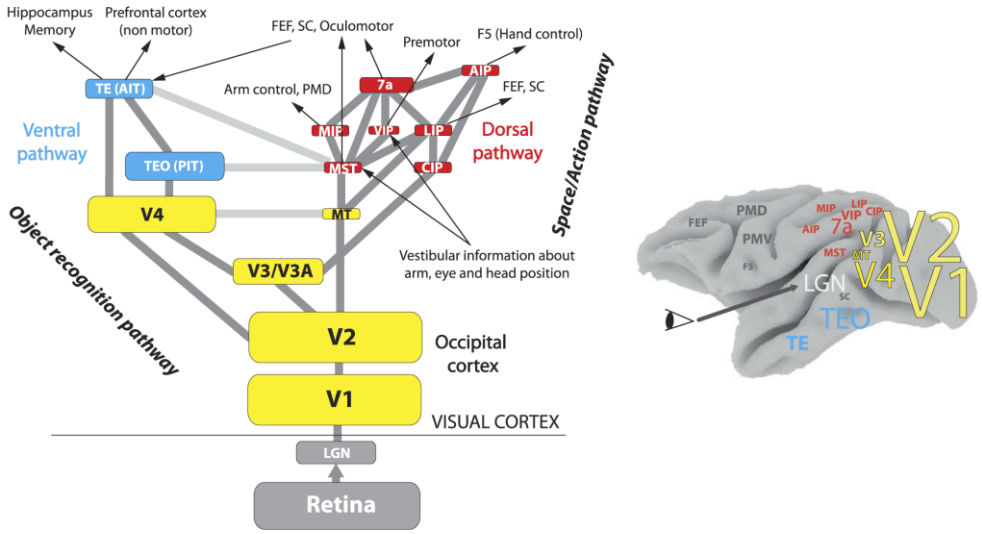

Figure 8.3: Projections of visual information from the retina to the visual cortex with areas in the dorsal and ventral streams are presented in a simplified hierarchical structure. The areas are arranged retinotopically and presented with different box and font sizes relative to their size. (*Kruger N et al., 2012*)

Early detection of functional changes in glaucoma using Eye Movement Perimetry

To evaluate SRT behaviour in the early detection of glaucoma, we selected glaucoma patients from our database in whom structural changes such as retinal nerve fibre layer abnormalities via Optical Coherence Tomography were not associated with detectable functional loss in SAP. These patients are often referred to as ‘pre-perimetric’ glaucoma patients (Susanna Jr. and Vessani, 2009).

One case is presented in fig 8.4. This patient exhibited a normal visual field with structural changes in the right eye (RNFL thinning inferiorly) which was definitive of glaucoma in the first visit (fig 8.4, left panel). The EMP report, that was created on the same day shows delayed SRTs in the nasal area (Fig 8.4, centre panel). The left eye of the same patient presented with both structural and functional glaucomatous

changes in the first visit. The visual field in left eye revealed depressed areas extending from the central visual field towards the blind spot also called coecocentral scotoma (fig 8.5, left panel) and structural evaluation showed RNFL thinning. The EMP report depicted significantly delayed SRT in the superior visual field and scattered delayed areas inferiorly involving the central visual field in the left eye (fig 8.5, centre panel).

After 4 months, the same patient underwent a follow-up measurement. Comparable to that of EMP report of the first visit, the HFA visual field report revealed depressed areas nasally and scattered depressed areas in the superior visual field in the right eye (fig 8.4, right panel) which was not present in the first visit. In the left eye, the follow up visual field report presented similar areas of reduced sensitivity as that of EMP in the first visit (fig 8.5, right panel).

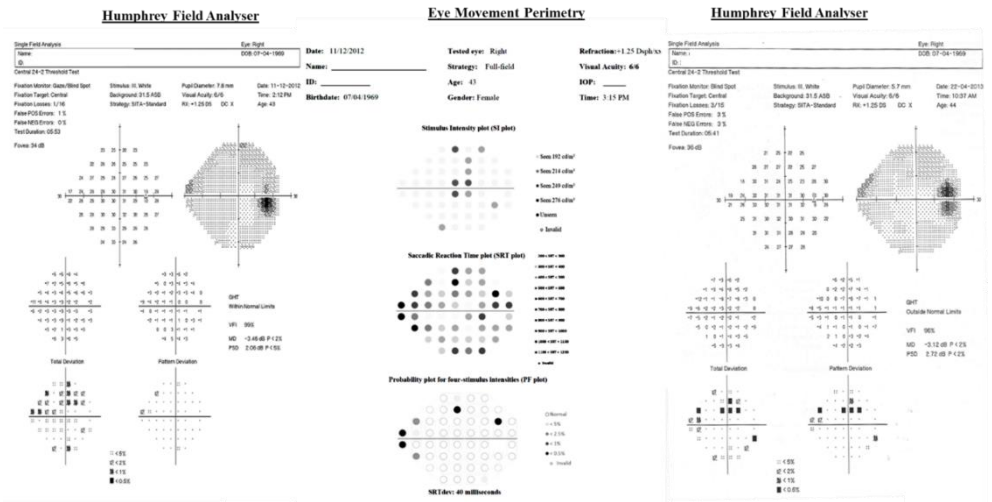

Figure 8.4: Presents visual field analysis reports of a glaucoma patient with 'pre-perimetric glaucoma' in the right eye. *Left panel*, SAP single field analysis for the right eye in the first visit; *Centre panel,* EMP visual field showed significantly delayed areas of SRT nasally; *Right panel,* The SAP visual field at the follow up visit after 4 months presenting nasal defects with scattered depressed areas in the superior visual field.

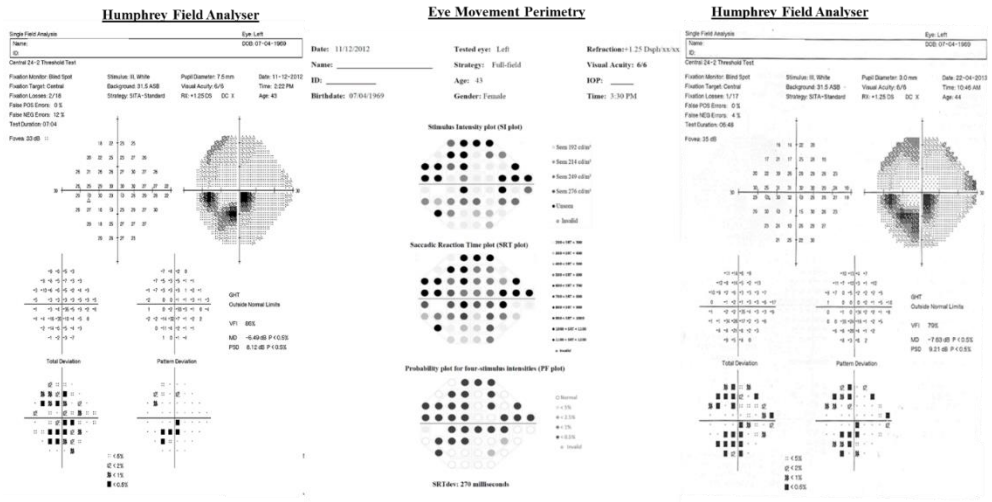

Figure 8.5: Presents visual field analysis reports of a glaucoma patient with moderate glaucoma in the left eye. *Left panel*, SAP single field analysis presented with depressed areas extending from the central visual field towards the blind spot in the first visit; *Centre panel*, EMP visual field depicted significantly delayed areas of SRT in the superior visual field and scattered delayed areas inferiorly; *Right panel,* The SAP visual field at the follow up visit after 4 months presenting depressed areas as that of present in EMP.

This patient is an interesting case; we see SRT changes in EMP and at the same time no detectable visual field loss on SAP. This case underlines the importance of quantifying the oculomotor responses as an index of measuring visual field responsiveness in patients with glaucoma and exploring the possibilities of early detection of glaucoma. Alterations in saccadic eye movement in POAG pre perimetric glaucoma patients were reported by Najjar et al. Their experimental set-up contained prosaccade and anti-saccade tasks (Najjar et al., 2017). A possible explanation could be that only after a substantial amount of Retinal Ganglion cell loss, SAP is able to detect functional changes (Quigley, Dunkelberger, and Green 1989; Hood, D.C., 2019). And the fact that altered SRTs are detectable might relate to the axonopathy of the RGCs at the level of the superior colliculus which precedes that at the level of the retina. To investigate these mechanisms and the potential contribution of EMP, further study is needed that includes a long-term follow up of ‘pre-perimetric’ cases.

Ethnic Variations in Saccadic Reaction Time by Eye Movement Perimetry

The empiric probability plots that have been calculated in this thesis are based on the normative values obtained from a healthy Indian population. Previous research has reported differences in saccadic reaction time as well as in fixations across different ethnic groups when tested with gap and overlap paradigm in a prosaccade task (Delinte, 2002; Rayner, 2007; Alotaibi, Underwoord, and Smith 2017). Another study on eye movement behaviour suggested that the genetic, racial, and cultural differences affect the morphology of the eye movement behaviour and should be considered while studying saccadic behaviours (Mardanbegi et al., 2020). Although the eye movement behaviour among ethnic groups is well reported in the literature, their combined effect when tested in a visual field test has not been reported. Thus, to introduce EMP into other communities, we need to address the question of whether there is a need for normative databases in different ethnicities. Since this thesis is a collaborative work between India and The Netherlands, this induced a unique opportunity to compare SRTs between Indian and Dutch populations. In chapter 4, a first attempt was made to compare normative SRT values in different visual field eccentricities and 5 age bins of 10 years each. Overall, statistically significant differences were found in SRTs between Indian and Dutch adults using a generalised linear mixed model analysis. The healthy Indian adults (irrespective of the groups and stimulus intensity) showed a trend of delayed SRTs in the central visual field compared to the Dutch counterparts. However, in the mid periphery to the peripheral visual field, Indians presented with faster SRT. Since the criteria for diagnosing glaucoma patients are comparable in India and the Netherlands, we further analysed the EMP results obtained in a group of age-matched glaucoma patients [n= 28 Indian and 38 Dutch]. Comparison between the Mean Deviation (MD) from HFA showed no statistically significant difference between both groups (Indian [Mean: -11. 05 (SD:10)dB] and Dutch [Mean: -9.02 (SD:7.23)dB]; p=0.37; Independent t-test). The patients that we selected were aged 50 years and older. To compare the SRTs with their age-matched healthy

counterparts we divided the patients into 2 age bins: 50-59, 60 and above.

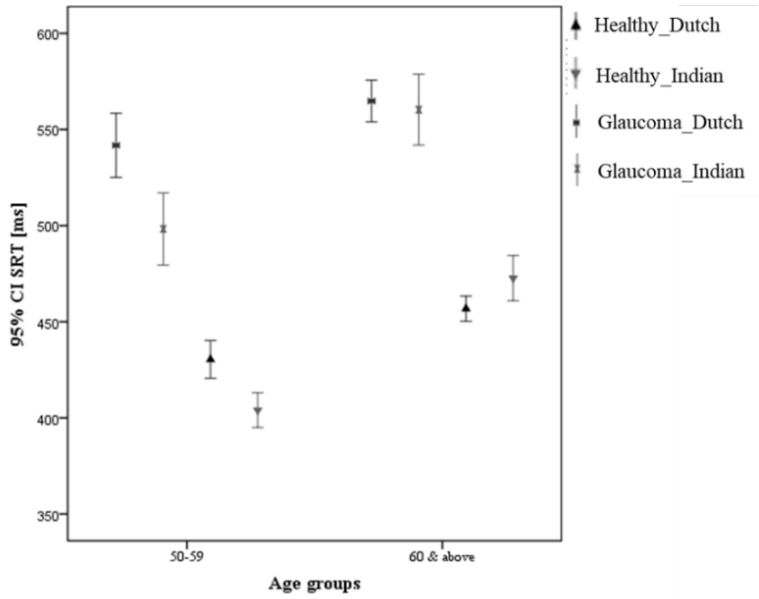

Figure 8.6: The illustration was generated using the mean and corresponding 95% CI* of SRT for the healthy subjects and patients diagnosed with glaucoma for age groups 50-59, 60 years and above. Mean SRT plotted between age-matched healthy and glaucoma individuals irrespective of the disease severity. *CI, Confidence Interval

Figure 8.6 illustrates the mean SRT with corresponding error bars representing 95% confidence interval (CI). The mean SRT was plotted for healthy and glaucoma (irrespective of their disease severity), for the age 50-59 and 60 years and above. It shows that for both age groups, the SRTs were delayed when compared with age-matched controls in both ethnicities. Yet, this example outlines a large difference in SRTs between healthy with glaucoma. A statistically significant SRT interaction was found between the effects of ethnicities and age groups in healthy adults, $p<0.001$ (Two-way anova). Pairwise comparison analysis with Bonferroni posthoc test showed that SRTs from 50-59 years Indian adults [mean 404 (SD 147) ms] were significantly ($p<0.001$) faster than the Dutch counterparts [mean 430 (SD132) ms]. Whereas the 60 years and older Indian adults [mean 473 (SD 166) ms] showed significantly ($p<0.001$) delayed SRT compared to the age-

matched Dutch group [mean 457 (SD 153) ms]. Still, when comparing SRTs between the glaucoma groups, no statistically significant interaction found among the ethnicities.

This preliminary evaluation shows that there is a prominent difference in SRT between glaucoma and healthy controls irrespective of ethnicity. In chapter 4, we showed a statistically significant trend between the age groups among Indian and Dutch participants. When, we compare glaucoma patients with age-matched healthy groups no overlap was found between the groups across ethnicities. Thus, from this interim analysis, a first assumption could be that for the first line of screening test the Indian normative database is sharable for the age group 50 years and above. However, additional evaluation of SRTs within the visual field is also necessary to establish whether the same follows for the younger patients with glaucoma (below 50 years) and across glaucoma severity. My view is that, to establish EMP measurements in clinics, it is advisable to consider age-matched ethnicity-based normative databases for SRT.

The impact of Binocular visual field testing in Eye Movement Perimetry

A key feature of EMP is to obtain visual field properties under binocular viewing conditions. The current clinical practice relies on monocular visual field testing for diagnosing and monitoring glaucoma course. Although the binocular functional visual field provides clinicians more information about patient's actual functional field of vision, at the clinical level quantifying the binocular visual field testing is still in its infancy. Humphrey Field Analyser's Esterman test assess visual field under binocular viewing condition with a bright fixed stimulus intensity of 10dB. This makes the test to overestimate the actual functional visual field (Smissth 1988). We used the EMP test set up to assess visual field properties under binocular viewing condition which allowed us to maintain a near real-life scenario as well as to map the extent and depth of the visual field defect manifested under binocular viewing condition (chapter 7). Our findings indicate that as hypothesized, EMP under binocular viewing condition showed more preserved visual field

responsiveness in cases with glaucomatous visual field defects compared to the monocular visual field. This could be explained by the fact that binocular viewing doubles the chances to detect a stimulus than in monocular conditions, statistical considerations of predicting improved binocular sensitivity from monocular sensitivity of each eye, as has been put forward in the binocular summation model (Blake et al., 1981). Since the use of various statistical predicting models in the simulated binocular visual field is well documented (Nelson-Quigg, Cello, and Johnson 2000; Crabb et al., 1998; Crabb & Viswanathan, 2005) further studies comparing the EMP binocular result with such models would tell us about the type of summation that is taking place in the brain.

Improved responses in binocular viewing may also be explained by asymmetric glaucomatous visual field defects. The preliminary findings in a small set of cases with asymmetric glaucomatous visual field defect indicate that EMP can be explored further to assess quantifiable visual field under binocular viewing condition. Particularly when a patient presents with an asymmetric visual field defect, a complete picture of the patient's functional visual field responsiveness is outlined. One of the hurdles in our study of estimating the binocular visual field is the absence of a clinical standard to compare its diagnostic accuracy. A first step could be to compare EMP binocular visual field results with those from the Esterman test (Esterman, B. 1982) would provide new insights.

Several studies have been conducted to examine the link between visual field restriction and activities of daily living (ADL) especially driving (Sippel K, 2014; Kasneci, Black, and Wood 2017; Kübler et al., 2015). The conventional monocular field tests are poor predictors of useful field of view. Health-related quality of life survey reported that an individual with glaucomatous visual field loss reports more difficulty in driving than subjects with a normal field of vision (McKean-Cowdin R, 2008). Visual field defects also reported having an impact on hand-eye coordination as well as increase the likelihood of falling (Freeman et al., 2007; Kotecha et al., 2009; Zwierko et al., 2019). In clinical practice, glaucoma specialists usually address patient's queries on ADL based

on the better eye. Since people use both eyes together, a binocular measure of the visual field is more likely to be the best way to predict the impact of visual field defect on a patient's quality of visual life (QoVL). It seems sensible to further investigate the visual field loss considering the summary measures from a binocular visual field measurement to evaluate the impact of the loss of useful vision in everyday function. Since EMP binocular visual field estimates the intactness of useful field of vision, it might expand the current knowledge about the 'tipping point' of when visual field defect becomes significant enough to cause disability, especially in ADL. This can be an integral contributory factor to understand the restrictions faced by the patients while participating in the activities of various domains of life including outdoor mobility/navigation, driving, crossing the road, household tasks and personal care that demands functional peripheral vision. The dynamic nature of the binocular saccade based EMP method will provide a way to investigate the visual field responsiveness and its use in real-life scenarios that will lead to the timely referral for low vision care and rehabilitation.

A roadmap towards modernising visual field testing

We showed that based on SRTs the EMP test can differentiate glaucomatous alterations in the visual field. Because we find such consistent SRT delays in patients diagnosed with glaucoma, I recommend clinical implementation of EMP especially for patients that fail to produce reliable SAP results. In multiple chapters, we addressed that EMP detects delays even in mild glaucoma patients without any noticeable functional changes in SAP. This implies that the EMP test is a potential tool to be implemented in the community, especially in the countries with remote/rural areas, for screening on possible early signs of the disease. Keeping the normative database as a basis, an attempt was made to make the testing time ideal for a screening device (Kadavath Meethal et al., 2018). Identifying the locations which were most susceptible to glaucomatous changes, we have reduced the 54-point EMP test grid to 26-point grid, which warranted an average test duration of ~2 minutes. This screening test grid showed 91% classification accuracy and the patients preferred the EMP screening

test over Frequency Doubling Perimetry (FDP) (Kadavath Meethal et al., 2019), the current clinical standard for screening glaucomatous visual field. This EMP based screening test is a promising development. It is easy to perform, and it does not require highly qualified personnel to administer the test. An important clinical consequence is that based on the eye movement responses obtained the glaucomatous visual field may be monitored and appropriate management with timely referral to the specialist can be planned to arrest the progress of this blinding disease.

APPENDICES

General Summary

References

Portfolio

List of Publications

Acknowledgement

Curriculum Vitae

General Summary

Visual information is one of the most essential senses for our survival. Any form of visual function loss, in isolation or combined, has an unfathomable impact on a person's life. One of the most frequent causes of visual function loss is glaucoma. Due to its asymptomatic nature in the early stages, ~90% of the affected remain unaware until the disease progresses to its moderate to severe form with significant visual field loss.

The glaucomatous degenerative change in primary visual sensory pathways is manifested in the form of permanent progressive visual field loss which, if left untreated, can turn into complete blindness. Evaluation of visual field defects is considered as one of the potential approaches for the detection and management of glaucoma. Standard automated perimetry (SAP) is the current clinical standard for testing a person's visual field. It requires considerable co-operation in the form of maintaining steady fixation and suppression of reflexive eye movements to perform the test reliably. At our laboratory (Vestibular and Oculomotor Research group, Department of Neuroscience, Erasmus MC, Rotterdam), a new method named Eye Movement Perimetry (EMP) was developed. The EMP technique consists of an infrared eye tracker to monitor eye movements made towards a visual target presented on a computer monitor. The saccadic eye movement responses towards detected stimuli in the visual field are used to map a patient's functional visual field responsiveness. In the EMP paradigm, the same test grid as used in SAP was adopted to present the visual stimuli. Subjects were instructed to make goal-directed prosaccades that were used to assess the extent of the intact visual field. In addition, the timing of the generation of the prosaccades i.e., the saccadic reaction time (SRT), the time needed to process visual information and initiate eye movement response, was calculated.

For this thesis, the EMP test paradigm was applied in healthy individuals and patients with glaucoma to evaluate its methodological properties for detecting glaucomatous visual field defects. The main purpose was to identify characteristics of eye movement responses

and to evaluate its diagnostic accuracy in a population-based cohort of patients with glaucoma aged 20 years and above.

In chapter 2, I discussed the applicability of EMP in glaucoma and its effect on SRT. We compared the SRTs between healthy subjects and glaucoma patients with different disease severity. We showed that the average SRT is delayed in glaucomatous eyes when compared to healthy eyes in subjects of the same age. An additional observation was that, when I grouped the patients with increasing glaucoma disease severity into 'mild', 'moderate' and 'severe', an increase in average SRT was found. These findings of delayed SRTs underline the importance of quantifying the oculomotor responses as an index of visual field responsiveness in glaucoma.

In chapter 3, I assessed the interaction of age, sex, and the factors within the visual field with SRT using a mixed model analysis. I found delayed SRTs with decreasing stimulus intensity and increasing eccentricity, especially when presented at the extreme periphery i.e., from 16 degrees onwards. The study population was paradigmatic of healthy adults from the Indian subcontinent. The results show an approximately 40% delay in SRT in adults aged 60 years and above when compared with 20-29 years. These results suggest a significant interaction between these factors with SRT, except for sex. The characteristics of SRT presented in this chapter provided a framework for estimating the normative limits of SRT. Next, an estimation was made of the normative reference limits adjusted for age, stimulus intensity and eccentricity. Because of the non-Gaussian nature of the distribution of SRT, the normal limits were calculated based on empirically ascertained deviations i.e., at the significance levels of 5%, 2.5%, 1% and 0.5% separately at each tested location in different age bins from the age corrected normal SRT. This normative reference for SRT has been applied for the subsequent studies (i.e., chapter 4, 5 and 6) to evaluate the clinical applicability of this testing paradigm.

In chapter 4, a comparison was made between the SRT behaviour among the Indian and Dutch adults. In this exploratory chapter, the results from chapter 3 were expanded and compared the SRTs obtained in healthy Indians with healthy Dutch adults aged 20 years

and above. The initial analysis of Indian and Dutch SRT behaviour demonstrated significant differences. One important observation was that elderly Indians i.e., subjects aged 60 years and above presented with remarkably delayed SRT values when compared with the Dutch counterparts. Overall, the result from this initial analysis implies the presence of ethnic variations in SRT derived from visual field testing. These findings suggest that ethnic variations should be considered when developing a normative database for EMP.

In chapter 5, we studied the diagnostic accuracy and validity of EMP compared with the current clinical standard, SAP, in differentiating glaucomatous visual field defects from normal visual fields. In this chapter, we have introduced the EMP plots which are customised to present the pictorial depiction about the presence, location, extent, and depth of a visual field defect especially useful to be applied in clinics. When compared with the SAP reports, by 2 glaucoma specialists, the grading revealed that the EMP visual field plots exhibit excellent agreement for discriminating normal and glaucomatous visual field defects (kappa 0.92 & 0.96). An additional observation from the specialists was that they found EMP plots easy to comprehend despite that it is a new testing paradigm.

In Chapter 6, I assessed SRT across the hemifield sectors to have an additional index pertinent to glaucomatous visual field defects. The normative reference data from chapter 3 were expanded and compared with a new dataset of participants with healthy and glaucoma aged 20-70 years. The hemi-field sectors used in this analysis are derived from the Glaucoma Hemi-field Test (GHT). The GHT sectors are developed based on the course of Retinal Nerve Fibre Layer (RNFL) arrangements, which is a more concise approach to interpreting visual field reports with respect to glaucomatous field defects. We found moderate sensitivity and specificity of SRT when assessed in hemi-field sectors to detect glaucoma. The result showed an overall delay in SRT in glaucomatous visual fields and that SRTs obtained in hemi-fields cannot be used as an independent index to differentiate normal from a glaucomatous field defect.

In chapter 7, I explored the possibility of using Eye Movement Perimetry in assessing binocular visual fields, in terms of the extent of the tested field as well as its responsiveness. This exploratory work provided the first insight into binocular SRTs in patients with glaucomatous visual field defects. The rationale for assessing a quantifiable binocular visual field responsiveness in patients with visual field defect is important when it comes to answering their questions regarding their eligibilities to perform activities in daily living such as driving or navigating. Our findings suggest that for patients with asymmetric visual field loss, the binocular visual field in EMP showed more preserved responsiveness than the monocular visual field of the worse eye. The result from this analysis necessitates further investigation of binocular visual field assessment in addition to monocular ones and evaluating its impact on day-to-day functions and quality of life.

Overall, we conclude that the Eye Movement Perimetry can identify visual field defects based on seen / unseen stimuli in combination with Saccadic Reaction Times of the seen stimuli. Given the use of reflexive eye movement and valid diagnostic accuracy, this method can be an addition to the conventional visual field testing in the glaucoma clinics especially for elderly patients with difficulties in pressing the button and postural constraints. The findings from this thesis provides a groundwork to use EMP in the visual field testing and considering its ease of performance this method can be useful in screening glaucomatous visual field in the community level without any experienced perimetrist.

In this way, the EMP method can contribute to earlier detection of the disease and increase the quality of life of these patients.

Reference list

Alotaibi, A., Underwood, G., & Smith, A. D. (2017). Cultural differences in attention: Eye movement evidence from a comparative visual search task. *Consciousness and Cognition*, *55*, 254–265.

Asaoka, R., Crabb, D. P., Yamashita, T., Russell, R. A., Wang, Y. X., & Garway-Heath, D. F. (2011). Patients have two eyes!: Binocular versus better eye visual field indices. *Investigative Ophthalmology and Visual Science*, *52*(9), 7007–7011.

Asfaw, D. S., Jones, P. R., Smith, N. D., & Crabb, D. P. (2018). Data on eye movements in people with glaucoma and peers with normal vision. *Data in Brief*, *19*, 1266–1273.

Åsman, P. (1992). Evaluation of Methods for Automated Hemifield Analysis in Perimetry. *Archives of Ophthalmology*, *110*(6), 820.

Åsman, P., & Heijl, A. (1992). Glaucoma Hemifield Test: Automated Visual Field Evaluation. *Archives of Ophthalmology*, *110*(6), 812–819.

Bahill, A. T., & Troost, B. T. (1979). Types of saccadic eye movements. *Neurology*, *29*(8), 1150–1152.

Bell, A. H., Meredith, M. A., Van Opstal, A. J., & Munoz, D. P. (2006). Stimulus intensity modifies saccadic reaction time and visual response latency in the superior colliculus. *Experimental Brain Research*, *174*(1), 53–59.

Bengtsson, B., & Heijl, A. (2000). False-negative responses in glaucoma perimetry: Indicators of patient performance or test reliability? *Investigative Ophthalmology and Visual Science*, *41*(8), 2201–2204.

Blais, C., Jack, R. E., Scheepers, C., Fiset, D., & Caldara, R. (2008). Culture shapes how we look at faces. *PLoS ONE*, *3*(8).

Blake, R., & Fox, R. (1973). The psychophysical inquiry into binocular summation. *Perception & Psychophysics*, *14*(1), 161–185.

Boxer, A. L., Garbutt, S., Rankin, K. P., Hellmuth, J., Neuhaus, J., Miller, B. L., & Lisberger, S. G. (2006). Medial versus lateral frontal lobe contributions to voluntary saccade control as revealed by the study of patients with frontal lobe degeneration. The Journal of Neuroscience : The Official Journal of the Society for Neuroscience, 26(23), 6354–6363.

Brigell, M. G., Goodwiaf, J. A., & Lorance, R. (1988). *Saccadic Latency as a Measure of Afferent Visual Conduction*. *29*(8), 1331–1338.

Broadway, D. C. (2012). Visual field testing for glaucoma - a practical guide. *Community Eye Health / International Centre for Eye Health*, *25*(79–80), 66–70.

Brusini, P., Salvetat, M. L., Parisi, L., & Zeppieri, M. (2005). Probing glaucoma visual damage by rarebit perimetry. *British Journal of Ophthalmology*, *89*(2), 180–184.

Brusini, Paolo, & Johnson, C. A. (2007). *MAJOR REVIEW Staging Functional Damage in Glaucoma : Review of Different Classification Methods*. *52*(2).

Carpenter, R. H. S. (2004). *Contrast , Probability , and Saccadic Latency : Evidence for Independence of Detection and Decision*. *14*, 1576–1580.

Census 2011. Available from: http://www.censusindia.gov.in/2011-common/census_2011.html (Last accessed on 2021 May 14)

Chew, S. S. L., Kerr, N. M., Wong, A. B. C., Craig, J. P., Chou, C., & Danesh-meyer, H. V. (2016). *Anxiety in visual fi eld testing*. 1128–1133.

Chylack, L. T., Khu, P., Kashiwagi, T., Mccarthy, D., Leske, M. C., & Sperduto, R. (1989). Lens opacities classification system ii (locs ii). *Archives of Ophthalmology*, *107*(7), 991–997.

Crabb, D. P., Smith, N. D., Rauscher, F. G., Chisholm, C. M., Barbur, J. L., Edgar, D. F., & Garway-Heath, D. F. (2010). Exploring eye movements in patients with glaucoma when viewing a driving scene. *PloS One*, *5*(3), e9710.

Crabb, D. P., & Viswanathan, A. C. (2005a). Integrated visual fields: A new approach to measuring the binocular field of view and visual disability. *Graefe's Archive for Clinical and Experimental Ophthalmology*, *243*(3), 210–216.

Crabb, D. P., & Viswanathan, A. C. (2005b). Integrated visual fields: A new approach to measuring the binocular field of view and visual disability. *Graefe's Archive for Clinical and Experimental Ophthalmology*, *243*(3), 210–216.

Crabb, D. P., Viswanathan, A. C., McNaught, A. I., Poinoosawmy, D., Fitzke, F. W., & Hitchings, R. A. (1998a). Simulating binocular visual field status in glaucoma. *British Journal of Ophthalmology*, *82*(11), 1236–1241.

Crabb, D. P., Viswanathan, A. C., McNaught, A. I., Poinoosawmy, D., Fitzke, F. W., & Hitchings, R. A. (1998b). Simulating binocular visual field status in glaucoma. *British Journal of Ophthalmology*, *82*(11), 1236–1241.

Crawford, T. J., Devereaux, A., Higham, S., & Kelly, C. (2015). The disengagement of visual attention in Alzheimer's disease: A longitudinal eye-tracking study. *Frontiers in Aging Neuroscience*, *7*(JUN), 1–10.

Crish, S. D., Sappington, R. M., Inman, D. M., Horner, P. J., & Calkins, D. J. (2010). Distal axonopathy with structural persistence in glaucomatous neurodegeneration. *Proceedings of the National Academy of Sciences of the United States of America*, *107*(11), 5196–5201.

Dafoe, J. M., Armstrong, I. T., & Munoz, D. P. (2007). The influence of stimulus

direction and eccentricity on pro- and anti-saccades in humans. *Experimental Brain Research*, *179*(4), 563–570.

Damato, B. E. (1985). Oculokinetic perimetry: a simple visual field test for use in the community. *The British Journal of Ophthalmology*, *69*(12), 927–931.

Darrien, J. H., Herd, K., Starling, L. J., Rosenberg, J. R., & Morrison, J. D. (2001). An analysis of the dependence of saccadic latency on target position and target characteristics in human subjects. *BMC Neuroscience*, *2*(area 8).

Daw, N. W. (2006). Visual development (Vol. 9). New York: Springer.

Delinte, A., Gomez, C. M., Decostre, M. F., Crommelinck, M., & Roucoux, A. (2002). Amplitude transition function of human express saccades. *Neuroscience Research*, *42*(1), 21–34.

Editor, C. G. G. (2007). Textbook of Clinical Neurology. *Textbook of Clinical Neurology*, 2007.

Enger, C., & Sommer, A. (1987). Recognizing Glaucomatous Field Loss With the Humphrey STATPAC. *Archives of Ophthalmology*, *105*(10), 1355–1357.

Esterman, B. E. N. (1982). Functionru Scoring of the. *Ophthalmology*, *89*(11), 1226–1234.

Farkas, & G. (2001). (1989). Apoptosis, Neuroprotection, and Retinal Ganglion Cell Death: An Overview. *Glaucoma - Basic and Clinical Concepts*, 111–130.

Fischer, B., Biscaldi, M., & Gezeck, S. (1997). On the development of voluntary and reflexive components in human saccade generation. *Brain Research*, *754*(1–2), 285–297.

Flaxman, S. R., Bourne, R. R. A., Resnikoff, S., Ackland, P., Braithwaite, T., Cicinelli, M. V., Das, A., Jonas, J. B., Keeffe, J., Kempen, J. H., Leasher, J., Limburg, H., Naidoo, K., Pesudovs, K., Silvester, A., Stevens, G. A., Tahhan, N., Wong, T. Y., Taylor, H. R., … Zheng, Y. (2017). Global causes of blindness and distance vision impairment 1990–2020: a systematic review and meta-analysis. *The Lancet Global Health*, *5*(12), e1221–e1234.

Fleuriet, J., & Goffart, L. (2012). Saccadic interception of a moving visual target after a spatiotemporal perturbation. *Journal of Neuroscience*, *32*(2), 452–461.

Foster, P. J., Buhrmann, R., Quigley, H. A., & Johnson, G. J. (2002). *prevalence surveys*. 238–242.

Freeman, E. E., Muñoz, B., Rubin, G., & West, S. K. (2007). Visual field loss increases the risk of falls in older adults: The salisbury eye evaluation. *Investigative Ophthalmology and Visual Science*, *48*(10), 4445–4450.

Frezzotti, P., Giorgio, A., Motolese, I., De Leucio, A., Iester, M., Motolese, E., Federico, A., & De Stefano, N. (2014). Structural and functional brain changes beyond visual system in patients with advanced glaucoma. *PLoS ONE*, *9*(8).

Friedman, D. S., Freeman, E., Munoz, B., Jampel, H. D., & West, S. K. (2007). Glaucoma and Mobility Performance. The Salisbury Eye Evaluation Project. *Ophthalmology*, *114*(12), 2232–2238.

Fukushima, J., Hatta, T., & Fukushima, K. (2000). Development of voluntary control of saccadic eye movements. I. Age-related changes in normal children. *Brain & Development*, *22*(3), 173–180.

Fuller, J. H. (1996). Eye position and target amplitude effects on human visual saccadic latencies. *Experimental Brain Research*, *109*(3), 457–466.

Garway-Heath, D F, Viswanathan, A., Westcott, M., Kamal, D., Fitzke, F., & Hitchings, R. A. (1999). Relationship between perimetric light sensitivity and optic disk neuroretinal rim area. *Perimetry Update*, 381–389.

Garway-Heath, David F., Holder, G. E., Fitzke, F. W., & Hitchings, R. A. (2002). Relationship between electrophysiological, psychophysical, and anatomical measurements in glaucoma. *Investigative Ophthalmology and Visual Science*, *43*(7), 2213–2220.

Gella, L., Nittala, M. G., & Raman, R. (n.d.). *Original Article Retinal sensitivity in healthy Indians using microperimeter*. 1–3.

George, R., der Steen, J., Mazumdar, D., Pel, J., Panday, M., Asokan, R., Vijaya, L., & Shantha, B. (2014). Comparison of saccadic reaction time between normal and glaucoma using an eye movement perimeter. *Indian Journal of Ophthalmology*, *62*(1), 55.

George, R., Ve, R. S., & Vijaya, L. (2010). Glaucoma in India: Estimated burden of disease. *Journal of Glaucoma*, *19*(6), 391–397.

Glen, F. C., Baker, H., & Crabb, D. P. (2014). A qualitative investigation into patients' views on visual field testing for glaucoma monitoring. *BMJ Open*, *4*(1), 1–10.

Gutienez, P., Roy Wilson, M., Johnson, C., Gordon, M., Cioffi, G. A., Ritch, R., Sherwood, M., Meng, K., & Mangione, C. M. (1997). Influence of glaucomatous visual field loss on health-related quality of life. *Archives of Ophthalmology*, *115*(6), 777–784.

Heijl, A., Lindgren, G., & Olsson, J. (1989). The effect of perimetric experience in normal subjects. Archives of ophthalmology, 107(1), 81-86.

Heijl, A., Lindgren, G., Olsson, J., & Åsman, P. (1989). Visual field interpretation with empiric probability maps. Archives of Ophthalmology, 107(2), 204-208.Helen Creasey, D. S. R. (1985). *The ageing Human Brain*. *17*(1).

Hendrickx, K. H., van den Enden, A., Rasker, M. T., & Hoyng, P. F. J. (1994). Cumulative Incidence of Patients with Disc Hemorrhages in Glaucoma and the Effect of Therapy. *Ophthalmology*, *101*(7), 1165–1172.

Hodgson, T. L. (2002). The location marker effect: Saccadic latency increases with target eccentricity. *Experimental Brain Research*, *145*(4), 539–542.

Hood, D. C. (2019). Does Retinal Ganglion Cell Loss Precede Visual Field Loss in Glaucoma? *Journal of Glaucoma*, *28*(11), 945–951.

Inoue, K. (2014). Managing adverse effects of glaucoma medications. *Clinical Ophthalmology*, *8*, 903–913.

Irving, E. L., Steinbach, M. J., Lillakas, L., Babu, R. J., & Hutchings, N. (2006). Horizontal saccade dynamics across the human life span. *Investigative Ophthalmology and Visual Science*, *47*(6), 2478–2484.

Jóhannesson, Ó. I., Ásgeirsson, Á. G., & Kristjánsson, Á. (2012). Saccade performance in the nasal and temporal hemifields. *Experimental Brain Research*, *219*(1), 107–120.

Johansson, J. E., Pansell, T., Ygge, J., & Seimyr, G. Ö. (2014). The effect of contrast on monocular versus binocular reading performance. *Journal of Vision*, *14*(5), 1–14.

John Findlay and Robin Walker (2012) Human saccadic eye movements. Scholarpedia, 7(7):5095., revision #126768

Johnson, C. A., Wall, M., & Thompson, H. S. (2011a). A history of perimetry and visual field testing. *Optometry and Vision Science*, *88*(1).

Johnson, C. A., Wall, M., & Thompson, H. S. (2011b). *A History of Perimetry and Visual Field Testing*. *88*(1), 8–15.

Johnson, L. N. (2016). Glaucoma as a Neurodegenerative Disease: Why We Must "Look for the Protein." *Rhode Island Medical Journal (2013)*, *99*(6), 18–21.

Jonas, J. B., Aung, T., Bourne, R. R., Bron, A. M., Ritch, R., & Panda-Jonas, S. (2017). Glaucoma. *The Lancet*, *390*(10108), 2183–2193.

Meethal, N. K., Mazumdar, D., Asokan, R., Panday, M., van der Steen, J., Vermeer, K. A., ... & Pel, J. J. M. (2018). Development of a test grid using eye movement perimetry for screening glaucomatous visual field defects. Graefe's Archive for Clinical and Experimental Ophthalmology, 256(2), 371-379.

Kanjee, R., Yücel, Y. H., Steinbach, M. J., González, E. G., & Gupta, N. (2012). Delayed saccadic eye movements in glaucoma. *Eye and Brain*, *4*, 63–68.

Kardon, R. H. (1992). Pupil perimetry. *Current Opinion in Ophthalmology*, *3*(5), 565–

570.

Kasneci, E., Black, A. A., & Wood, J. M. (2017). Eye-Tracking as a Tool to Evaluate Functional Ability in Everyday Tasks in Glaucoma. *Journal of Ophthalmology*, *2017*.

Kelly, D. J., Miellet, S., & Caldara, R. (2010). Culture shapes eye movements for visually homogeneous objects. *Frontiers in Psychology*, *1*(APR), 1–7.

Kenward, B., Koch, F. S., Forssman, L., Brehm, J., Tidemann, I., Sundqvist, A., Marciszko, C., Hermansen, T. K., Heimann, M., & Gredebäck, G. (2017). Saccadic reaction times in infants and adults: Spatiotemporal factors, gender, and interlaboratory variation. *Developmental Psychology*, *53*(9), 1750–1764.

Kim, D. E., Eizenman, M., Trope, G. E., & Kranemann, C. (1995, September). Eye movement perimetry. In Proceedings of 17th International Conference of the Engineering in Medicine and Biology Society (Vol. 2, pp. 1629-1630). IEEE.

Knox, P. C., Amatya, N., Jiang, X., & Gong, Q. (2012). Performance Deficits in a Voluntary Saccade Task in Chinese "Express Saccade Makers." *PLoS ONE*, *7*(10), 1–8.

Knox, P. C., & Wolohan, F. D. A. (2014). Cultural diversity and saccade similarities: Culture does not explain saccade latency differences between Chinese and Caucasian participants. *PLoS ONE*, *9*(4).

Kotecha, A., O'Leary, N., Melmoth, D., Grant, S., & Crabb, D. P. (2009). The functional consequences of glaucoma for eye-hand coordination. *Investigative Ophthalmology and Visual Science*, *50*(1), 203–213.

Kruger, N., Janssen, P., Kalkan, S., Lappe, M., Leonardis, A., Piater, J., Rodriguez-Sanchez, A. J., & Wiskott, L. (2012). Deep hierarchies in the primate visual cortex: What can we learn for computer vision? *IEEE Transactions on Pattern Analysis and Machine Intelligence*, *35*(8), 1847–1871.

Kübler, T. C., Kasneci, E., Rosenstiel, W., Heister, M., Aehling, K., Nagel, K., Schiefer, U., & Papageorgiou, E. (2015). Driving with glaucoma: Task performance and gaze movements. *Optometry and Vision Science*, *92*(11), 1037–1046.

Lamirel, C., Milea, D., Cochereau, I., Duong, M. H., & Lorenceau, J. (2014). Impaired saccadic eye movement in primary open-angle glaucoma. *Journal of Glaucoma*, *23*(1), 23–32.

Larrazabal, A. J., García Cena, C. E., & Martínez, C. E. (2019). Video-oculography eye tracking towards clinical applications: A review. *Computers in Biology and Medicine*, *108*(December 2018), 57–66.

Leffler, C. T., Schwartz, S. G., Hadi, T. M., Salman, A., & Vasuki, V. (2015). The early history of glaucoma: The glaucous eye (800 BC to 1050 AD). *Clinical*

Ophthalmology, *9*, 207–215.

Lopes-Ferreira, D., Neves, H., Queiros, A., Faria-Ribeiro, M., Peixoto-De-Matos, S. C., & González-Méijome, J. M. (2013). Ocular dominance and visual function testing. *BioMed Research International*, *2013*.

Mardanbegi, D., Wilcockson, T. D. W., Killick, R., Xia, B., Gellersen, H., Sawyer, P., & Crawford, T. J. (2020). A comparison of post-saccadic oscillations in European-Born and China-Born British University Undergraduates. *PLoS ONE*, *15*(2), 1–14.

Masgoret, X., Asper, L., Alexander, J., & Suttle, C. (2010). Enhancement of resolution acuity in a half-binocular viewing condition. *Investigative Ophthalmology and Visual Science*, *51*(11), 6066–6069.

Mazumdar, D., Meethal, N. S. K., George, R., & Pel, J. J. M. (2021). Saccadic reaction time in mirror image sectors across horizontal meridian in eye movement perimetry. *Scientific Reports*, *11*(1), 1–11.

Mazumdar, D., Meethal, N. S. K., Panday, M., Asokan, R., Thepass, G., George, R. J., van der Steen, J., & Pel, J. J. M. (2019). Effect of Age, Sex, Stimulus Intensity, and Eccentricity on Saccadic Reaction Time in Eye Movement Perimetry. *Translational Vision Science & Technology*, *8*(4), 13.

Mazumdar, D., Pel, J. J. M., Kadavath Meethal, N. S., Asokan, R., Panday, M., Steen, J. Van Der, & George, R. (2020). Visual Field Plots: A Comparison Study between Standard Automated Perimetry and Eye Movement Perimetry. *Journal of Glaucoma*, *29*(5), 351–361.

McKean-Cowdin R et al, 2008. (2008). Impact of Visual field loss on HRQOL. *Physiology & Behavior*, *176*(12), 139–148.

McTrusty, A. D., Cameron, L. A., Perperidis, A., Brash, H. M., Tatham, A. J., Agarwal, P. K., Murray, I. C., Fleck, B. W., & Minns, R. A. (2017). Comparison of Threshold Saccadic Vector Optokinetic Perimetry (SVOP) and Standard Automated Perimetry (SAP) in Glaucoma. Part II: Patterns of Visual Field Loss and Acceptability. *Translational Vision Science & Technology*, *6*(5), 4.

Meethal, N. S. K., Pel, J. J. M., Mazumdar, D., Asokan, R., Panday, M., van der Steen, J., & George, R. (2019). Eye Movement Perimetry and Frequency Doubling Perimetry: clinical performance and patient preference during glaucoma screening. *Graefe's Archive for Clinical and Experimental Ophthalmology*.

Munoz, D. P., Broughton, J. R., Goldring, J. E., & Armstrong, I. T. (1998). Age-related performance of human subjects on saccadic eye movement tasks. *Experimental Brain Research*, *121*(4), 391–400.

Murray, I. C., Fleck, B. W., Brash, H. M., MacRae, M. E., Tan, L. L., & Minns, R. A.

(2009). Feasibility of Saccadic Vector Optokinetic Perimetry. A Method of Automated Static Perimetry for Children Using Eye Tracking. *Ophthalmology*, *116*(10), 2017–2026.

Murray, I. C., Perperidis, A., Cameron, L. A., McTrusty, A. D., Brash, H. M., Tatham, A. J., Agarwal, P. K., Fleck, B. W., & Minns, R. A. (2017). Comparison of Saccadic Vector Optokinetic Perimetry and Standard Automated Perimetry in Glaucoma. Part I: Threshold Values and Repeatability. *Translational Vision Science & Technology*, *6*(5), 3.

Najjar, R. P., Sharma, S., Drouet, M., Leruez, S., Baskaran, M., Nongpiur, M. E., Aung, T., Fielding, J., White, O., Girard, M. J., Lamirel, C., & Milea, D. (2017). Disrupted eye movements in preperimetric primary open-angle glaucoma. *Investigative Ophthalmology and Visual Science*, *58*(4), 2430–2437.

Nelson-Quigg, J. M., Cello, K., & Johnson, C. A. (2000). Predicting binocular visual field sensitivity from monocular visual field results. *Investigative Ophthalmology and Visual Science*, *41*(8), 2212–2221.

Nelson, P., Aspinall, P., O'Brien, C., & Scott, I. U. (2001). Patients' perception of visual impairment in glaucoma: A pilot study. *Evidence-Based Eye Care*, *2*(2), 114–115.

Olsen, A. S., Alberti, M., Serup, L., La Cour, M., Damato, B., & Kolko, M. (2016). Glaucoma detection with damato multifixation campimetry online. *Eye (Basingstoke)*, *30*(5), 731–739.

Opper, J. K., & Volbrecht, V. J. (2017). Binocular vs. monocular hue perception. *Vision Research*, *131*, 1–15.

Anderson, D. R., & Patella, V. M. (1992). Automated static perimetry. Mosby.

Pel, J. J M, Manders, J. C. W., & van der Steen, J. (2010). Assessment of visual orienting behaviour in young children using remote eye tracking: Methodology and reliability. *Journal of Neuroscience Methods*, *189*(2), 252–256.

Pel, Johan J. M., van Beijsterveld, M. C. M., Thepass, G., & van der Steen, J. (2013). Validity and Repeatability of Saccadic Response Times Across the Visual Field in Eye Movement Perimetry. *Translational Vision Science & Technology*, *2*(7), 3.

Pepperberg, D. R. (2003). Bleaching desensitization: Background and current challenges. *Vision Research*, *43*(28), 3011–3019.

Popescu, M. L., Boisjoly, H., Schmaltz, H., Kergoat, M. J., Rousseau, J., Moghadaszadeh, S., Djafari, F., & Freeman, E. E. (2012). Explaining the relationship between three eye diseases and depressive symptoms in older adults. *Investigative Ophthalmology & Visual Science*, *53*(4), 2308–2313.

Pratt, J., Abrams, R. A., & Chasteen, A. L. (1997). Initiation and inhibition of saccadic eye movements in younger and older adults: An analysis of the gap effect. *Journals of Gerontology - Series B Psychological Sciences and Social Sciences*, *52*(2), 103–107.

Quigley, H. A., McKinnon, S. J., Zack, D. J., Pease, M. E., Kerrigan-Baumrind, L. A., Kerrigan, D. F., & Mitchell, R. S. (2000). Retrograde axonal transport of BDNF in retinal ganglion cells is blocked by acute IOP elevation in rats. *Investigative Ophthalmology and Visual Science*, *41*(11), 3460–3466.

Quigley, H., & Broman, A. T. (2006). The number of people with glaucoma worldwide in 2010 and 2020. *British Journal of Ophthalmology*, *90*(3), 262–267.

Quigley, Harry A., Dunkelberger, G. R., & Green, W. R. (1989). Retinal ganglion cell atrophy correlated with automated perimetry in human eyes with glaucoma. *American Journal of Ophthalmology*, *107*(5), 453–464.

Rayner, K., Li, X., Williams, C. C., Cave, K. R., & Well, A. D. (2007). Eye movements during information processing tasks: Individual differences and cultural effects. *Vision Research*, *47*(21), 2714–2726.

Reulen, J. P. (1984). Latency of visually evoked saccadic eye movements. Biological cybernetics, 50(4), 251-262.

Saslow, M. G. (1967). Effects of components of displacement-step stimuli upon latency for saccadic eye movement. *Journal of the Optical Society of America*, *57*(8), 1024–1029.

Satgunam, P., Joshi, D., Bobbili, K. R., Chillakala, K., & Datta, S. (2017). Pediatric Perimeter—A Novel Device to Measure Visual Fields in Infants and Patients with Special Needs. *Translational Vision Science & Technology*, *6*(4), 3.

Sippel, K., Kasneci, E., Aehling, K., Heister, M., Rosenstiel, W., Schiefer, U., & Papageorgiou, E. (2014). Binocular glaucomatous visual field loss and its impact on visual exploration - A supermarket study. *PLoS ONE*, *9*(8).

Smissth, T. J. (1988). The effect of regression towards the mean on visual disability rating scales. *Documenta Ophthalmologica*, *70*(4), 331–337.

Smith, N. D., Crabb, D. P., & Garway-Heath, D. F. (2011). An exploratory study of visual search performance in glaucoma. *Ophthalmic and Physiological Optics*, *31*(3), 225–232.

Smith, N. D., Glen, F. C., & Crabb, D. P. (2012). Eye movements during visual search in patients with glaucoma. *BMC Ophthalmology*, *12*(1).

Sommer, A. (1989). Intraocular pressure and glaucoma. American journal of ophthalmology, 107(2), 186-188.

Stamper, R. L., Lieberman, M. F., & Drake, M. V. (2009). Becker-Shaffer's Diagnosis and Therapy of the Glaucomas E-Book. Elsevier Health Sciences.

Jernigan, M. E. (1980). Structural analysis of eye movement response to visual field stimuli. Computers in biology and medicine, 10(1), 11-22.

State of Health in the EU- Netherlands country health profile 2017 from : https://www.oecd.org/publications/netherlands-country-health-profile-2017-9789264283503-en.html (Last accessed on 2021 May 14)

Susanna Jr., R., & Vessani, R. M. (2009). Staging Glaucoma Patient: Why and How? *The Open Ophthalmology Journal*, *3*(2), 59–64.

Tham, Y. C., Li, X., Wong, T. Y., Quigley, H. A., Aung, T., & Cheng, C. Y. (2014). Global prevalence of glaucoma and projections of glaucoma burden through 2040: A systematic review and meta-analysis. *Ophthalmology*, *121*(11), 2081–2090.

Thepass, G., Pel, J. J. M., Vermeer, K. A., Creten, O., Bryan, S. R., Lemij, H. G., & Van Der Steen, J. (2015). The effect of cataract on eye movement perimetry. *Journal of Ophthalmology*, *2015*.

Thomas, R., & George, R. (2001). Interpreting automated perimetry. *Indian Journal of Ophthalmology*, *49*(2), 125–140.

Toepfer, A., Kasten, E., Guenther, T., & Sabel, B. A. (2008). Perimetry while moving the eyes: Implications for the variability of visual field defects. *Journal of Neuro-Ophthalmology*, *28*(4), 308–319.

Trope, G. E., Eizenman, M., & Coyle, E. (1989). Eye movement perimetry in glaucoma. *Canadian Journal of Ophthalmology*, *24*(5), 197–199.

Vashist, P., Talwar, B., Gogoi, M., Maraini, G., Camparini, M., Ravindran, R. D., Murthy, G. V., Fitzpatrick, K. E., John, N., Chakravarthy, U., Ravilla, T. D., & Fletcher, A. E. (2011). Prevalence of cataract in an older population in India: The india study of age-related eye disease. *Ophthalmology*, *118*(2), 272–278.

Viswanathan, A. C. (1999). Severity and Stability of Glaucoma. *Archives of Ophthalmology*, *117*(4), 450.

Vrabec, J. P., & Levin, L. A. (2007). The neurobiology of cell death in glaucoma. *Eye (Basingstoke)*, *21*, S11–S14.

Wakayama, A., Matsumoto, C., Iwagaki, A., & OTORI, T. (1999). Binocular summation within the binocular visual field. Perimetry Update 1998/1999.

Warren, D. E., Thurtell, M. J., Carroll, J. N., & Wall, M. (2013). Perimetric evaluation of saccadic latency, saccadic accuracy, and visual threshold for peripheral visual stimuli in young compared with older adults. *Investigative Ophthalmology*

and Visual Science, *54*(8), 5778–5787.

Weber, H., Aiple, F., Fischer, B., & Latanov, A. (1992). Dead zone for express saccades. *Experimental Brain Research*, *89*(1), 214–222.

Weinreb, R. N., & Tee Khaw, P. (2004). Primary open-angle glaucoma. *Lancet*, *363*(9422), 1711–1720.

Wild, J. M., Dengler-Harles, M., Searle, A. E. T., O'Neill, E. C., & Crews, S. J. (1989). *The infuence of the learning effect on automated perimetry in patients withsuspected glaucoma*. *67*(5).

Williams, C., Azzopardi, P., & Cowey, A. (1995). Nasal and temporal retinal ganglion cells projecting to the midbrain: Implications for "blindsight." *Neuroscience*, *65*(2), 577–586.

World Medical Association. (2013). World Medical Association Declaration of Helsinki: ethical principles for medical research involving human subjects. Jama, 310(20), 2191-2194.

Wurtz, R. H., & Optican, L. M. (1994). Superior colliculus cell types and models of saccade generation. *Current Opinion in Neurobiology*, *4*(6), 857–861.

Yang, Q., Bucci, M. P., & Kapoula, Z. (2002). The latency of saccades, vergence, and combined eye movements in children and in adults. *Investigative Ophthalmology and Visual Science*, *43*(9), 2939–2949.

Yanjun Chen, PhD, Harry J. Wyatt, PhD, FAAO, William H. Swanson, PhD, FAAO, and M., & W. Dul, OD, MS, F. (2008). Rapid Pupil-Based Assessment of Glaucomatous Damage. *Optom Vis Sci.*, *85*(6).

Zwierko, T., Jedziniak, W., Lesiakowski, P., Śliwiak, M., Kirkiewicz, M., & Lubiński, W. (2019). Eye–hand coordination impairment in glaucoma patients. *International Journal of Environmental Research and Public Health*, *16*(22).

PhD PORTFOLIO

Name of PhD student:	Deepmala Mazumdar	**PhD Period:**	April 2016 - December 2021
Erasmus MC Dept:	Neuroscience	**Promotor:**	Prof. dr. Johannes van der Steen Dr. Ronnie J. George
Research School:	ONWAR	**Supervisor:**	Dr.ir. Johan JM Pel

1. PhD training

	Year	Workload (ECTS)
General Courses		
• Clinical Research Methodology and Statistics in Norwegian University of Life Sciences (NMBU), Oslo, Norway	2015	2
• Sensory Systems under Neuroscience programme by Erasmus university, Rotterdam, The Netherlands	2015	1
Specific Courses/ Lectures		
• Eye movement analysis in Nystagmus - Professor Larry Abel	2018	0.25
• Interpreting visual field reports under Glaucoma diagnostics - glaucoma department, Medical Research Foundation, Chennai, India	2018	0.5
• Evaluation of Optic Nerve head in glaucoma under Glaucoma diagnostics - glaucoma department, Medical Research Foundation, Chennai, India	2019	1

• How to write a research proposal & read a research paper? - Dr Ronnie George, Glaucoma Department, Medical Research Foundation, Chennai, India	2020	1
• Pupil examination & assessment: A skill must for an optometrist - Dr Rashmin Gandhi	2020	0.25
• Clinical imaging in Glaucoma diagnosis - Dr Rashima A, Medical Research Foundation, Chennai, India	2020	1
• An overview of Research Methodology for clinicians - Conducted by Shroff's eye care hospital	2020	1
• Role of optometrist in Occupational health - Dr Krishnakumar R (Conducted by Optometry Association for Tamil Nanbargal)	2020	0.25
• Developing effective research skills - Dr. Rashima A. (Conducted by IRC)	2020	0.25
• How to start a research? - Dr Kalpa N. (Conducted by Optometry Association of Assam)	2020	0.50
• Ophthalmic imaging in Glaucoma diagnosis - Dr. Rashima A (Conducted by Optometry Association of Assam)	2020	0.50
• Enhancing research capacities for ophthalmologists - Conducted by Medical & Vision Research Foundation, Chennai, India	2020	1
• "Glaucoma evaluation & diagnosis: Key elements - Workshop on Glaucoma Detection & Referral How & When, conducted by The Sankara Nethralaya Academy and Optometric Association of Tamil Nanbargal, Chennai, India"	2020	1
• Pupils: Neural pathways & clinical aspects - Webinar conducted by Optometry Association of Assam, India	2020	1

Seminars and workshops

• Talk on “ESO-SN Visual Acuity Charts” The XV Dr E Vaithilingam Memorial Scientific session 2016	2016	1

• Introduction to scientific referencing' - Scientific writing workshop, conducted by Elite School of Optometry, Chennai, India	2017	1
• Scientific literature search tools' - Research Methodology workshop, conducted by Elite School of Optometry, Chennai, India	2017	1
• "Sample size calculation' - Research Methodology workshop, conducted by Elite School of Optometry, Chennai, India"	2017	1
• "Tools for storing & citing papers' – Literature review workshop, conducted by The Sankara Nethralaya Academy, Chennai, India"	2018	1
• Innovations in eye tracking technology for Ophthalmology in collaboration with College of Engineering Anna university - Medical & Vision Research Foundation, Chennai, India	2018	0.5
• "Sample size calculation – Research Methodology workshop, conducted by Elite School of Optometry, Chennai, India"	2019	1
• Scientific Referencing' - Scientific writing workshop, conducted by Elite School of Optometry, Chennai, India	2019	1
• Literature review: What & How? - Literature review workshop, conducted by The Sankara Nethralaya Academy, Chennai	2019	1
• Artificial intelligence in Ophthalmic diagnostics in collaboration with Google AI - Medical & Vision Research Foundation, Chennai, India	2019	1
• Tools for storing & citing papers' - Literature review workshop, conducted by The Sankara Nethralaya Academy, Chennai, India	2019	1
• Visual Field Interpretation – Glaucoma imaging and diagnostics workshop, conducted by 18th Dr. EV Memorial Scientific Session, The Imaging Conference 2K19, Chennai, India	2019	1

• Basics on research methodology & hands-on on basic analysis using statistical tools' - Workshop on Research Methodology for Diplomate of National Board candidates in Ophthalmology - Conducted by Sankara Nethralaya, Chennai, India	2019	1
• How to appropriately use search engines to select & save published articles? - Conducted by Shroff Charity Eye Hospital (SCEH), Delhi, India on an overview of Research Methodology for clinicians	2020	1
• Scientific Referencing and Rules of citation – Conducted by The Sankara Nethralaya Academy, Chennai for the Post-graduate Optometry students	2020	1
• Visual Field Interpretation- Conducted by Malabar Institute of Optometry, Kerala, India (11th July 2020)	2020	0.5
• Doing a good literature search and managing your bibliography- Workshop on Research Methodology for Diplomate of National Board candidates in ophthalmology, Conducted by Sankara Nethralaya, Chennai, India (12th Aug 2020)	2020	1
• Writing an Introduction – NethraVidya comprehensive research methodology workshop conducted by Elite School of Optometry	2021	1
• Emerging technological trends in vision research – “Choose to Challenge” seminar to celebrate International Women’s Day conducted by Vision Science Academy, London, UK (7th March 2021)	2021	1
• How to read Humphrey visual field reports - "Irvin Borish Event”, conducted by University of Hyderabad school of Medical Sciences, Hyderabad, India (23rd March 2021)	2021	1

Presentations

• Clinical research cell meeting, Medical research Foundation, Chennai, India (2x)	2017, 2019	1
• Lab talks - Department of Neuroscience, Erasmus MC, Rotterdam, The Netherlands (2x)	2019	1
• Departmental Talk - Glaucoma Department. Medical Research Foundation, Chennai, India (2x)	2020	1

(Inter) national conferences

• The XV Dr E Vaithilingam Memorial Scientific session 2016 (attendance)	2016	0.25
• International orthoptic congress, IOA, June - 2016 (attendance)	2016	0.25
• The XVI Dr E Vaithilingam Memorial Scientific session 2017 (attendance)	2017	0.25
• Vision 2017 (12th International conference by the ISLRR, The Hague, The Netherlands (Oral presentation)	2017	2
• Sankara Nethralaya Glaucoma Meet (SANGAM), Chennai, India (Oral presentation)	2017	2
• World Congress of Optometry (WCO), Hyderabad, India (oral presentation)	2017	2
• Indian Eye Research Group – ARVO - India Chapter (25th IERG-ARVO-IC), Hyderabad, India (Poster presentation)	2018	1
• The XVIII Dr E Vaithilingam Memorial Scientific session 2019 (Glaucoma Workshop moderator)	2019	1
• World Glaucoma Congress (8th WGC), Melbourne, Australia (Poster presentation)	2019	1

Others

• Research associate in development of eye tracking prototype in collaboration with Bulbi Tech. Trondheim, Norway - Vision Research Foundation, Chennai, India	2016 - 2017	2

• Introduction & Familiarisation of recent ophthalmic devices, Lamirus, Ede, The Netherlands	2017	0.25
• Demonstrated the eye tracking test on strabismus patient - VUMC, Amsterdam, The Netherlands	2017	0.25
• Member of Research Methodology workshop series - Elite School of Optometry	2017-2019	2
• Member of Research Advisory board for the project " Development of a prototype eye tracking technology to evaluate oculomotor functions' - Bulbi Tech. Trondheim, Norway	2018-present	1
• Member of organising committee in The XVIII Dr E Vaithilingam Memorial Scientific session 2019	2019	0.50
• Institutional visit and discussion on current research activities, The Department of Optometry & Vision Science, University of Melbourne, Australia 2019	2019	0.25

2. Teaching

	Year	Workload (ECTS)
Lecturing		
• Optometric Optics, 2nd year Bachelor students, Optometry, Elite School of Optometry, Chennai, India (2 years)	2016-2017	0.50
• Inter college Continuous Medical Education & Case discussion - Moderator (4x)	2017-2019	2
• Clinical mentoring - 4th year Bachelor students (clinical Internship), Optometry, Elite School of Optometry	2017-2019	1
• Common Clinical Conditions - 3rd year Bachelor students, Optometry, Elite School of Optometry, Chennai, India	2019	0.25

Supervising clinical optometry practicals

• Optometric Optics, 2nd year bachelor's in optometry, Elite School Optometry, Chennai, India	2016-2017	1
• Common Clinical Conditions - 3rd year Bachelor students, Optometry, Elite School of Optometry, Chennai, India	2019	0.5

Supervising Undergraduate and postgraduate theses

• Anantha Padmanavan, Master's in optometry thesis on "Development of visual field screening prototype"	2019-present	2
• Vaishali G, Master's in optometry thesis on "Comparing central visual field test points in 24-2 with 10-2 in patients with different grades of glaucoma"	2016-2018	2
• Manideepak, Master's in optometry thesis on "Structural and functional analysis in different severities of glaucoma using Spectral domain optical coherence tomography and Humphrey visual field analyzer"	2017-2019	2
• Nandhini Ravi, Undergraduate thesis on "Assessment of compliance with anti-glaucoma medication in a tertiary eye care centre"	2017-2018	2

Others

• Supervised research protocol writing for 3rd year, bachelor's in medical electronics engineering, College of Engineering Anna university, Chennai, India	2018	0.5
• Author (three chapters) - EcSelO (Eso's Case Scenario based e-learning in Optometry - learning application	2018	1
• External Examiner for Optometry- eye & systemic diseases, advanced ophthalmic diagnostics, ocular disease & therapeutics, Kasturba Medical College, MAHE Manipal, India	2018	1
• External examiner for 3rd year bachelor's in optometry project literature review - Department of Optometry, SRM institute of science and technology, Chennai, India	2018	1

• External Examiner for bachelor’s in optometry theses & Defence presentation, Department of Optometry, SRM institute of science and technology, Chennai, India	2019	1
• External Examiner for Optometry clinics and clinical examination of visual system, Department of Optometry, SRM institute of science and technology, Chennai, India	2018-2019	1
• Moderated journal club session for Glaucoma Department "LOGIX" (2019-2020) - Glaucoma Department. Medical Research Foundation, Chennai, India	2019-2020	1
• Khaarthiyaa Lokanathan, conference presentation pilot project supervision	2021	1
• Sangeetha Nagarajan, conference presentation pilot project supervision	2021	1
• A Technical writeup for "eOphtha"- A online portal of ophthalmology, Title: Mendeley Reference Manager: A Step-by-step Guide	2021	1
Total		**74.25**

List of publications

Mazumdar D, Pel JM, Panday M, Asokan R, Vijaya L, Shantha B, George R, Van Der Steen J. Comparison of saccadic reaction time between normal and glaucoma using an eye movement perimeter. *Indian journal of ophthalmology*. 2014 Jan;62(1):55.

Negiloni K, **Mazumdar D**, Neog A, Das B, Medhi J, Choudhury M, George RJ, Ramani KK. Construction and validation of logMAR visual acuity charts in seven Indian languages. *Indian journal of ophthalmology*. 2018 May;66(5):641.

Meethal NK, **Mazumdar D**, Asokan R, Panday M, van der Steen J, Vermeer KA, Lemij HG, George RJ, Pel JJ. Development of a test grid using eye movement perimetry for screening glaucomatous visual field defects. *Graefe's Archive for Clinical and Experimental Ophthalmology*. 2018 Feb;256(2):371-9.

Mazumdar D, Meethal NS, Panday M, Asokan R, Thepass G, George RJ, van der Steen J, Pel JJ. Effect of age, sex, stimulus intensity, and eccentricity on saccadic reaction time in eye movement perimetry. *Translational vision science & technology*. 2019 Jul 1;8(4):13-.

Meethal NS, Pel JJ, **Mazumdar D**, Asokan R, Panday M, van der Steen J, George R. Eye Movement Perimetry and Frequency Doubling Perimetry: clinical performance and patient preference during glaucoma screening. *Graefe's Archive for Clinical and Experimental Ophthalmology*. 2019 Jun;257(6):1277-87.

Mazumdar D, Lal B, Asokan R. Anterior segment optical coherence tomography of intrastromal corneal cysts. *Asian Journal of Ophthalmology*. 2019;17(1):41-4.

Mazumdar D, Pel JJ, Kadavath Meethal NS, Asokan R, Panday M, v.d. Steen J, George R. Visual Field Plots: A Comparison Study Between Standard Automated Perimetry and Eye Movement Perimetry. *Journal of glaucoma*. 2020 May 21;29(5):351-61.

Datta S, Varadharajan S, **Mazumdar D**, Narayanan A, Monira S, Panda S, Hyvärinen L, Satgunam P. Construction and Validation of LEA Hindi Chart: A Multicenter Study. *Optometry and Vision Science*. 2020 May 1;97(5):351-9.

Mazumdar D, Meethal NS, George R, Pel JJ. Saccadic reaction time in mirror image sectors across horizontal meridian in eye movement perimetry. *Scientific Reports*. 2021 Jan 29;11(1):1-1.

List of Awards and Accolades

Travel grant of amount $1,100 from Association for Research in Vision and Ophthalmology (ARVO) 2017, Baltimore, Md. for the submission titled "Variability of Saccadic Reaction Time across the visual field on an Eye tracker-based perimeter".

All India Ophthalmological Society – Indian Journal of Ophthalmology (AIOS-IJO) Platinum Award for the year 2017-18 for the paper "Construction and validation of logMAR visual acuity charts in seven Indian languages".

The Best Research Clinical science in Ophthalmology for the year 2019 [Ruby Banik Memorial Endowment Award – 2019], Vision Research Foundation, Chennai, India for the research work titled *"Evaluation of Saccadic Reaction Time within Glaucoma Hemi-field test in Eye Movement Perimetry".*

The Young Clinical Mentor Award of the year 2018-2019 [For the contribution towards optometric education and teaching in Elite School of Optometry].

Aspiring Researcher Award by 18th Dr. EV Memorial Scientific Session, The Imaging Conference 2K19, Chennai, India.

The Best Research Clinical science in Ophthalmology for the year 2020 [Ruby Banik Memorial Endowment Award – 2020], Vision Research Foundation, Chennai, India for the research work titled "*A haploscopic based automated binocular pupillometer to quantify the dynamics of direct and consensual Pupillary Light Reflex: methodology & feasibility*".

Acknowledgement

Curriculum Vitae

Deepmala Mazumdar was born on November 1st, 1989, in Assam, India. After graduated in optometry with a bachelor's degree in 2011, she enrolled in post-graduation studies in optometry at the Birla Institute of Technology & Science, Pilani in collaboration with Elite School of Optometry, Chennai, India. From 2011-2013, she studied glaucoma as her speciality under the supervision of Dr Ronnie George. She completed her master thesis titled "Eye Movement Perimeter in Glaucoma Diagnosis" in a collaborative project with the vestibular and oculomotor research group, department of Neurosciences, Erasmus MC Rotterdam. In 2013, she joined with dual designation of research associate and clinical optometrist in the department of visual psychophysics, Sankara Nethralaya, Chennai, India. During this time, she was involved in research works in different specialities in optometry specifically at the glaucoma clinic. This is when she developed her interest in research with a clinically focused view. She has also undergone a course on clinical Research Methodology and Statistics at the Norwegian University of Life Sciences (NMBU), Oslo, Norway.

At the beginning of 2016, she started her PhD research in the vestibular and oculomotor research group, department of Neurosciences, Erasmus MC, Rotterdam. Her research project was the continuation of the collaboration between Erasmus MC, The Netherlands, Sankara Nethralaya, Chennai, India to develop an eye-tracking based diagnostic test for glaucoma. First, her PhD was jointly funded by Netherlands Organisation for Health Research and Development (ZonMw) and Bulbi Tech., Trondheim, Norway. From 2018, her project was funded by the foundations Glaucoomfonds, Oogfonds, Rotterdamse Stichting Blindenbelangen, and Stichting Blindenhulp contributed through UitZicht. During her PhD period, she was affiliated as Senior Research Optometrist at Sankara Nethralaya, Chennai, India.